Hydrographic Observations at the Woods Hole Oceanographic Institution Hawaii Ocean Time-series Site: 2014 – 2015 Data Report #11

Fernando Santiago-Mandujano, Daniel McCoy, R. Walter Deppe, Kellen Rosburg, Albert Plueddemann, Robert Weller, Roger Lukas, Jefrey Snyder, Sean Whelan and Nan Galbraith

January, 2019

SCHOOL OF OCEAN AND EARTH SCIENCE AND TECHNOLOGY
UNIVERSITY OF HAWAI'I AT MĀNOA
SOEST Publication no. 10635

Acknowledgments

Many people participated in the WHOTS mooring deployment/recovery cruises. They are listed in Tables 2.1 and 2.4. We gratefully acknowledge their contributions and support. Thanks are due to all the personnel of the Upper Ocean Processes Group (UOP) at WHOI who prepared the WHOTS buoy's instrumentation and mooring; to Branden Nakahara, Thanh-Van Tran, Kelly Lance, Adela Dumitrascu, and Ryan Tabata, for their technical assistance with the moored and shipboard instrumentation; to Kellie Terada for her excellent project support, to Ksenia Trifonova for editing support, and to Joseph Gum for his shore-based support. We gratefully acknowledge the support from the colleagues at Sea-Bird for helping us maintain the quality of the CTD data. We would also like to thank the captains and crew of the Ship *Hi'ialakai* and especially the University of Hawaii (UH) Marine Center staff for their efforts. The WHOTS project is funded in part by the Ocean Observing and Monitoring Division, Climate Program Office (FundRef number 100007298). National Oceanic and Atmospheric Administration, US Department of Commerce under grant NA14OAR4320158. This work is also supported by the National Science Foundation grant OCE12-60164.

Table of Contents

1. Introduction 1
2. Description of the WHOTS-11 Mooring Cruises 3
   A. WHOTS-11 Cruise: WHOTS-11 Mooring Deployment 3
   B. WHOTS-12 Cruise: WHOTS-11 Mooring Recovery 5
3. Description of WHOTS-11 Mooring 7
4. WHOTS-10 and -11 cruise shipboard observations 11
   A. Conductivity, Temperature and Depth (CTD) profiling 11
      1. Data acquisition and processing 11
      2. CTD sensor calibration and corrections 12
         Pressure 12
         Temperature/Conductivity 12
         Dissolved Oxygen 12
   B. Water sampling and analysis 13
      1. Salinity 13
   C. Thermosalinograph data acquisition and processing 14
      1. WHOTS-11 Cruise 14
         Temperature Calibration 14
         Nominal Conductivity Calibration 14
         Data Processing 14
         Bottle Salinity and CTD Salinity Comparisons 15
         CTD Temperature Comparisons 15
      2. WHOTS-12 Cruise 16
         Temperature Calibration 16
         Nominal Conductivity Calibration 16
         Data Processing 16
         Bottle Salinity and CTD Salinity Comparisons 17
         CTD Temperature Comparisons 18
   D. Shipboard ADCP 18
      1. WHOTS-11Deployment Cruise 18
      2. WHOTS-12 Deployment Cruise 18
5. Moored Instrument Observations 20
   A. MicroCAT/SeaCAT data processing procedures 20
      1. Internal Clock Check and Missing Samples 21
      2. Pressure Drift Correction and Pressure Variability 21
      3. Temperature Sensor Stability 23
         Comparisons with VMCM and ADCP temperature sensors 25
      4. Conductivity Calibration 30
   B. Acoustic Doppler Current Profiler 39
      1. Compass Calibrations 39
      2. ADCP Configurations 42
      3. ADCP data processing procedures 43
   C. Vector Measuring Current Meter (VMCM) 52
   D. Global Positioning System Receiver and ARGOS Positions 55
6. Results 58
   A. CTD Profiling Data 60

B. Thermosalinograph data 73
C. MicroCAT/SeaCAT data 77
D. Moored ADCP data 96
E. Moored and Shipboard ADCP comparisons 102
F. Next Generation Vector Measuring Current Meter data (VMCM) 121
G. GPS data 122
H. Mooring Motion 123
7. References 125
8. Appendices 127
A. Appendix 1: WHOTS-9 300 kHz ADCP Configuration ...**Error! Bookmark not defined.**
B. Appendix 2: WHOTS-9 600 kHz ADCP Configuration ...**Error! Bookmark not defined.**
C. Appendix 3: WHOTS-9 VMCM report 129

1. Introduction

In 2003, Robert Weller (Woods Hole Oceanographic Institution [WHOI]), Albert Plueddemann (WHOI) and Roger Lukas (University of Hawaii [UH]) proposed to establish a long-term surface mooring at the Hawaii Ocean Time-series (HOT) Station ALOHA (22°45'N, 158°W) to provide sustained, high-quality air-sea fluxes and the associated upper ocean response as a coordinated part of the HOT program, and as an element of the global array of ocean reference stations supported by the National Oceanic and Atmospheric Administration's (NOAA) Office of Climate Observation.

With support from NOAA and the National Science Foundation (NSF), the WHOI HOT Site (WHOTS) surface mooring has been maintained at Station ALOHA since August 2004. The objective of this project is to provide long-term, high-quality air-sea fluxes as a coordinated part of the HOT program and contribute to the goals of observing heat, fresh water and chemical fluxes at a site representative of the oligotrophic North Pacific Ocean. The approach is to maintain a surface mooring outfitted for meteorological and oceanographic measurements at a site near Station ALOHA by successive mooring turnarounds. These observations are being used to investigate air-sea interaction processes related to climate variability and change.

The original mooring system is described in the mooring deployment/recovery cruise reports (Plueddemann et al., 2006; Whelan et al., 2007). Briefly, a Surlyn foam surface buoy is equipped with meteorological instrumentation including two complete Air-Sea Interaction Meteorological (ASIMET) systems (Hosom et al. (1995), Colbo and Weller (2009)), measuring air and sea surface temperatures, relative humidity, barometric pressure, wind speed and direction, incoming shortwave and longwave radiation, and precipitation. Complete surface meteorological measurements are recorded every minute, as required to compute air-sea fluxes of heat, freshwater and momentum. Each ASIMET system also transmits hourly averages of the surface meteorological variables via the Argos satellite system and via iridium. The mooring line is instrumented in order to collect time series of upper ocean temperatures, salinities and velocities with the surface forcing record. This includes vector measuring current meters, conductivity, salinity and temperature recorders, and two Acoustic Doppler current profilers (ADCPs). See the WHOTS-11 mooring diagram in Figure 1-1.

The subsurface instrumentation is located vertically to resolve the temporal variations of shear and stratification in the upper pycnocline to support study of mixed layer entrainment. Experience with moored profiler measurements near Hawaii suggests that Richardson number estimates over 10 m scales are adequate. Salinity is clearly important to the stratification, as salt-stratified barrier layers are observed at HOT and in the region (Kara et al., 2000), so we use Sea-Bird MicroCATs with vertical separation ranging from 5-20 m to measure temperature and salinity. We use an RDI ADCP to obtain current profiles across the entrainment zone and another in the mixed layer. Both ADCPs are in an upward-looking configuration, one is at 125 m, using 4 m bins, and the other is a 47.5 m using 2 m bins. To provide near-surface velocity (where the ADCP estimates are less reliable) we deploy two Vector Measuring Current Meters (VMCMs). The nominal mooring design is a balance between resolving extremes versus typical annual cycling of the mixed layer (see WHOTS Data Report 1-2, Santiago-Mandujano et al., 2007).

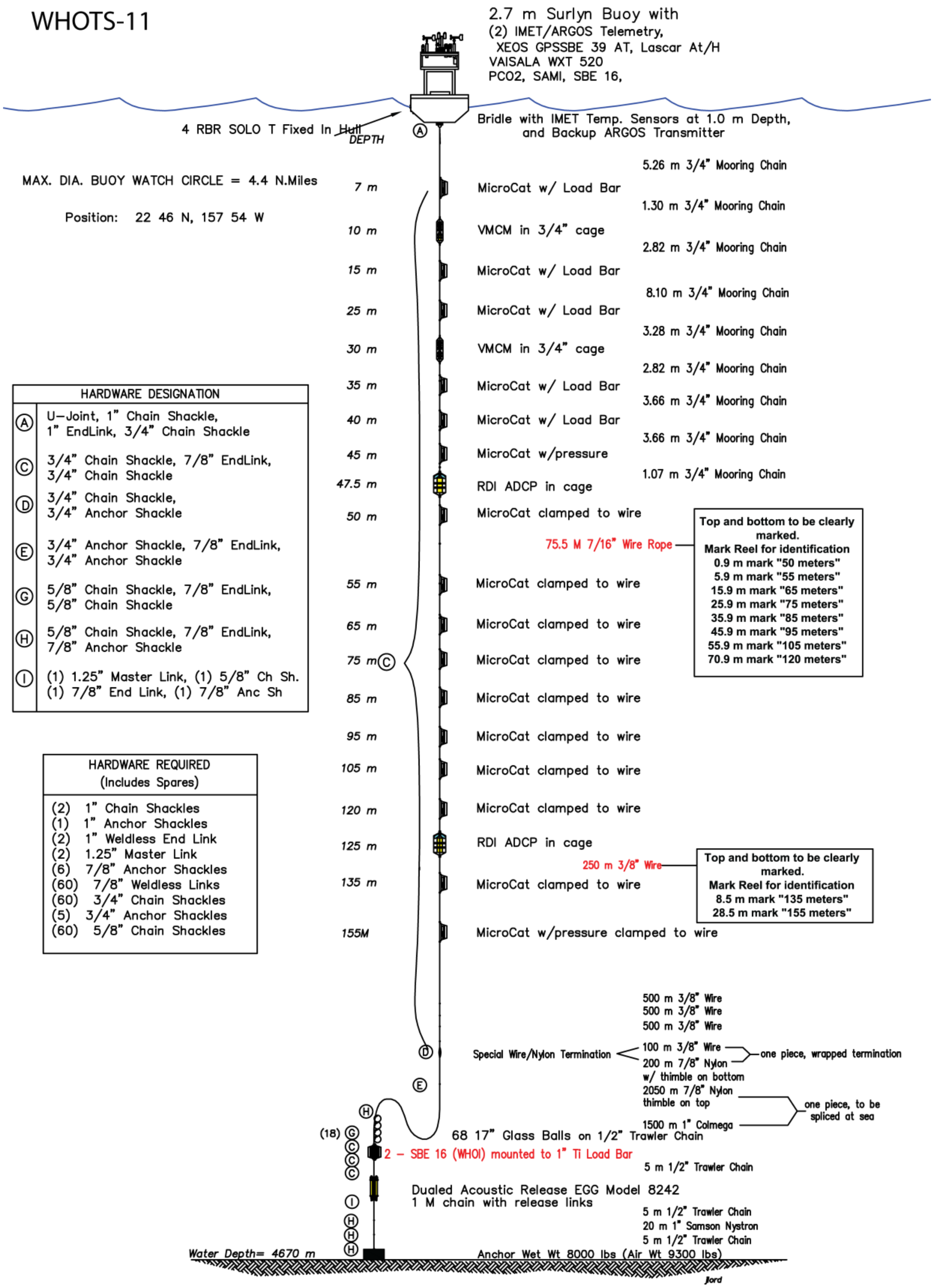

Figure 1-1. WHOTS-11 mooring design.

The eleventh WHOTS mooring (WHOTS-11 mooring) was deployed in July 2014 during a 9-day cruise (WHOTS-11 cruise), and it was recovered in July 2015 during an 8-day cruise (WHOTS-12 cruise); both cruises aboard the NOAA Ship *Hi'ialakai*. An twelfth mooring (WHOTS-12 mooring) was deployed during the WHOTS-12 cruise; to be recovered in June 2016.

This report documents and describes the oceanographic observations made on the eleventh WHOTS mooring during a period of nearly one year, and from shipboard during the two cruises when the mooring was deployed and recovered. Sections 2 and 3, respectively, include a detailed description of the cruises and the mooring. Sampling and processing procedures of the hydrographic casts, thermosalinograph, and shipboard ADCP data collected during cruises are in Section 4. Section 5 includes the processing procedures for the data collected by the moored instruments: SeaCATs, MicroCATs, VMCMs, and moored ADCP. Plots of the resulting data and a preliminary analysis are included in Section 6.

2. Description of the WHOTS-11 Mooring Cruises

A. WHOTS-11 Cruise: WHOTS-11 Mooring Deployment

The Woods Hole Oceanographic Institution Upper Ocean Processes Group (WHOI/UOP), with the assistance of the UH group conducted the eleventh deployment of the WHOTS mooring on board the NOAA Ship *Hi'ialakai* during the WHOTS-11 cruise between 15 and 23 July 2014. The WHOTS-11 mooring was deployed at HOT Station 50 on 17 July 2014 at 02:40 UTC at 22° 45.98'N, 157° 53.96'W. The scientific personnel that participated during the cruise are listed in Table 2-1.

Table 2-1. Scientific personnel on Ship Hi'ialakai during the WHOTS-11 deployment cruise.

Cruise	Name	Title or function	Affiliation
WHOTS-11	Plueddeman, Albert	Chief Scientist	WHOI
	Whelan, Sean	Senior Engineering Assistant	WHOI
	Pietro, Ben	Engineering Assistant	WHOI
	Snyder, Jefrey	Marine Electronic's Technician	UH
	Santiago-Mandujano, Fernando	Research Associate	UH
	McCoy, Daniel	Research Associate	UH
	Tabata, Ryan	Marine Research Technician	UH
	Nakahara, Branden	Marine Research Technician	UH
	Tran, Thanh-Van	Undergraduate Student	UH
	Lance, Kelly	Undergraduate Student	UH
	Blomquist, Byron	Researcher	NOAA

The shipboard oceanographic observations during the cruise were conducted by the UH group.

A Sea-Bird CTD (conductivity, temperature and depth) system was used to measure T, S, and O_2 profiles during ten CTD casts. The time, location, and maximum CTD pressure for each of the profiles are listed in Table 2-2. One cast was conducted at a test site near Oahu to 1020 dbar. Five CTD casts were made at station 50 near the WHOTS-11 mooring for comparison with subsurface instruments after the WHOTS-11 mooring deployment; each cast was to 200 dbar. Five CTD casts were conducted at station 52 near the WHOTS-10 mooring for comparison with subsurface instruments before its recovery; each cast was to 200 dbar. Following these casts, one more CTD cast to 200 dbar was made at station 50 near the WHOTS-11 mooring. These casts were sited approximately 200 to 500 m from the buoys and consisted of 5 yo-yo cycles between 10 dbar and 200 dbar. Four salinity samples were taken from each 200 dbar cast to calibrate the conductivity sensors used for the CTD profiling. One final CTD cast to 1000 dbar was conducted at Station ALOHA and six salinity samples were taken.

Table 2-2. CTD stations occupied during the WHOTS-11 cruise

Station/cast	Date	Time (GMT)	Location *(using NMEA data)*	Maximum pressure (dbar)
1 / 1	7/16/14	00:41	21° 28.04´ N, 158° 21.07´ W	1024
50 / 1	7/17/14	16:10	22° 46.38´ N, 157° 57.37´ W	945
50 / 2	7/17/14	19:54	22° 45.79´ N, 157° 56.15´ W	206
50 / 3	7/18/14	00:05	22° 46.77´ N, 157° 55.64´ W	206
50 / 4	7/18/14	04:28	22° 46.40´ N, 157° 55.86´ W	201
50 / 5	7/18/14	08:11	22° 46.50´ N, 157° 55.87´ W	203
52 / 1	7/18/14	16:09	22° 40.42´ N, 157° 58.79´ W	205
52 / 2	7/18/14	19:57	22° 40.72´ N, 157° 58.78´ W	206
52 / 3	7/18/14	23:49	22° 40.89´ N, 157° 58.56´ W	204
52 / 4	7/19/14	03:53	22° 41.04´ N, 157° 58.74´ W	205
52 / 5	7/19/14	07:45	22° 40.99´ N, 157° 58.74´ W	208
50 / 6	7/22/14	16:02	22° 47.07´ N, 157° 55.65´ W	204
2 / 1	7/23/14	01:59	22° 44.93´ N, 157° 59.55´ W	1001

In addition, continuous acoustic Doppler current profiler (ADCP) and near surface thermosalinograph data were obtained while underway.

The Ship Hi'ialakai was equipped with an RD Instruments Ocean Surveyor 75 kHz ADCP, set to function in broadband and narrowband configurations. Broadband data was unavailable for this cruise. Configurations for each system are shown in Table 2-6. The ADCP used input from a S.G. Brown gyrometer and a Furuno GP 90 GPS receiver to establish the heading and attitude of the ship while an Applanix POSMV4 system archived attitude data for use in post-processing.

A complete description of these operations is available in the WHOTS-11 cruise report (Plueddemann *et al*., 2015).

Table 2-3. Configuration of the Ocean Surveyor 75kHz ADCP on board the Ship Hi'ialakai during the WHOTS-11 cruise.

	OS75NB
Sample interval (s)	900
Number of bins	60
Bin Length (m)	16
Pulse Length (m)	16
Transducer depth (m)	5
Blanking length (m)	24

Near-surface temperature and salinity data during the WHOTS-11 cruise were acquired from the thermosalinograph (TSG) system installed on the NOAA Ship Hi'ialakai. The sensors were sampling water from the continuous seawater system running through the ship, and were comprised of a thermosalinograph model SBE-21 (SN 3233) with (internal) temperature and conductivity sensors located in the ship's wet lab, about 67 m from the intake, and an SBE-38 (SN 227) external temperature sensor located at the water intake. The ship's system running SeaSave (Sea-Bird) recorded data from these sensors every 10 seconds. The Hi'ialaki has a water intake depth of 2 m located at the bow of the ship, next to the starboard side bow thruster. The water pressure at the thermosalinograph is between 5 and 7 psi.

B. WHOTS-12 Cruise: WHOTS-11 Mooring Recovery

The WHOI/UOP Group conducted the mooring turnaround operations during the WHOTS-12 cruise between 9 and 16 July 2015. The WHOTS-11 mooring was recovered, and the WHOTS-12 mooring was deployed at Station 52 on 12 July 2015 02:40 UTC at 22 40.06 'N, 157 56.96'W.

The scientific personnel that participated during the cruise are listed in Table 2-4.

Table 2-4. Scientific personnel on Ship Hi'ialakai during the WHOTS-12 cruise (WHOTS-11 mooring recovery).

Cruise	**Name**	**Title or function**	**Affiliation**
WHOTS-12	Weller, Robert	Chief Scientist	WHOI
	Smith, Jason	Senior Engineering Assistant	WHOI
	Pietro, Ben	Engineering Assistant	WHOI
	Snyder, Jefrey	Marine Electronic's Technician	UH
	Santiago-Mandujano, Fernando	Research Associate	UH
	McCoy, Daniel	Research Associate	UH
	Deppe, R. Walt	Research Associate	UH
	Tabata, Ryan	Marine Research Technician	UH
	Ko, Whitney	Marine Research Technician	UH
	Dumitrascu, Adela	Graduate Student	UH
	Otto, Bill	Met Technician	NOAA

The shipboard oceanographic observations during the cruise were conducted by the UH group. A complete description of these operations is available in the WHOTS-12 cruise report (Santiago-Mandujano *et al*., 2015).

A Sea-Bird CTD system was used to measure T, S, and O_2 profiles during ten CTD casts. The time, location, and maximum CTD pressure for each of the profiles are listed in Table 2-5. Thirteen CTD casts were conducted during the WHOTS-12 cruise, from July 10 – 15. CTD profile data were collected at Station 50 (near the WHOTS-11 buoy), and Station 52 (near the WHOTS-12 buoy). The first cast at Station 50 was 1500 m deep, and three acoustic releases (two for the WHOTS-12 mooring and one backup) were attached to the rosette frame for function testing. Seven CTD yo-yo casts were conducted to obtain profiles for comparison with subsurface instruments on the WHOTS-12 mooring after deployment, and five yo-yo casts were conducted for comparison with the WHOTS-11 mooring before recovery. These were started approximately 200 to 500 m from the buoys with varying drift during each cast. The comparison casts consisted of 5 up-down cycles between 5 and 200 dbar, except during the last two casts at Station 52, which consisted of 10 up-down cycles between 5 and 200 dbar. Water samples were taken from all casts; 4 samples for each of the yo-yo casts, and 6 from the first cast at Station 50.

Table 2-5. CTD stations occupied during the WHOTS-12 cruise (WHOTS-11 mooring recovery).

Station/cast	Date	Time (UTC)	Location *(using NMEA data)*	Maximum pressure (dbar)
50 / 1	7/10/15	19:34	22° 46.13´ N, 157° 53.08´ W	1458
52 / 1	7/12/15	15:58	22° 38.31´ N, 157° 58.54´ W	207
52 / 2	7/12/15	20:00	22° 38.56´ N, 157° 58.43´ W	204
52 / 3	7/13/15	00:06	22° 38.75´ N, 157° 58.91´ W	200
52 / 4	7/13/15	03:59	22° 38.76´ N, 157° 58.72´ W	218
52 / 5	7/13/15	07:58	22° 38.91´ N, 157° 58.80´ W	202
50 / 2	7/13/15	16:00	22° 44.87´ N, 157° 56.09´ W	208
50 / 3	7/13/15	19:55	22° 45.44´ N, 157° 56.02´ W	203
50 / 4	7/14/15	00:04	22° 45.50´ N, 157° 56.01´ W	200
50 / 5	7/14/15	03:56	22° 45.61´ N, 157° 56.04´ W	203
50 / 6	7/14/15	07:53	22° 45.57´ N, 157° 55.85´ W	203
52 / 6	7/15/15	18:02	22° 39.18´ N, 157° 58.86´ W	204
52 / 7	7/15/15	22:57	22° 39.02´ N, 157° 59.17´ W	204

In addition, continuous acoustic Doppler current profiler (ADCP) and near surface thermosalinograph data were obtained while underway.

The Ship *Hi'ialakai* was equipped with an RD Instruments Ocean Surveyor 75 kHz ADCP, set to function in broadband and narrowband configurations. The configuration information is shown in Table 2-3. The ADCP used input from a S.G. Brown gyrometer and a Furuno GP 90 GPS receiver to establish the heading and attitude of the ship while an Applanix POSMV4 system archived attitude data for use in post-processing.

Table 2-6. Configuration of the Ocean Surveyor 75kHz ADCP on board the Ship Hi'ialakai during the WHOTS-11 cruise.

	OS75BB	OS75NB
Sample interval (s)	900	900
Number of bins	80	60
Bin Length (m)	8	16
Pulse Length (m)	8	16
Transducer depth (m)	5	5
Blanking length (m)	16	24

Near-surface temperature and salinity data during the WHOTS-12 cruise were acquired through the use of a thermosalinograph (TSG) system aboard Ship *Hi'ialakai.* The sensors were sampling water from the continuous seawater system running through the ship, and were comprised of one thermosalinograph model SBE-21 and a micro-thermosalinograph model SBE-45, both with (internal) temperature and conductivity sensors located in the ship's wet lab, about 67 m from separate hull intakes; and an SBE-38 external temperature sensor located at the entrance to one of the water intakes. The SBE-21 recorded data every 5 seconds, and the other two instruments recorded data every second. The water intake for the SBE-21 and SBE-38 is located at the bow of the ship, next to the starboard side bow thruster, at a depth of 2 m. The intake for the SBE-45 is located near the middle of the ship, also 2 m deep. The water pressure at the thermosalinograph is between 5 and 7 psi.

Thermosalinograph data exhibited large spikes in conductivity, which often occur due to bubble entrainment from the surface, especially during bad weather or while the ship is pitching in transit. The SBE-45 exhibited a large number of conductivity glitches, indicating a possible problem with the system. The rest of the conductivity data and the calculated salinity for the SBE-21 seem to be of good quality. The records from the external and internal temperature sensors are also of good quality, the internal temperature from the SBE-21 appears to be consistently about 0.2 ℃ lower than the external temperature, probably due to cooling from the ship's A/C system while the water travels from the intake to the thermosalinograph. The temperature from the SBE-45 was about 0.3 ℃ lower than the external temperature early in the cruise, but increased drastically by more than 1 ℃ by the end of the cruise. This micro-thermosalinograph uses a much smaller volume of water as compared to the SBE-21, and it seems to be affected more significantly by the wet-lab's temperature changes than the SBE-21.

3. Description of WHOTS-11 Mooring

The WHOTS-11 mooring, deployed on 17 July 2014 from NOAA's Ship *Hi'ialakai*, was outfitted with two complete sets (L19 and L07) of ASIMET sensors on the buoy and underneath, and subsurface instruments from 7 to 155 m depth (Figure 1-1). The WHOTS-11 recovery on 14-15 July 2015 resulted in about 363 days on station.

The buoy tower also contains a radar reflector, two marine lanterns, and two independent Argos satellite transmission systems that provide continuous monitoring of buoy position. A Xeos Melo Global Positioning System (GPS) receiver, a SBE-39 temperature sensor adapted to measure air temperature and a Vaisala WXT-520 multi-variable (temperature, humidity, pressure, wind and precipitation) were also mounted on the tower. A fourth positioning system (SiS Argos transmitter) was mounted beneath the hull. Several other instruments were mounted on the buoy. A Battelle pCO_2 system, a pumped SBE-16 CTD and a SEAFET pH sensor were mounted to the underside of the buoy. The SHB-16 hosted turbidity and dissolved oxygen sensors. Three downlooking radiometers were mounted on the buoy. One hyperspectral sensor is mounted facing upward near the radiometers as a reference for the incoming spectral irradiance. A chlorophyll fluorometer was also mounted on the buoy hull.

Four internally-logging RBR Solo-T temperature sensors and two SBE-37 MicroCATs were bolted to the underside of the buoy hull measuring sea surface temperature (SST) and salinity. The RBRs measured SST once every 60 sec between 80-98 cm below the surface, and the MicroCATs were at 1.51 m.

Instrumentation provided by UH for the WHOTS-11 mooring included 16 SBE-37 Microcats, an RDI 300 kHz Workhorse ADCP, and an RDI 600 kHz Workhorse ADCP. The Microcats all measured temperature and conductivity, with 6 also measuring pressure. WHOI provided two Vector Measuring Current Meters (VMCMs), and two Seacats (SBE-16) installed near the bottom of the mooring.

Table 3-1a provides a listing of the WHOTS-11 subsurface instrumentation at their nominal depths on the mooring, along with serial numbers, sampling rates and other pertinent information. Table 3-1b includes the four RBR Solo-T's and two MicroCATs from WHOI bolted to the underside of the buoy hull. A cold water spike was induced to the UH MicroCATs before deployment and after recovery by placing an ice pack in contact with their temperature sensor to check for any drift in their internal clock.

The RDI 300 kHz Workhorse Sentinel ADCP, SN 7637, with an additional external battery pack, was deployed at 125 m with transducers facing upwards. The instrument was set to ping at 4-second intervals for 160 seconds every 10 minutes. This burst sampling was designed to minimize aliasing by occasional large ocean swell orbital motions. Bin size was set for 4 m. The total number of ensemble records was 52,860. The first ensemble was at 7/14/2014 00:00:00Z, and the last was at 7/16/2015 01:49:59Z. This instrument also measured temperature.

The RDI 600 kHz Workhorse Sentinel ADCP, SN 13917, with an additional external battery pack, was deployed at 47.5 m with transducers facing upwards. The instrument was set to ping at 2-second intervals for 160 seconds every 10 minutes. This burst sampling was designed to minimize aliasing by occasional large ocean swell orbital motions. Bin size was set for 2 m. The total number of ensemble records was 44,104. The first ensemble was at 7/14/2014 00:00:00Z, and the last was at 5/16/2015 06:30:00Z. This instrument also measured temperature.

A spike was induced in each of the ADCPs before deployment and after recovery (except for the 600 kHz ADCP at 47.5 m which was not pinging on recovery, see below), by gently rubbing by hand for 20 seconds each of their transducers, to check for any drift in their internal clock.

The two VMCMs, SN 62 and 83 were deployed at 10 m and 30 m depth respectively. The instruments were prepared for deployment by the WHOI/UOP group and set to sample at 1-minute intervals. These instruments also measured temperature.

Table 3-1a. WHOTS-11 mooring subsurface instrument deployment information. All times are in UTC.

SN:	Instrument	Depth	Pressure SN	Sample Interval (sec)	Start Logging Data(UTC)		Spike begin (UTC)		Spike end (UTC)		Time in Water (UTC)	
6892	Microcat	7	2651324	75	07/14/14	0:00:00	07/15/14	19:10:00	07/15/14	19:20:00	07/16/14	19:05
62	VMCM	10	N/A	60	07/09/14	19:06:00	N/A	N/A	N/A	N/A	07/16/14	18:42
3382	Microcat	15	N/A	180	07/14/14	0:00:00	07/15/14	19:10:00	07/15/14	19:20:00	07/16/14	18:26
4663	Microcat	25	N/A	180	07/14/14	0:00:00	07/15/14	19:10:00	07/15/14	19:20:00	07/16/14	18:37
83	VMCM	30	N/A	60	07/09/14	19:06:00	N/A	N/A	N/A	N/A	07/16/14	18:16
3633	Microcat	35	N/A	180	07/14/14	0:00:00	07/15/14	19:10:00	07/15/14	19:20:00	07/16/14	18:12
3381	Microcat	40	N/A	180	07/14/14	0:00:00	07/15/14	19:10:00	07/15/14	19:20:00	07/16/14	18:07
3668	Microcat	45	2651319	240	07/14/14	0:00:00	07/15/14	19:10:00	07/15/14	19:20:00	07/16/14	18:01
13917	600 kHz ADCP	47.5	N/A	600	07/14/14	0:00:00	07/15/14	22:29:40	07/15/14	22:30:40	07/16/14	19:30
3619	Microcat	50	N/A	180	07/14/14	0:00:00	07/15/14	19:10:00 PM	07/15/14	19:20:00	07/16/14	19:30
3620	Microcat	55	N/A	180	07/14/14	0:00:00	07/15/14	19:10:00 PM	07/15/14	19:20:00	07/16/14	19:31
3621	Microcat	65	N/A	180	07/14/14	0:00:00	07/15/14	19:10:00 PM	07/15/14	19:20:00	07/16/14	19:33
3632	Microcat	75	N/A	180	07/14/14	0:00:00	07/15/14	19:10:00 PM	07/15/14	19:20:00	07/16/14	19:34
4699	Microcat	85	3418742	240	07/15/14	2:00:00	07/15/14	19:10:00 PM	07/15/14	19:20:00	07/16/14	19:36
3791	Microcat	95	N/A	180	07/14/14	0:00:00	07/15/14	19:10:00 PM	07/15/14	19:20:00	07/16/14	19:37
2769	Microcat	105	2651321	240	07/14/14	0:00:00	07/15/14	19:10:00PM	07/15/14	19:20:00	07/16/14	19:38
4700	Microcat	120	2651322	240	07/14/14	0:00:00	07/15/14	19:10:00	07/15/14	19:20:00	07/16/14	19:45
7637	300 kHz ADCP	125	N/A	600	07/14/14	0:00:00	07/15/14	22:20:10	07/15/14	22:21:10	07/16/14	19:45
3669	Microcat	135	N/A	240	07/14/14	0:00:00	07/15/14	19:10:00	07/15/14	19:20:00	07/16/14	19:47
4701	Microcat	155	2651323	240	07/14/14	0:00:00	07/15/14	19:10:00	07/15/14	19:20:00	07/16/14	19:49
1881	SBE 16-04	36m off bottom	N/A	1800	07/09/14	21:00:00	07/10/14	17:04:00	07/10/14	18:06:00	07/17/14	2:08
1880	SBE 16-04	36m off bottom	N/A	1800	07/09/14	21:00:00	07/10/14	17:04:00	07/10/14	18:06:00	07/17/14	2:08

Table 3-1b. WHOTS-11 RBR Solo-T Temperature, and SBE-37 sensors installed in the buoy. The buoy was deployed on 7/16/2014 at 19:07z.

Instrument	SN	Depth (m)	Sample Interval (sec)
RBR Solo-T	76107	0.80	60
RBR Solo-T	76112	0.98	60
RBR Solo-T	76105	0.80	60
RBR Solo-T	76113	0.80	60
SBE-37	1306	1.51	300
SBE-37	1727	1.51	300

All WHOTS-11 instruments were successfully recovered. One of the MicroCATs installed in the buoy (SN 1727) had no data, since the sensor died before deployment. Recovery information for the underwater instruments is shown in Table 3-2. All UH MicroCATs were in good condition after recovery except for the one at 135 m (SN 3669), which flooded due to a broken bulkhead connector. The data were downloaded on board ship, and all instruments returned full data records, except for SN 3669. Table 3-2 has an initial evaluation of the data quality; more details are in Section 5-A.

Table 3-2. WHOTS-11 MicroCAT Recovery Information. All times stated are in UTC.

Depth (m)	Sea-Bird Serial #	Time out of water	Time of Spike	Time Logging Stopped	Samples Logged	Data Quality
7	SBE 37-6892	7/15/15 01:31:26	7/15/15 05:00:00	7/15/15 18:35:00	422,524	good
15	SBE 37-3382	7/15/15 01:34:26	7/15/15 05:00:00	7/15/15 18:47:00	176,055	good
25	SBE 37-4663	7/15/15 01:38:40	7/15/15 05:00:00	7/15/15 18:54:30	176,058	good
35	SBE 37-3633	7/15/15 01:45:06	7/15/15 05:00:00	7/15/15 18:38:00	176,053	good
40	SBE 37-3381	7/15/15 01:45:43	7/15/15 05:00:00	7/15/15 18:49:00	176,056	good
45	SBE 37-3668	7/15/15 01:50:19	7/15/15 05:00:00	7/15/15 18:40:00	132,040	good
47.5	ADCP 13917	7/14/15 23:47:29	NA	NA	44,104	Good up to 5/16/2015 Not pinging on recovery
50	SBE 37-3619	7/14/15 23:47:27	7/15/15 05:00:00	7/15/15 06:25:30	175,808	good
55	SBE 37-3620	7/14/15 23:46:48	7/15/15 05:00:00	7/15/15 06:04:00	175,800	good
65	SBE 37-3621	7/14/2015 23:44:38	7/15/15 05:00:00	7/15/15 18:42:00	176,054	good
75	SBE 37-3632	7/14/15 23:43:43	7/15/15 05:00:00	7/15/15 06:22:00	175,807	good
85	SBE 37-4699	7/14/15 23:43:10	7/15/15 05:00:00	7/15/15 06:29:00	131,317	good
95	SBE 37-3791	7/14/15 23:42:25	7/15/15 05:00:00	7/15/15 06:00:30	175,800	good
105	SBE 37-2769	7/14/15 23:41:42	7/15/15 05:00:00	7/15/15 05:53:30	131,848	good
120	SBE 37-4700	7/14/15 23:40:23	7/15/15 05:00:00	7/15/15 06:07:30	131,852	good
125	ADCP 7637	7/14/15 23:37:25	7/15/15 22:30:45	7/16/15 02:07:00	52,860	Good, pinging on recovery
135	SBE 37-3669	7/14/15 23:36:25	7/15/15 05:00:00	NA	NA	Instrument flooded Bulkhead connector broken
155	SBE 37-4701	7/14/15 23:34:58	7/15/15 05:00:00	7/15/15 06:19:00	131,855	good
36 mab	SBE-16-04-1880	7/14/15 19:15:23	7/15/15 05:00:00	7/16/15 01:20:00	17,817	good
36 mab	SBE-16-04-1881	7/14/15 19:15:23	7/15/15 05:00:00	7/15/15 23:46:00	17,814	good

The data from the upward-looking 300 kHz ADCP at 125 m were good; the instrument was pinging upon recovery. There appeared to be no obviously questionable data from this ADCP, apart from near-surface artifacts; more details are in Section 5-B.

The data from the upward-looking 600 kHz ADCP at 47.5 m was good until May 16, 2015; the instrument was not pinging upon recovery. There appeared to be no initial questionable data from this ADCP, apart from near-surface artifacts; more details are in Section 5-B.

4. WHOTS-11 and -12 cruise shipboard observations

The hydrographic profile observations made during the WHOTS cruises were obtained with a Sea-Bird CTD package with dual temperature, salinity and oxygen sensors. This CTD was installed on a rosette-sampler with 5-liter Niskin bottles for calibration water samples. In addition, the *Hi'ialakai* came equipped with a thermosalinograph system which provided a continuous depiction of temperature and salinity of the near-surface layer. Horizontal currents over the depth range of 30-1000 m were measured from the shipboard 75 kHz Ocean Surveyor ADCP in narrowband (OS75NB) with a vertical resolution of 16m for the WHOTS-11 and WHOTS-12 cruises. Broadband mode on the ADCP (OS75BB) was unavailable for the WHOTS-11 cruise due to problem with one of the ADCP cables. Broadband mode was available in addition for WHOTS-12 cruise, providing additional current data over the range of 20-650 m with a vertical resolution of 8m.

A. Conductivity, Temperature and Depth (CTD) profiling

Continuous measurements of temperature, conductivity, dissolved oxygen and pressure were made with the UH Sea-Bird SBE-9/11Plus CTD underwater unit #09P43777-0850 (referred to as #0850) during the WHOTS-11 and WHOTS-12 cruises. The CTD was equipped with an internal Digiquartz pressure sensor and pairs of external temperature, conductivity, and oxygen sensors.

Each of the temperature-conductivity sensor pairs used a Sea-Bird TC duct which circulated seawater through independent pump and plumbing installations. The CTD configuration also included two oxygen sensors, installed in the plumbing for each sensor set. In both cruises, the CTD was mounted in a vertical position in the lower part of a rosette sampler, with the sensors' water intakes located at the bottom of the 12-place rosette.

The package was deployed on a conducting cable, which allowed for real-time data acquisition and display. The deployment procedure consisted in lowering the package to 10-15 dbar and waiting until the CTD pumps started operating. The CTD was then raised until the sensors were close to the surface to begin the CTD cast. The time and position of each cast was obtained via a GPS connection to the CTD deck box. Six Niskin bottles were used on the rosette. Four salinity samples were taken on each cast for calibration of the conductivity sensors.

1. Data acquisition and processing.

CTD data were acquired at the instrument's highest sampling rate of 24 samples per second. Digital data were stored on a laptop computer and the analog signal was recorded on VHS video tapes for redundancy. Backups of CTD data were made onto USB storage cards.

The raw CTD data were quality controlled and screened for spikes as described in the WHOTS Data Report 1 (Santiago-Mandujano et al., 2007). Data alignment, averaging, correction and reporting were done as described in Tupas *et al*. (1993). Spikes in the data occur when the CTD samples the disturbed water of its wake. Therefore, samples from the downcast were rejected when the CTD was moving upward or when its acceleration exceeded 0.5 m s^{-2} in magnitude. The data were subsequently averaged into 2-dbar pressure bins after calibrating the CTD conductivity with the bottle salinities.

The data were additionally screened by comparing the T-C sensor pairs. These differences permitted identification of problems with the sensors. The data from only one T-C pair, whichever was deemed most reliable, is reported here. Only data from the downcast are reported, as upcast data are contaminated by rosette wake effects.

Temperature is reported in the ITS-90 scale. Salinity and all derived units were calculated using the UNESCO (1981) routines; salinity is reported in the practical salinity scale (PSS-78). Oxygen is reported in μmol kg^{-1}.

2. CTD sensor calibration and corrections

Pressure

The pressure calibration strategy for CTD pressure transducer SN 101430 used during WHOTS-11 and WHOTS-12 cruises employed a high-quality quartz pressure transducer as a transfer standard. Periodic recalibrations of this lab standard were performed with a primary pressure standard. The only corrections applied to the CTD pressures were a constant offset determined at the time that the CTD first enters the water on each cast. In addition, a span correction determined from bench tests on the sensor against the transfer standard was applied. These procedures and corrections are thoroughly documented in the HOT-2014 and 2015 data reports (Fujieki, et al. 2016 and 2017)

Temperature/Conductivity

Sea-Bird SBE-3-Plus temperature and SBE 4C conductivity transducers were used during WHOTS-11 and -12 cruises. The history and performance of these sensors have been monitored during HOT cruises, and calibrations and drift corrections applied during WHOTS cruises are thoroughly documented in the HOT-2014 and 2015 data reports (Fujieki, et al. 2016 and 2017).

Dissolved Oxygen

Sea-Bird SBE-43 oxygen sensors were used during the WHOTS-11 and -12 cruises. Oxygen data from the WHOTS-11 cruise were calibrated using empirical calibrations coefficients obtained during the HOT-264 cruise conducted on 29 June to 3 July 2014, before the WHOTS-11 cruise, which used the same oxygen sensors (Fujieki, et al., 2016). Similarly, the WHOTS-12 oxygen data were calibrated using calibration coefficients obtained during the HOT-274 cruise conducted on 18 to 22 July 2015, after the WHOTS-12 cruise, which used the same oxygen sensors. Fujieki, et al. (2017) have details on these calibrations. The CTD empirical calibration was conducted using oxygen water samples and the procedure from Owens and Millard (1985). See Tupas et al. (1997) for details on these calibrations procedures.

B. Water sampling and analysis

1. Salinity

Salinity samples were collected by rosette sampler during CTD casts at selected depths during WHOTS-11 and -12, and sub-sampled in 250 ml glass bottles. The top of each bottle and thimble were thoroughly dried before being tightly capped to prevent water from being trapped between the cap or thimble and the bottle's mouth. It has been observed that residual water trapped in this way increases its salinity due to evaporation, and it can leak into the sample when the bottle is opened for measuring. Samples from each cruise were measured after the cruise in the laboratory at the UH using a Guildline Autosal 8400B (SN 70168). IAPSO[1] standard seawater samples were measured to standardize the Autosal, and samples from a large batch of "secondary standard" (substandard) seawater were measured after every 24-48 samples to detect drift in the Autosal. Standard deviations of the secondary standard measurements were less than ± 0.001 for WHOTS-11 and -12 cruises (Table 4-1).

The substandard water was collected by rosette sampler from 1020 m at station ALOHA during HOT cruises and drained into a 50-liter Nalgene plastic carboy. In the laboratory, the water was then thoroughly mixed in a glass carboy for 20 minutes by manually shaking, rolling and tilting the carboy vigorously, after which a 2-inch protective layer of white oil was added on top to deter evaporation. The substandard water was allowed to stand for approximately three days before it was used, and was stored in the same temperature controlled room as the Autosal, protecting it from the light with black plastic bags to inhibit biological growth. Substandard seawater batches #57 and #59 were prepared on 14 February 2014, and 11 December 2014, respectively and used for WHOTS-11 and -12 samples respectively.

Salinity samples from the WHOTS-11 and HOT-264 were run together from July 28th to July 31st 2014. Salinity samples from the WHOTS-12 and HOT-274 were run together from July 27th to July 30th 2015. The substandard statistics in Table 4-1 include the substandard samples measured for the combined WHOTS-11 / HOT-264 samples and the combined WHOTS-12 / HOT-274 samples.

Table 4-1. Precision of salinity measurements of secondary lab standards.

Cruise	Mean Salinity +/- SD	# Samples	Substandard Batch #	IAPSO Batch #
WHOTS-11 / HOT-264	34.4723 ± 0.0006	25	57	P154
WHOTS-12 / HOT-274	34.4674 ± 0.0003	30	59	P156

[1] International Association for Physical Sciences of the Ocean

C. Thermosalinograph data acquisition and processing

1. WHOTS-11 Cruise

Near-surface temperature and salinity data for the WHOTS-11 cruise were acquired through the use of the thermosalinograph system aboard the Ship *Hi'ialakai* (described above). The system included an SBE-21 (SN 3233) thermosalinograph sensor measuring conductivity and internal temperature; and an SBE-38 (SN 0277) external temperature sensor installed near the seawater intake. Temperature data were acquired every 10 seconds for the duration of the cruise. Salinity samples were taken periodically throughout the cruise for calibration from an outlet in the flowthrough system located less than 0.5 m from the SBE-21.

Temperature Calibration

External temperature data from the SBE-38 sensor (last calibrated at Sea-Bird on 04 December 2012) were used as a measure of the seawater temperature. These data were compared to data collected during CTD casts.

Nominal Conductivity Calibration

Data from the SBE-21 conductivity and temperature sensors were used to calculate the intake seawater salinity. These sensors were last calibrated at Sea-Bird on 27 November 2012. All conductivity data from the thermosalinograph were nominally calibrated with coefficients from this calibration. However, all the final salinity data reported here were calibrated against bottle data as explained below.

Data Processing

Daily files containing navigation data recorded every 10 seconds were concatenated with the thermosalinograph data. The thermosalinograph data were then screened for gross errors, with upper and lower bounds of 18 °C and 35 °C for temperature and 3 Siemens m^{-1} and 6 Siemens m^{-1} for conductivity. There were no points outside the valid temperature and conductivity ranges.

A 5-point running median filter was used to detect one- or two-point temperature and conductivity glitches in the thermosalinograph data. Glitches in temperature and conductivity detected by the 5-point median filter were immediately replaced by the median. Threshold values of 0.3 °C for temperature and 0.1 Siemens m^{-1} for conductivity were used for the median filter. After running the filter, there were 346 conductivity points replaced by the median. No temperature points were replaced. A three-point triangular running mean filter was used to smooth the temperature and conductivity data after passing the glitch detection.

The thermosalinograph aboard the NOAA Ship *Hi'ialakai* was set to record data every 10 seconds, but occasionally, due to an error in the acquisition software rounding routine, a record can be written at a longer interval. However, there were no timing errors observed during WHOTS-11.

Data were visually scanned to flag spikes/glitches. These are usually caused by the introduction of bubbles into the flow through system during transit or during rough conditions. The *Hi'ialakai's* flow through system is not equipped with a de-bubbler. Of the 67,158 conductivity data points, 6,081 were flagged BAD as spikes.

Bottle Salinity and CTD Salinity Comparisons

The thermosalinograph salinity was calibrated by comparing it to bottle salinity samples drawn from a water intake next to the thermosalinograph every 8 hours throughout the cruise. Of the 24 bottles sampled, 2 were considered outliers, while the final 3 bottles were sampled after the system stopped collecting conductivity data. The remaining 21 salinity samples were analyzed as described in Section 0. The comparison was made in conductivity in order to eliminate the effects of temperature. The conductivity of the bottle sample was computed using the salinity of the bottle, thermosalinograph temperature and a pressure of 3.44 dbar, which includes the pressure of the flow through system's pump.

Salinity samples were drawn from the flow through system, located less than 0.5 m from the SBE-21 and consequently there should be virtually no delay between when the water passes through the thermosalinograph and it being sampled. A 90 second average centered on the sample draw time was chosen for processing purposes.

The CTD salinity data at 2 dbar from the 12 casts conducted during the cruise were used to compare with the thermosalinograph conductivity. Using the thermosalinograph temperature data and a pressure of 3.44 dbar the CTD conductivity was calculated for the 12 casts conducted while the thermosalinograph was running. Two CTD casts (station 1 cast 1 and station 50 cast 6) were excluded from the processing as outliers. The SBE-21 conductivity sensor had a mean offset of 0.0043 Sm^{-1} with respect to the CTD data.

A cubic spline was fit to the time series of the differences between the bottle and thermosalinograph conductivity and a correction was obtained for the thermosalinograph conductivities. Salinity was calculated using these corrected conductivities, the thermosalinograph temperatures, and 6-dbar pressure. After correction, the mean difference between the bottle and thermosalinograph salinities was 0.000001 with a standard deviation of 0.0142. The mean CTD - thermosalinograph difference was -0.00221 with a standard deviation of 0.0105.

CTD Temperature Comparisons

There were 12 CTD casts conducted during the WHOTS-11 cruise. The 2 dbar CTD temperature data were used to compare with the thermosalinograph external temperature. Two

CTD casts (station 1 cast 1 and station 50 cast 6) were excluded from the processing as outliers. The mean difference between the external sensor and the CTD was -0.17127 ± 0.03063 °C, while the mean difference between the internal sensor and the CTD was -0.22439 ± 0.02666 °C.

2. WHOTS-12 Cruise

Near-surface temperature and salinity data during the WHOTS-12 cruise were acquired from the thermosalinograph (TSG) system installed on the NOAA Ship *Hi'ialakai*. The sensors, located in the ship's wet lab ~67 meters astern of the seawater intake, were sampling water from separate continuous seawater systems running through the ship, and were comprised of one TSG model SBE-21 (SN 3155) and a micro-thermosalinograph model SBE-45 (SN 4537642-0121), both with (internal) temperature and conductivity sensors, and an SBE-38 (SN 215) external temperature sensor located at the seawater intake. The SBE-21 recorded data every five seconds and the other two instruments recorded data every second. The seawater intakes aboard the *Hi'ialakai* are 2 m below the water surface at the bow of the ship, next to the starboard bow thruster, and by the middle of the ship respectively. Water pressure at the TSG is between 5 and 7 psi. Only data from the SBE-21 and the SBE-38 are reported here because the SBE-45 had many conductivity glitches, indicating some problems with the instrument.

Temperature Calibration

External temperature data from the SBE-38 sensor (last calibrated at Sea-Bird on 04 December 2012) were used as a measure of the seawater temperature. These data were compared to the data collected during CTD casts.

Nominal Conductivity Calibration

Data from the SBE-21 conductivity and temperature sensors were used to calculate the intake seawater salinity. These sensors were last calibrated at Sea-Bird on 18 November 2011. All conductivity data from the thermosalinograph were nominally calibrated with coefficients from this calibration. However, all the final salinity data reported here were calibrated against bottle data as explained below.

Data Processing

Daily files containing navigation data recorded every second were concatenated with the thermosalinograph data. The thermosalinograph data were then screened for gross errors, with upper and lower bounds of 18 °C and 35 °C for temperature and 3 Siemens m^{-1} and 6 Siemens m^{-1} for conductivity. There were no points outside the valid temperature range and no points outside the valid conductivity range.

A 5-point running median filter was used to detect one- or two-point temperature and conductivity glitches in the thermosalinograph data. Glitches in temperature and conductivity detected by the 5-point median filter were immediately replaced by the median. Threshold values of 0.3 °C for temperature and 0.1 Siemens m^{-1} for conductivity were used for the median filter. After running the filter, there were 18 conductivity points replaced by the median. No temperature points were replaced. A 3-point triangular running mean filter was used to smooth the temperature and conductivity data after passing the glitch detection.

The thermosalinograph aboard the Ship *Hi'ialakai* was set to record data every second, but occasionally, due to an error in the acquisition software rounding routine, a record is written at a longer interval. Only 36 timing errors occurred during this cruise; all of these were between 30 and 32 seconds.

Data were visually scanned to flag glitches probably caused by contamination due to the introduction of bubbles to the flow through system during transits or rough conditions. Of a total of 19,699 data points, 660 conductivity data points were flagged as bad. The *Hi'ialakai's* flow through system was not equipped with a de-bubbler.

Bottle Salinity and CTD Salinity Comparisons

The thermosalinograph salinity was calibrated by comparing it to bottle salinity samples drawn from a water intake next to the thermosalinograph every 8 hours throughout the cruise. Of the 21 bottles sampled, none were considered outliers. Samples were analyzed as described in Section 0. The comparison was made in conductivity in order to eliminate the effects of temperature. Conductivity of each bottle sample was computed using the salinity of the bottle, thermosalinograph temperature and a pressure of 3.44 dbar, which includes the pressure of the flow through system's pump.

Salinity samples were drawn from the flow through system, located less than 0.5 m from the SBE-21 and consequently there should be virtually no delay between when the water passes through the thermosalinograph and it being sampled. A 90 second average centered on the sample draw time was chosen for processing purposes.

The CTD salinity data at 2 dbar from the 13 casts conducted during the cruise was used to compare with the thermosalinograph conductivity. Using the thermosalinograph temperature data and a pressure of 3.44 dbar, the CTD conductivity was calculated for the 13 casts conducted while the thermosalinograph was running. Three CTD casts were excluded from processing as they were obvious outliers. The SBE-21 conductivity sensor had a mean offset of 0.0024 Sm^{-1} with respect to the CTD data.

A cubic spline was fit to the time series of the differences between the bottle and TSG conductivity and a correction was obtained for the TSG conductivities. Salinity was calculated using these corrected conductivities, the thermosalinograph temperatures, and 3.44 dbar pressure. After correction, the mean difference between the bottle and thermosalinograph salinities was 0.000001 psu with a standard deviation of 0.0029 psu. The mean CTD - thermosalinograph difference was -0.0020 with a standard deviation of 0.0044.

CTD Temperature Comparisons

There were 13 CTD casts conducted during the WHOTS-12 cruise. The 2 dbar CTD temperature data were used to compare with the thermosalinograph internal temperature. Three CTD casts were excluded from processing as obvious outliers. The mean difference between the internal sensor and the CTD was -0.2796 °C, with a standard deviation of ±0.0338 °C.

D. Shipboard ADCP

1. WHOTS-11 Cruise

Currents measured by the Ship Hi'ialakai's Ocean Surveyor 75 kHz narrowband ADCP were processed using the CODAS ADCP processing suite. Horizontal velocity data, latitude and longitude were processed with 15 minute ensemble averages and 10 m depth resolution. The times of the datasets from the OS75 are shown in Table 4-2. Broadband mode for the ADCP was not available during the WHOTS-11 cruise due to a cable problem.

Table 4-8. ADCP record times (UTC) for the Narrow Band 75 kHz ADCP during the WHOTS-11 cruise.

WHOTS-11	**OS75nb**
File beginning time	11-Jul-2014 21:22:02
File ending time	23-Jul-2014 18:03:49

2. WHOTS-12 Cruise

Currents were measured for the duration of the cruise over the depth range of 30-1000 m with the Hi'ialakai's 75 kHz RDI Ocean Surveyor (OS75) ADCP working in narrowband mode with a vertical resolution of 16 m, and in broadband mode with vertical resolution of 8 m. The system yielded good data. File start and end times are listed in Table 4-2 below. Gaps in the data occurred when the system was shut down during communications with the acoustic releases used for the moorings. A gap on July 10 from about 9:00 to 19:00 UTC was during triangulation of the WHOTS-12 anchor after deployment. The times of the datasets from the OS75 are shown in Table 4-2.

Table 4-2. ADCP record times (UTC) for the 75 kHz ADCP during the WHOTS-12 cruise.

WHOTS-12	**OS75nb**	**OS75bb**

File beginning time	09-Jul-2015 18:02:33	09-Jul-2015 18:02:33
File ending time	16-Jul-2015 18:43:51	16-Jul-2015 18:41:21

5. Moored Instrument Observations

A. MicroCAT/SeaCAT data processing procedures

Each moored MicroCAT and SeaCAT temperature, conductivity and pressure (when installed) was calibrated at Sea-Bird prior to their deployment and after their recovery on the dates shown in Table 5-1. The internally-recorded data from each instrument were downloaded on board the ship after the mooring recovery, and the nominally-calibrated data were plotted for a visual assessment of the data quality. The data processing included checking the internal clock data against external event times, pressure sensor drift correction, temperature sensor stability, and conductivity calibration against CTD data from casts conducted near the mooring during HOT and WHOTS cruises. The detailed processing procedures are described in this section.

Table 5-1. WHOTS-11 MicroCAT/SeaCAT temperature sensor calibration dates, and sensor drift.

Nominal deployment depth (m)	Sea-Bird Serial number	Pre-deployment calibration	Post-recovery calibration	Temperature sensor drift (mili^{o}C/year)
7	SBE37SM-6892	3-Apr-2009	29-Sep-2015	-0.02
15	SBE37SM-3382	17-Aug-2013	29-Sep-2015	0.38
25	SBE37SM-4663	9- Aug-2013	29-Sep-2015	-0.01
35	SBE37SM-3633	17- Aug-2013	25-Sep-2015	-0.07
40	SBE37SM-3381	29- Aug-2013	1-Oct-2015	0.14
45	SBE37SM-3668	17- Aug-2013	25-Sep-2015	-0.44
50	SBE37SM-3619	9- Aug-2013	25-Sep-2015	-0.18
55	SBE37SM-3620	3- Aug-2013	29-Sep-2015	-0.04
65	SBE37SM-3621	8- Aug-2013	19-Sep-2015	0.20
75	SBE37SM-3632	17- Aug-2013	21-Nov-2015	-0.21
85	SBE37SM-4699	29- Aug -2013	2-Oct-2015	-0.16
95	SBE37SM-3791	17- Aug -2013	30-Sep-2015	-0.28
105	SBE37SM-2769	9- Aug-2013	29-Sep-2015	0.19
120	SBE37SM-4700	17- Aug-2013	2-Oct -2015	-0.27
135	SBE37SM-3669	29- Aug-2013	Instrument flooded	NA
155	SBE37SM-4701	28- Aug-2013	2-Oct -2015	-0.04
4671	SBE16-1880	16-Oct-2013	2-Dec-2015	0.03
4671	SBE16-1881	16-Oct-2013	8-Dec-2015	0.01

1. Internal Clock Check and Missing Samples

Before the WHOTS-11 mooring deployment and after its recovery (before the data logging was stopped), the MicroCATs temperature sensors were placed in contact with an ice pack to create a spike in the data, to check for any problems with their internal clocks, and for possible missing samples (Table 3-2). The cold spike was detected by a sudden decrease in temperature. For all the instruments, the clock time of this event matched correctly the time of the spike (within the sampling interval of each instrument). No missing samples were detected for any of the instruments.

2. Pressure Drift Correction and Pressure Variability

Some of the MicroCATs used in the moorings were outfitted with pressure sensors (Table 3-1). Biases were detected in the pressure sensors by comparing the on-deck pressure readings (which should be zero for standard atmospheric pressure at sea level of 1029 mbar) before deployment and after recovery. Table 5-2 shows the magnitude of the bias for each of the sensors before and after deployment. To correct for this offset, a linear fit between the initial and final on-deck pressure offset as a function of time was obtained, and subtracted from each sensor. Figure 5-1 shows the linearly corrected pressures measured by the MicroCATs during the WHOTS-11 deployment. For all the sensors, the mean difference from the nominal instrument pressure (based on the deployed depth) was less than 1.1 dbar. The standard deviation of the pressure for the duration of the record was less than 1 dbar for all sensors, with the deeper sensors showing a slightly larger standard deviation. The range of variability for all sensors was about ± 3 dbar.

The causes of pressure variability can be several, including density variations in the water column above the instrument; horizontal dynamic pressure (not only due to the currents, but also due to the motion of the mooring); mooring position, etc. (see WHOTS Data Report 1, Santiago-Mandujano et al., 2007).

Table 5-2. Pressure bias of MicroCATs with pressure sensor.

Deployment	Depth (m)	Sea-Bird Serial #	Bias before deployment (dbar)	Bias after recovery (dbar)
WHOTS-11	7	37SM31486-6892	-0.04	-0.15
WHOTS-11	45	37SM31486-3668	0.07	-0.04
WHOTS-11	85	37SM31486-4699	0.60	0.55
WHOTS-11	105	37SM31486-2769	0.05	-0.02
WHOTS-11	120	37SM31486-4700	0.09	-0.45
WHOTS-11	135	37SM31486-3669	Instrument flooded	NA
WHOTS-11	155	37SM31486-4701	0.00	-0.07

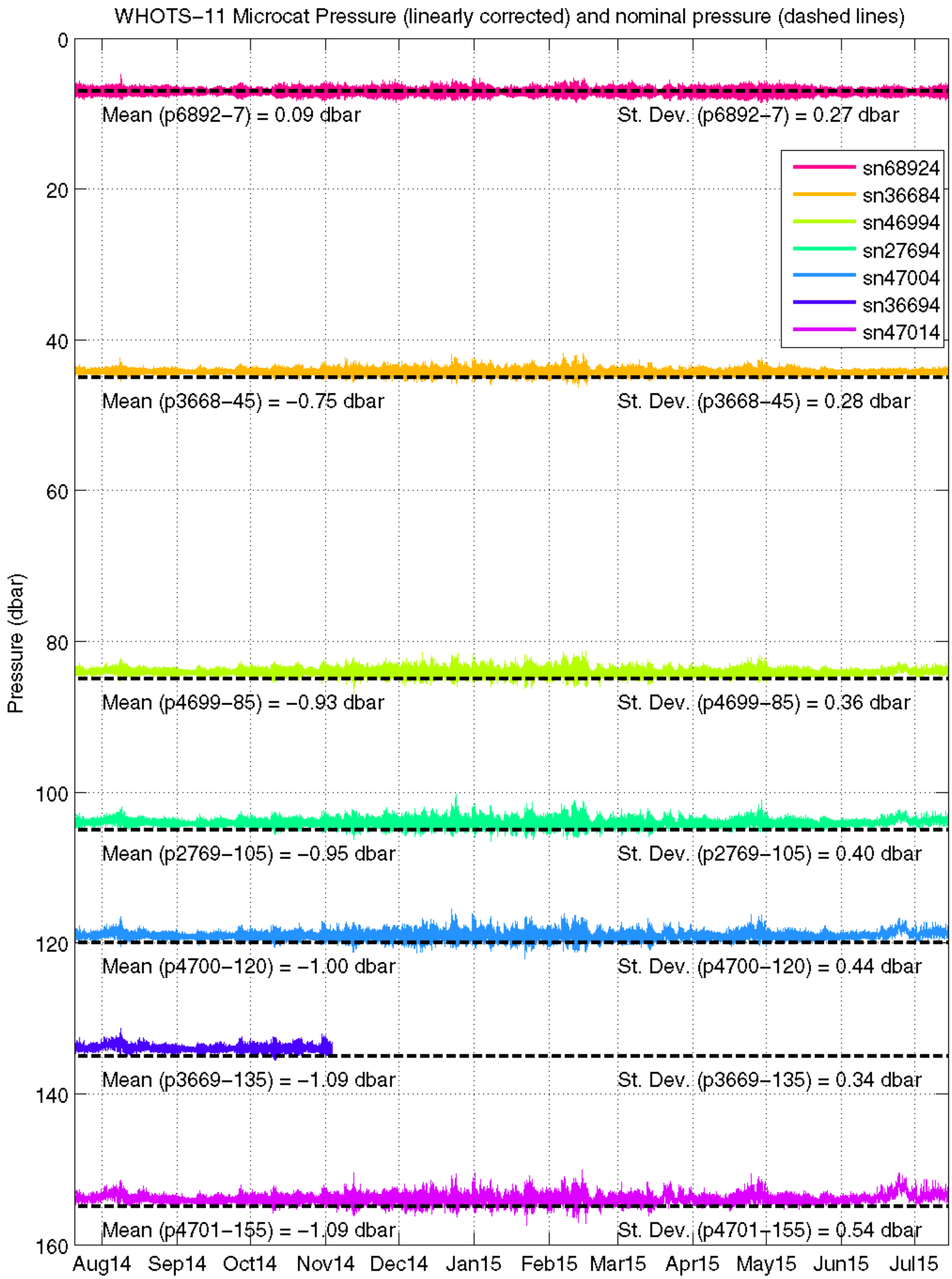

Figure 5-1. Linearly corrected pressures from MicroCATs during WHOTS-11 deployment. The horizontal dashed line is the sensor's nominal pressure, based on deployed depth.

3. Temperature Sensor Stability

The MicroCAT and SeaCAT temperature sensors were calibrated at Sea-Bird before and after each deployment, and their annual drift evaluations are shown in Table 5-1. These values turned out to be insignificant (not higher than 1 milli °C) for all sensors. Comparisons between the MicroCAT and CTD data from casts conducted near the mooring during HOT cruises confirmed that the temperature drift of the rest of the moored instruments was insignificant. The two SeaCATs (SN 1880 and SN 1881) deployed near the bottom were drift corrected. Figure 5-7 (upper panel) shows the temperature differences between both instruments before and after the correction. After the correction the temperature differences were in the -1.0 to 1.0 milli°C range.

Temperature comparisons between one of the WHOTS-11 near-surface MicroCATs (SN 1306, the other MicroCAT SN 1727 malfunctioned during the whole deployment) and three of the four RBR surface temperature sensors in the buoy hull (Table 3-1) are shown in Figure 5-2. Three of the RBR instruments (#76107, #76112 and #76113) returned full records; instrument #76105 was damaged during recovery and was not able to communicate. Sensor #76107 shows a bias of nearly 0.1 °C as compared to the Microcat measurements.

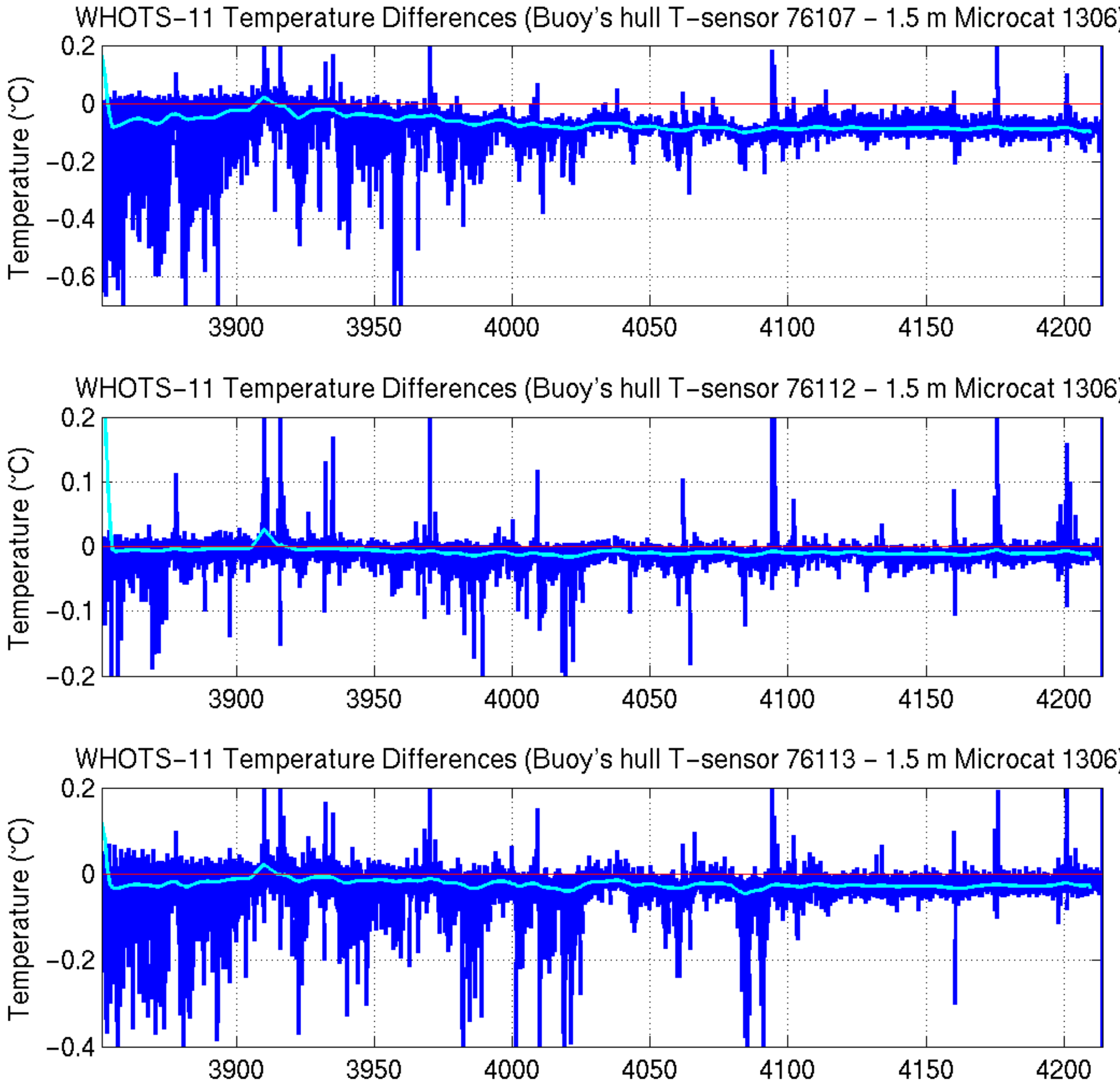

Figure 5-2. Temperature difference between MicroCAT SN 1306 at 1.5 m, and near-surface temperature sensors SN 76107 (upper panel), 76112 (second panel), and 76113 (bottom panel), during WHOTS-11 deployment. The light blue line is a 24-hour running mean of the differences.

In addition to the temperature sensors in the Sea-Bird and the RBR instruments, there were additional temperature sensors in the VMCMs (at 10 and 30 m), and in the ADCPs (at 47.5 m and 125 m). In order to evaluate the quality of the temperatures from these sensors, comparisons with the temperatures from adjacent MicroCATs were conducted.

Comparisons with VMCM and ADCP temperature sensors

The upper panel of

Figure 5-3 shows the temperature differences between the 10-m VMCM and the temperatures from adjacent MicroCATs at 7 and 15-m during WHOTS-11. For comparison, the differences between the MicroCATs temperatures are also shown. These plots indicate that there was no offset in the 10-m VMCM with respect to the adjacent MicroCATs (top and middle plots).

The upper panel of

Figure 5-3 shows the difference between the 30-m MicroCAT and the 25-m VMCM temperatures during WHOTS-11, after adding a 0.031 °C offset correction to the VMCM. The offset was the mean difference between the uncorrected VMCM and the 25-m MicroCAT data. The lower panel of the figure shows the differences between MicroCAT temperatures at 25 and 35 m. The temperature fluctuations in the differences between the 25 and 35-m MicroCATs seem to be around zero.

Temperature differences between the 47.5-m ADCP and the temperatures from adjacent MicroCATs at 45 and 50-m during WHOTS-11 are shown in Figure 5-5. For comparison, the differences between the MicroCATs temperatures are also shown. These plots indicate that there was no offset in the 47.5-m ADCP with respect to the adjacent MicroCATs (top and middle plots). The ADCP malfunctioned and stopped recording data after 27 May 2015.

Temperature differences between the 125-m ADCP and the temperatures from adjacent MicroCATs at 120 and 135-m during WHOTS-11 are shown in Figure 5-6. The MicroCAT at 135 m flooded and stopped recording data after 3 November 2014. For comparison, the differences between the MicroCATs temperatures are also shown. It is difficult to assess the quality of the ADCP temperature from these comparisons, as these sensors were located at the top of the thermocline, where we expect to find large temperature differences between adjacent sensors. However, an indication of the quality of the ADCP temperatures is given in the upper panel plot, which shows temperatures fluctuating closely around zero.

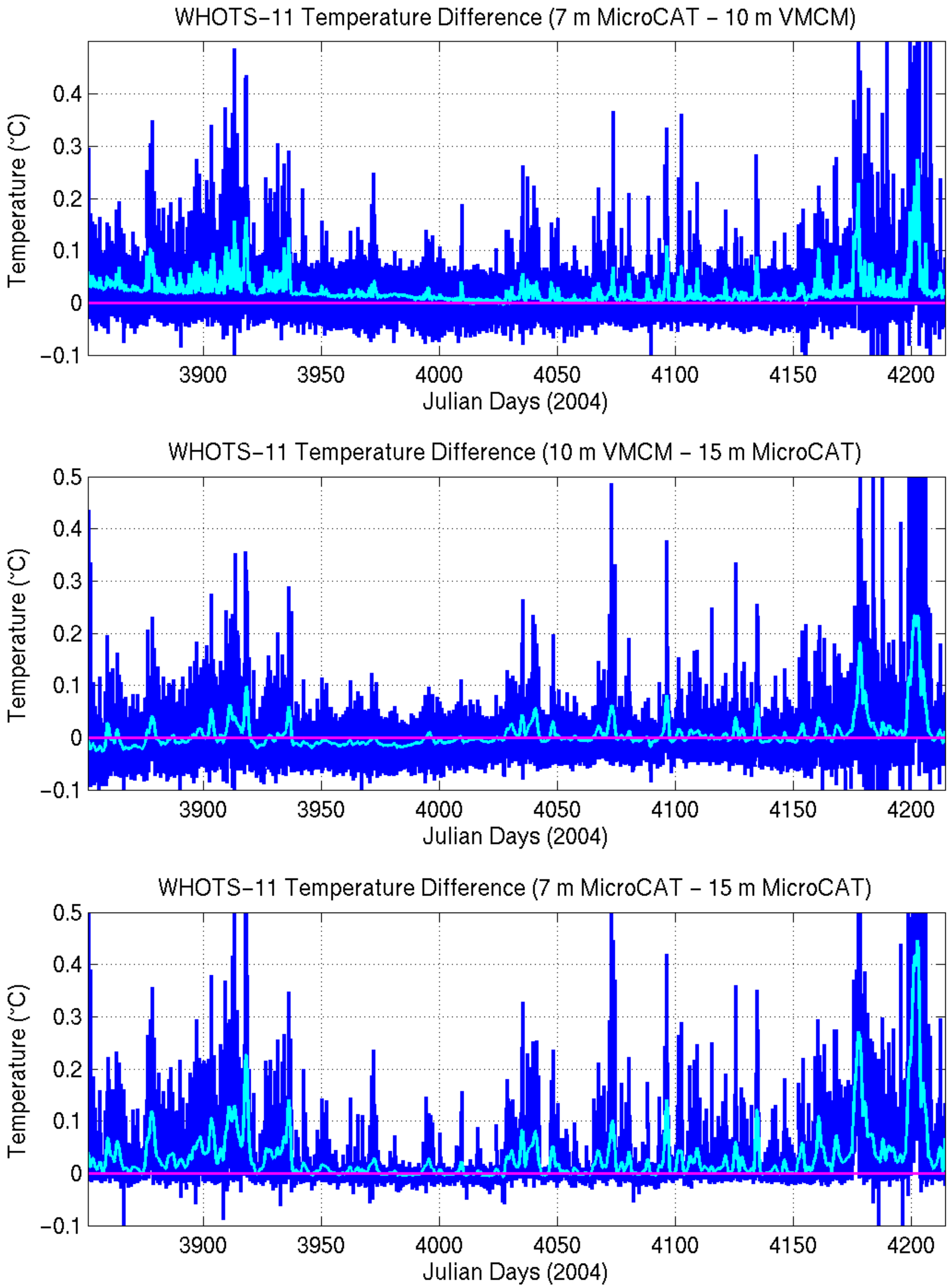

Figure 5-3. Temperature difference between the 7-m MicroCAT and the 10-m VMCM (upper pane)l; between the 15-m MicroCAT and the 10-m VMCM (middle panel); and between the 7-m and the 15-m MicroCATs (lower panel) during the WHOTS-11 deployment. The light blue line is a 24-hour running mean of the differences.

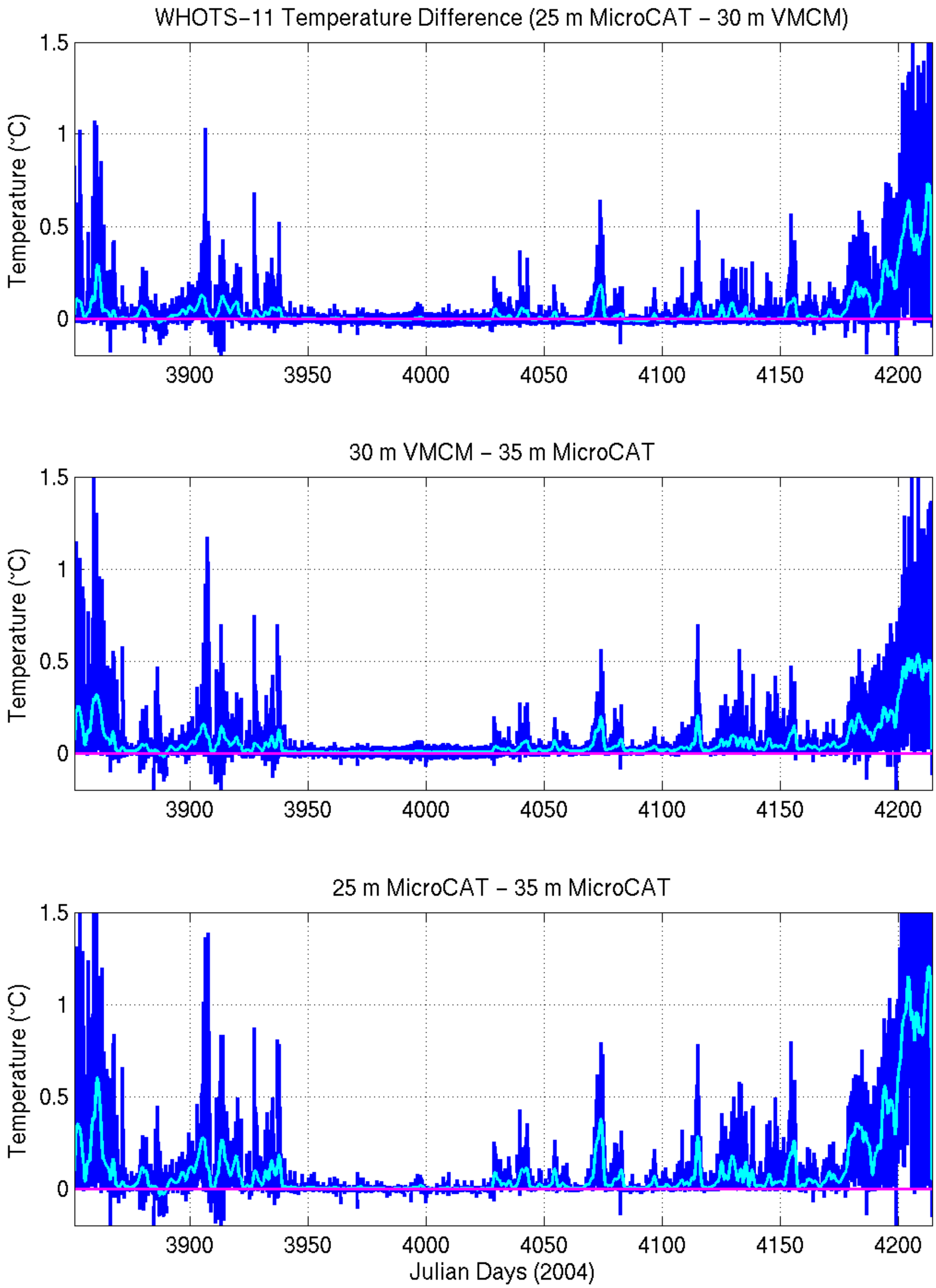

Figure 5-4. Temperature difference between the 25-m MicroCAT and the 30-m VMCM (upper panel); between the 35-m MicroCAT and the 30-m VMCM (middle panel); and between the 25-m and the 35-m MicroCATs (lower panel) during the WHOTS-11 deployment. The light blue line is a 24-hour running mean of the differences.

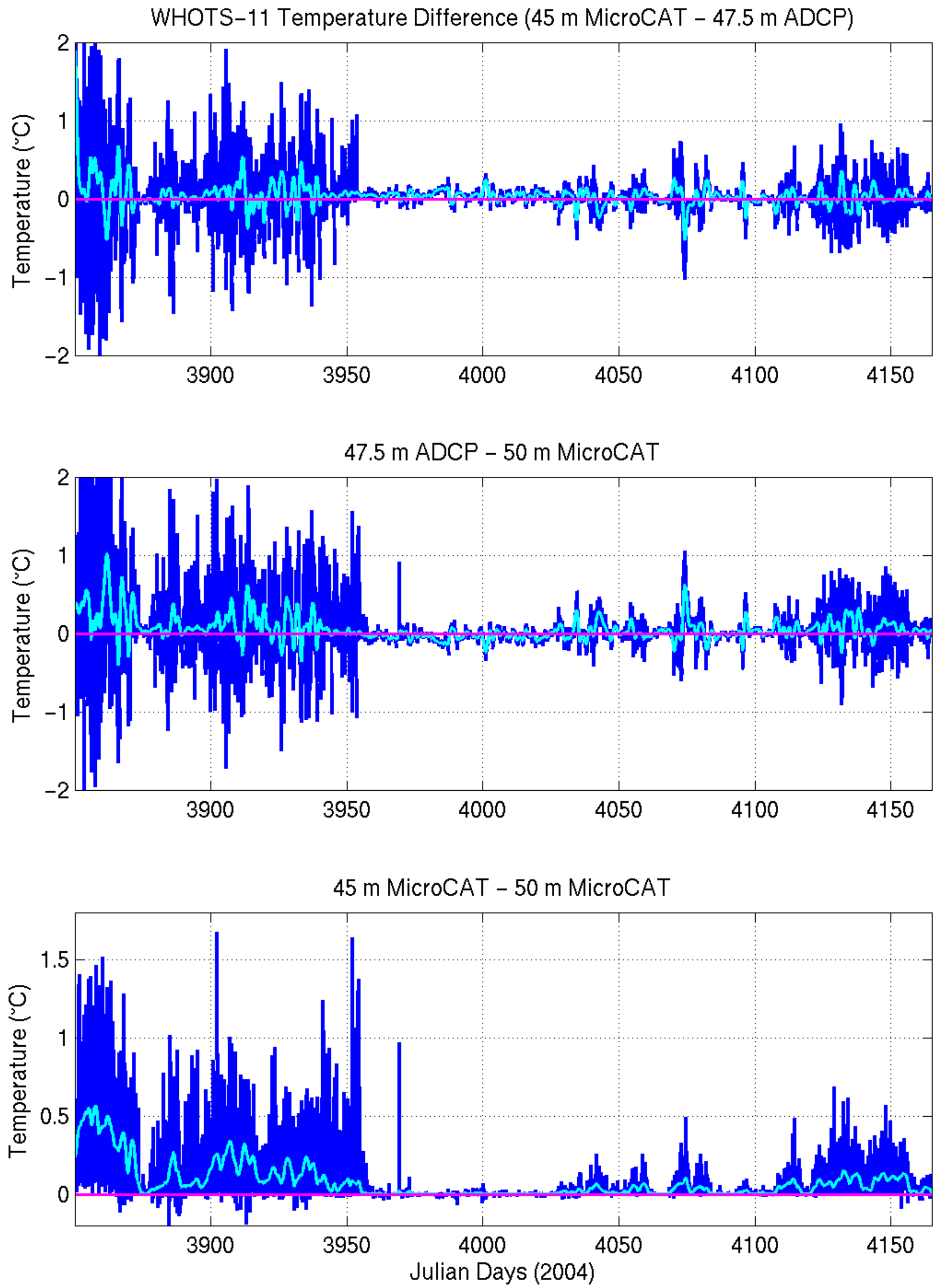

Figure 5-5. Temperature difference between the 45-m MicroCAT and the 47.5-m ADCP (upper panel); between the 50-m MicroCAT and the 47.5-m ADCP (middle panel); and between the 45-m and the 50-m MicroCATs (lower panel) during the WHOTS-11 deployment. The light blue line is a 24-hour running mean of the differences.

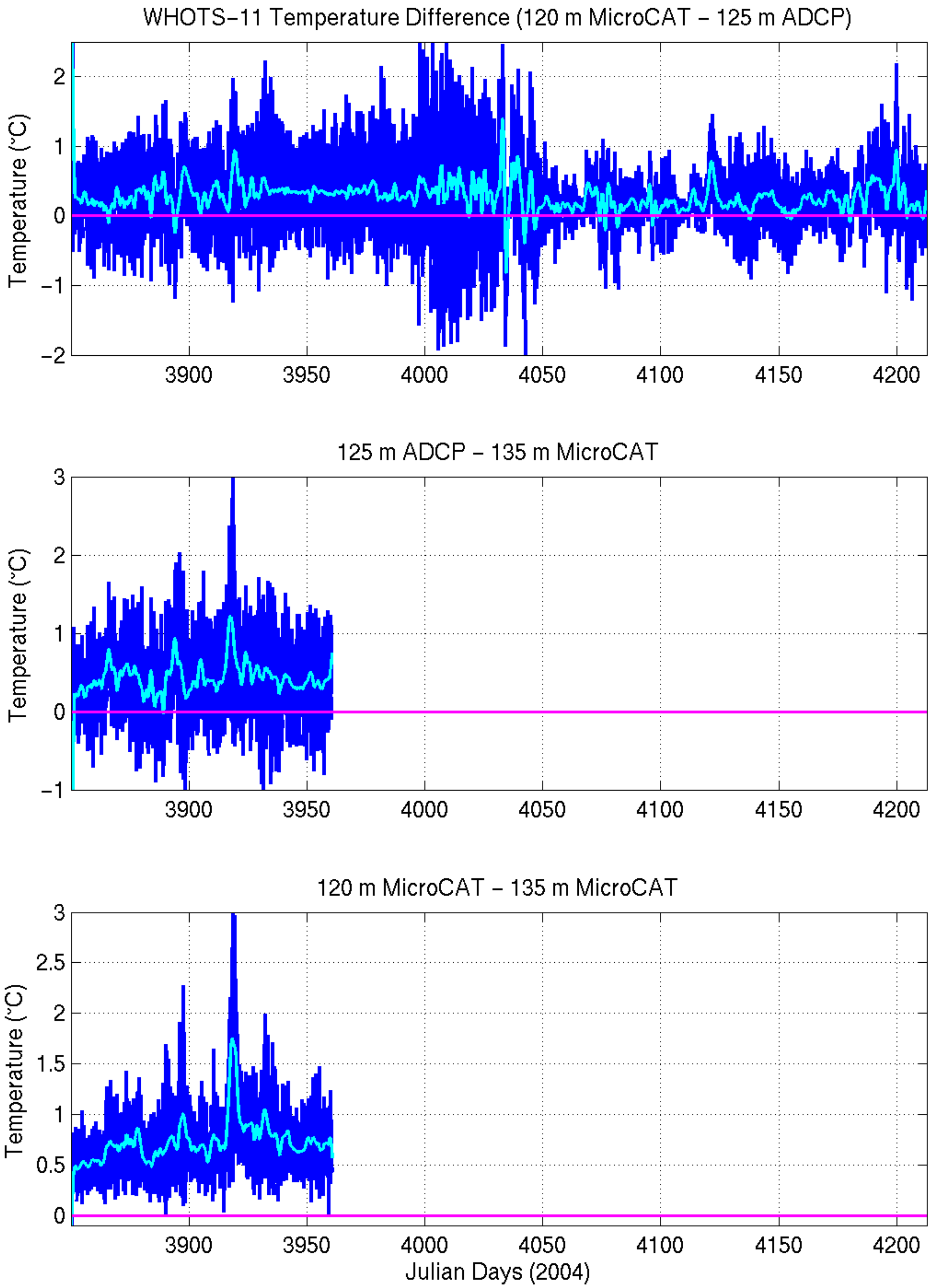

Figure 5-6. Temperature difference between the 120-m MicroCAT and the 125-m ADCP (upper panel); between the 135-m MicroCAT and the 125-m ADCP (middle panel); and between the 120-m and the 135-m MicroCATs (lower panel) during the WHOTS-11 deployment. The light blue line is a 24-hour running mean of the differences.

4. Conductivity Calibration

The results of the Sea-Bird post-recovery conductivity calibrations indicated that some of the MicroCAT and SeaCAT conductivity sensors experienced relatively large offsets from their pre-deployment calibration. These were qualitatively confirmed by comparing the mooring data against CTD data from casts conducted between 200 m and 5 km from the mooring during HOT cruises. The causes of the conductivity offsets are not clear, and there may have been multiple causes (see Freitag et. al, (1999) for a similar experience with conductivity cells during COARE). For some instruments the offset was negative, caused perhaps by biofouling of the conductivity cell while for others the offset was positive, caused possibly by scouring of the inside of the conductivity cell (possible by the continuous up and down motion of the instrument in an abundant field of diatoms). A visual inspection of the instruments after recovery did not show any obvious signs of biofouling, and there were no cell scourings reported in the post-recovery inspections at Sea-Bird.

Corrections of the MicroCATs conductivity data were conducted by comparing them against CTD data from profiles and yo-yo casts conducted near the mooring during HOT cruises, and during deployment/recovery cruises. Casts conducted between 200 and 1000 m from the mooring were given extra weight in the correction, as compared to those conducted between 1 and 5 km away. Casts more than 5 km away from the mooring were not used. Given that the CTD casts are conducted at least 200 m from the mooring, the alignment between CTD and MicroCAT data was done in density rather than in depth. For cases in which the alignment in density was not possible due to large conductivity offsets (causing unrealistic mooring density values), alignment in temperature space was done. A cubic least-squares fit (LSF) to the CTD-MicroCAT/SeaCAT differences against time was applied as a first approximation, and the corresponding correction was applied.

Some of the sensors had large offsets and/or obvious variability that could not be explained by a cubic LSF (see below). For these sensors, a stepwise correction was applied matching the data to the available CTD cast data, and then using the differences between consecutive sensors to determine when the sensor started to drift. For instance, during periods of weak stratification the conductivity difference between neighboring sensors A, B, and C could reach near-zero values, in particular for instruments near the surface, which are the ones most prone to suffer conductivity offsets. A sudden conductivity offset observed during this period between sensors A and B, but not between sensors A and C could indicate the beginning of an offset for sensor B.

Given that the deepest instruments on the mooring are less likely to be affected by biofouling and consequent sudden conductivity drift, the deep instruments served as a good reference to find any possible malfunction in the shallower ones. Therefore the deepest instruments' conductivity was corrected first, and the correction was continued sequentially upwards toward the shallower ones.

As a quality control to the conductivity corrections, the buoyancy frequency between neighboring instruments was calculated using finite differences. Over- or under-corrected conductivities yielded instabilities in the water column (negative buoyancy frequency) that were easy to detect and were obviously not real when lasting for several days. Based on this, the conductivity correction of the corresponding sensors was revised.

Corrections of the deep SeaCATs conductivity data were conducted following similar procedures as for the shallow instruments by comparing them against CTD data from near-bottom profiles conducted during HOT cruises.

Another characteristic of the offsets in the conductivity sensors is that their development is not always linear in time, and their behavior can be highly variable (see WHOTS Data Report 1, Santiago-Mandujano et al., 2007).

A correction was also applied to the deep SeaCATs conductivities. Both instruments were deployed at the same depth (4671 m). After correction, the salinity differences between both instruments were in the +-0.003 g/kg range (Figure 5-7).

The corrections applied to each of the conductivity sensors during WHOTS-11 can be seen in Figures 5-8. Most of the instruments had a drift of less than 0.01 Siemens/m for the duration of the deployment, which was corrected with a linear or cubic least-squares fit. Most of the instruments deployed above 65 m showed a sharp negative drift starting about two months before the end of the deployment, apparently due to the expiration of the anti-foulant.

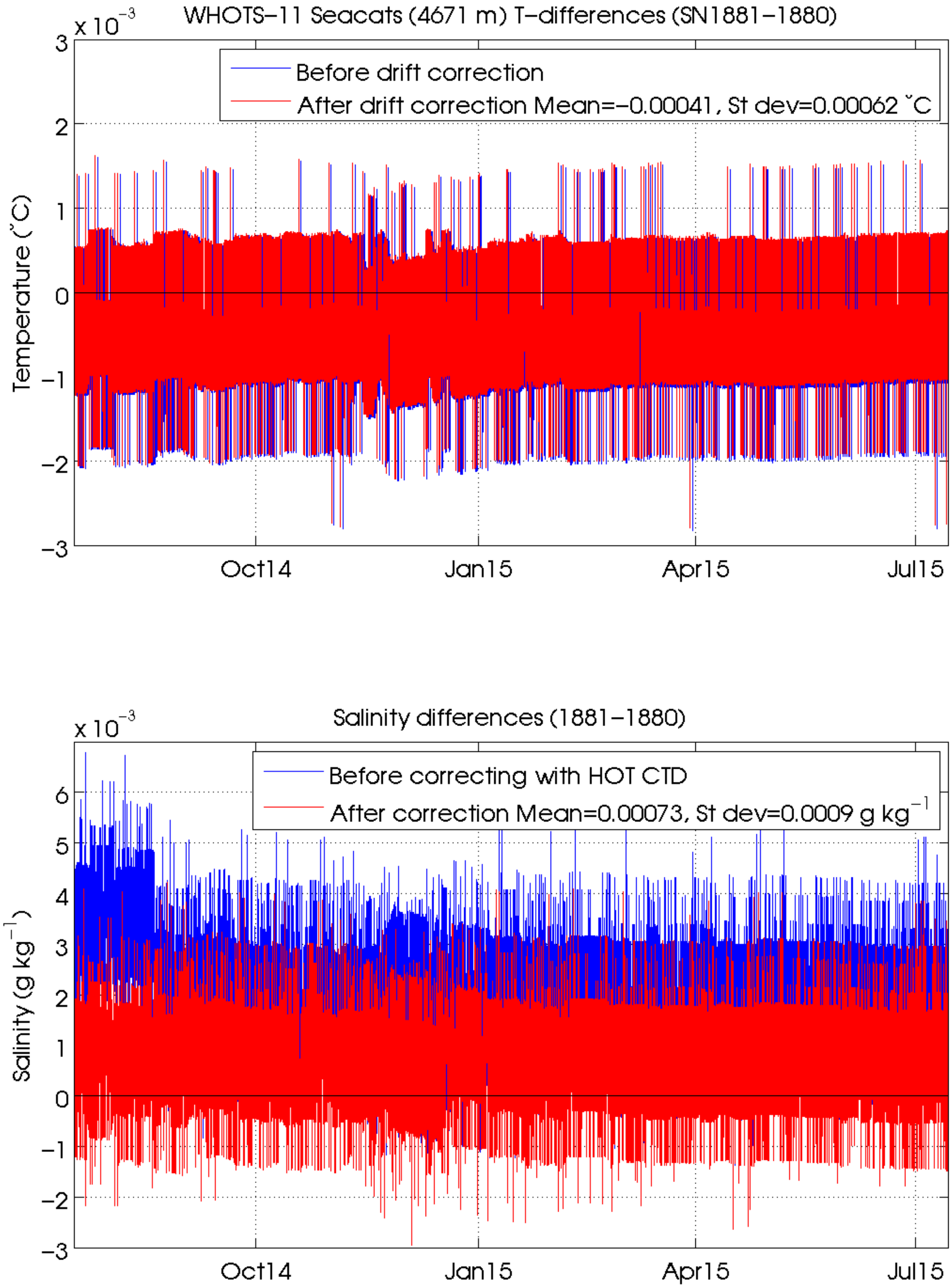

Figure 5-7. Temperature differences (top panel), and salinity differences (bottom panel) between SeaCATs #1881 and #1880 during WHOTS-11. The blue (red) lines are the differences before (after) correcting the data following procedures indicated in the this report's section.

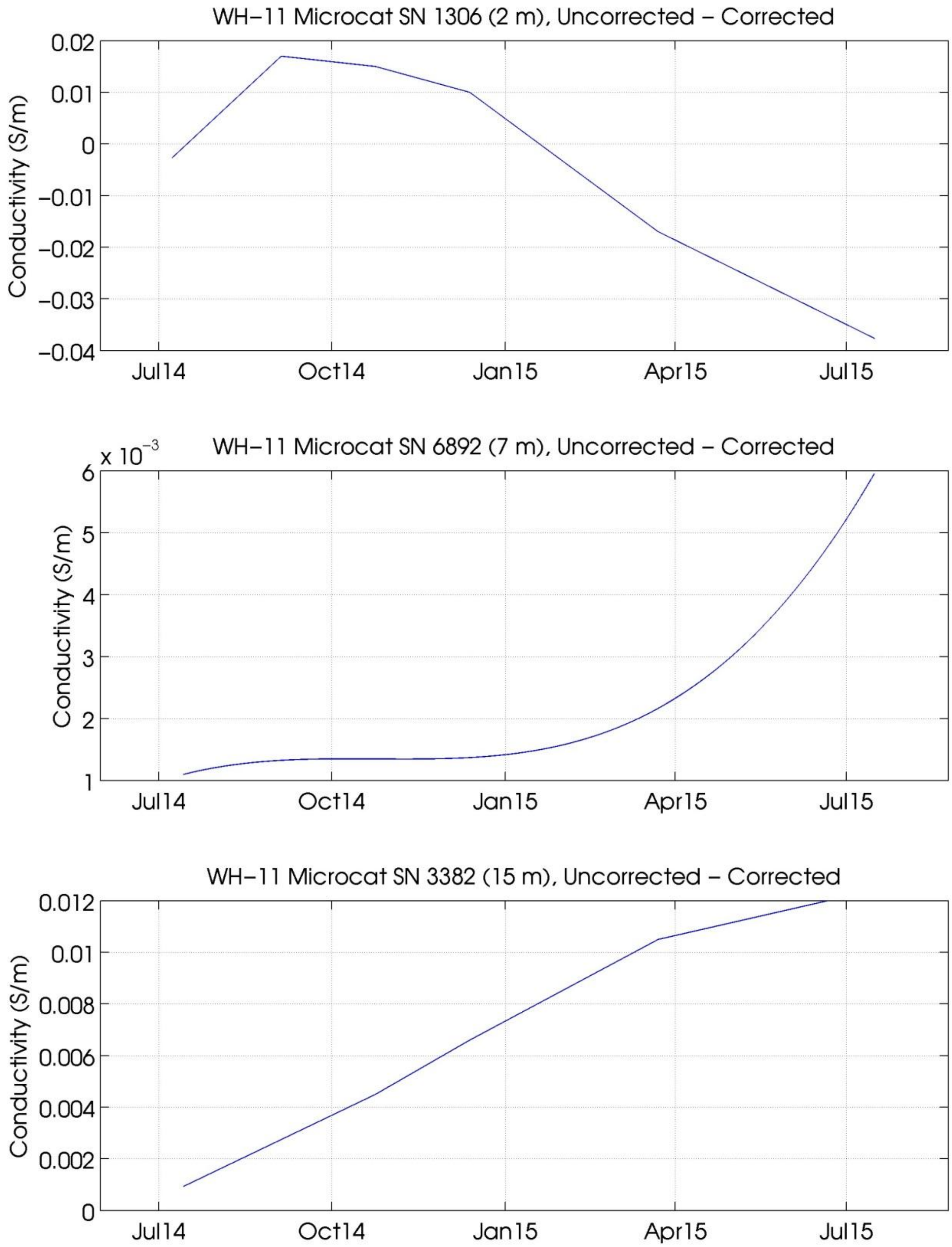

Figure 5-8a. Conductivity sensor corrections for MicroCATs during WHOTS-11.

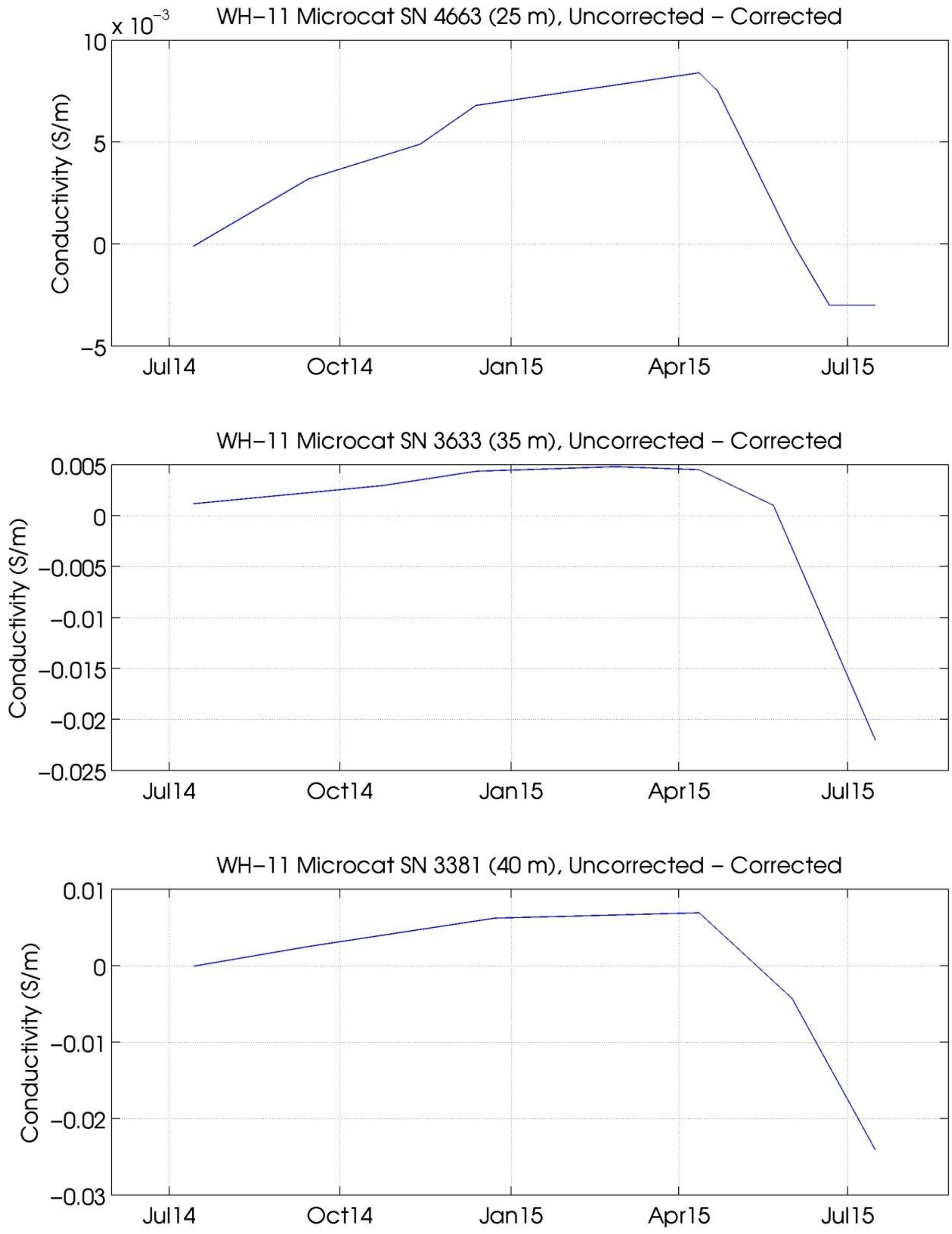

Figure 5-8b. Conductivity sensor corrections for MicroCATs during WHOTS-11.

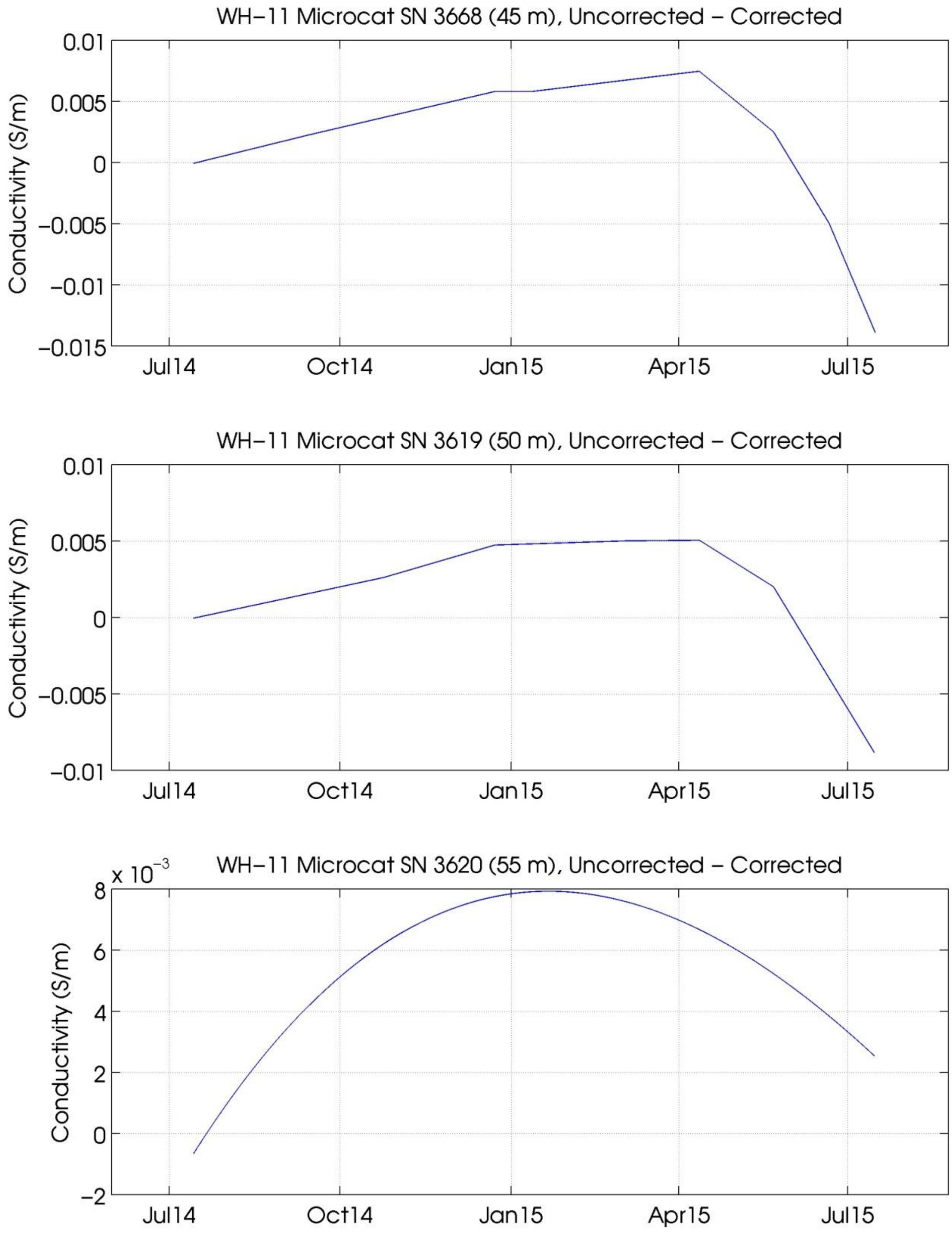

Figure 5-8c. Conductivity sensor corrections for MicroCATs during WHOTS-11.

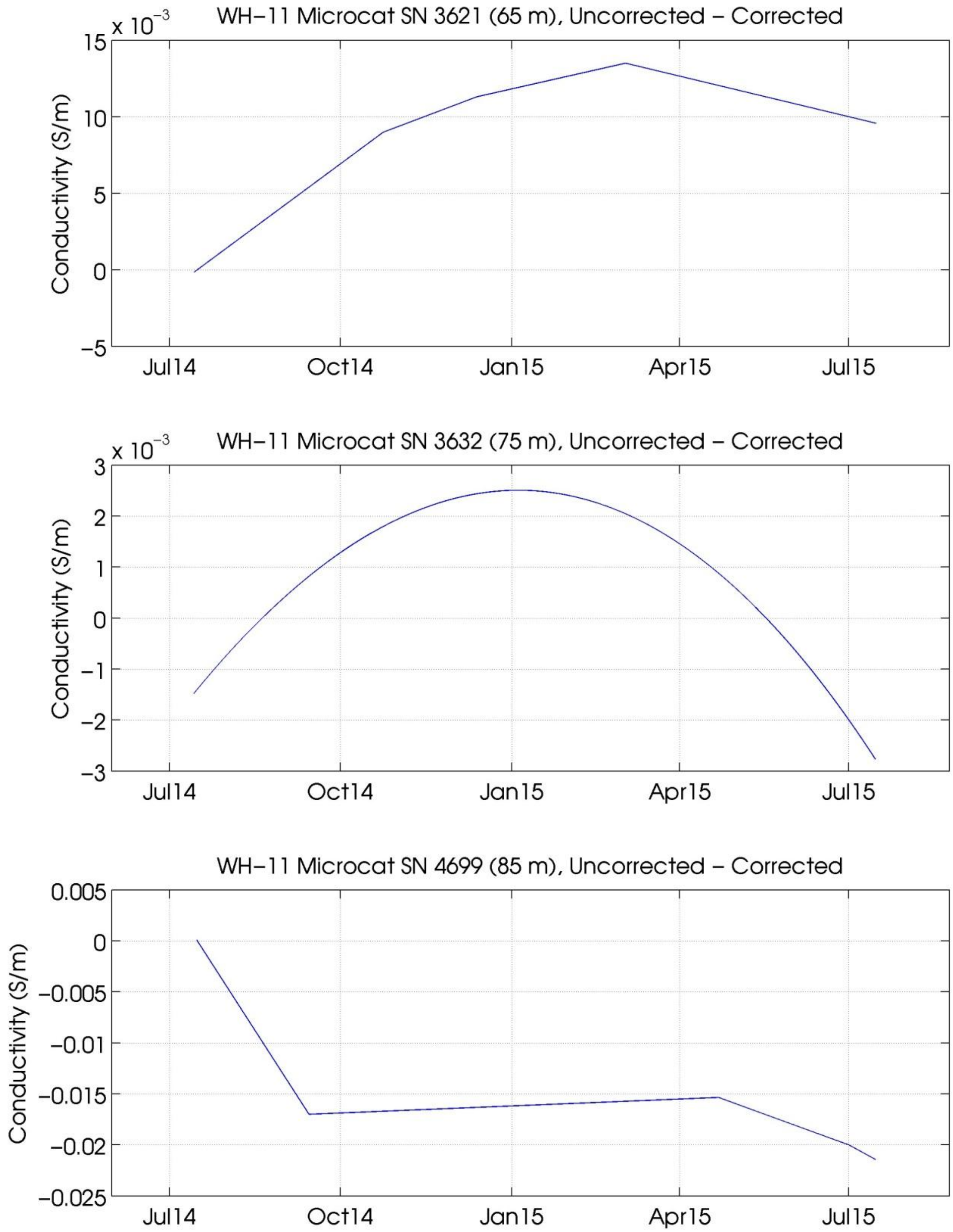

Figure 5-8d. Conductivity sensor corrections for MicroCATs during WHOTS-11.

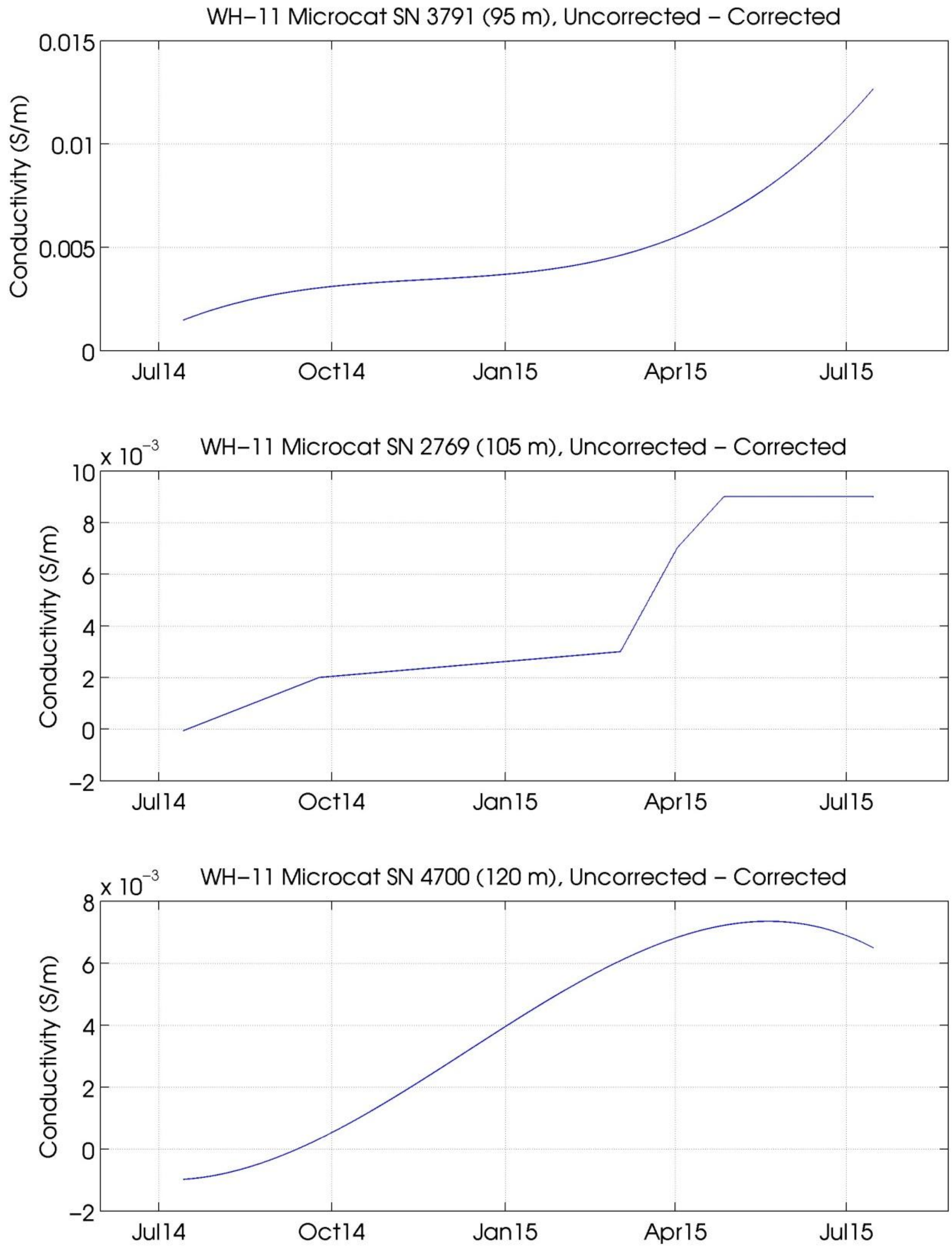

Figure 5-8e. Conductivity sensor corrections for MicroCATs during WHOTS-11.

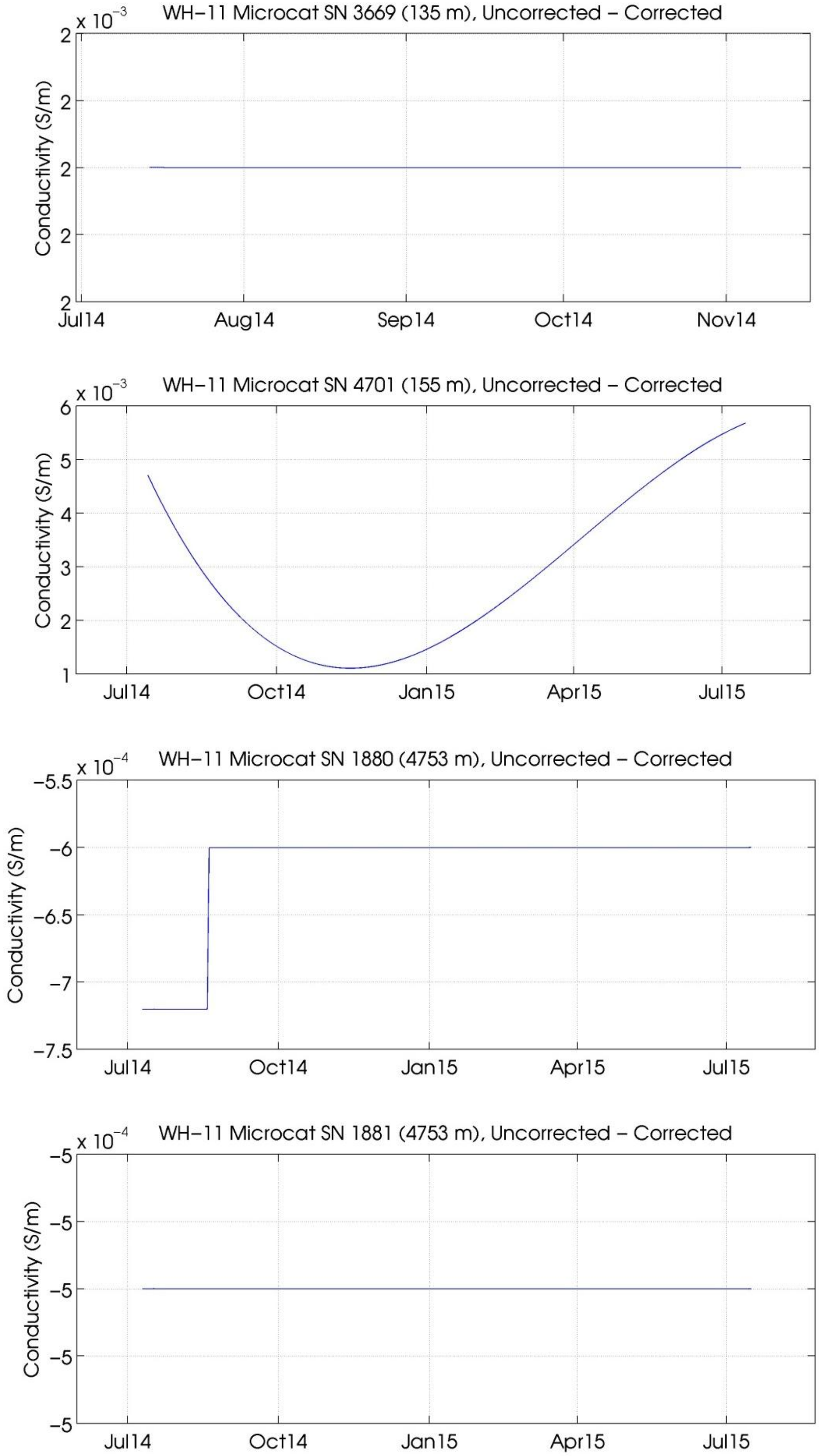

Figure 5-8f. Conductivity sensor corrections for MicroCATs and SeaCATs during WHOTS-11.

B. Acoustic Doppler Current Profilers

Two Teledyne/RD Instruments broadband Workhorse Sentinel ADCP's were deployed on the WHOTS-11 mooring. A 600 kHz ADCP was deployed at 47.5 m depth in the upward-looking configuration, and a 300 kHz ADCP was deployed at 125 m, also in the upward-looking configuration. The instruments were installed in aluminum frames along with an external battery module to provide sufficient power for the intended period of deployment. The four ADCP beams were angled at 20° from the vertical line of the instrument. The ADCP was set to profile across 30 range cells of 4 m with the first bin centered 6.2 m from the transducer. The maximum range of the instrument was just short of 125 m. The specifications of the instrument are shown in Table 5-3.

Table 5-3. Specifications of the ADCP's used for the WHOTS-11 mooring.

Instrument	Description
ADCP	*RDI Workhorse Sentinel, 300KHz* Model: WHS300-I-UG186; Serial Number: 7637 *RDI Workhorse Sentinel, 600KHz* Model: WHS600-I; Serial Number: 13917
Battery module	*300 kHz* Model: WH-EXT-BATTERY; Serial Number: 3426 *600 kHz* Model: WH-EXT-BCL; Serial Number: 3818

1. Compass Calibrations

Pre-Deployment

Prior to the WHOTS-11 deployment a field calibration of the internal ADCP compass was performed at the soccer field of the University of Hawai'i at Manoa on June 18th 2014 for both the 300 kHz and the 600 kHz instruments. Each instrument was mounted in the deployment cage along with the external battery module and was located away from potential sources of magnetic field disturbances. The ADCP was mounted to a turntable, which was aligned with magnetic north using a surveyor's compass. Using the built-in RDI calibration procedure, the instrument was tilted in one direction between 10 and 20 degrees and then rotated through 360 degrees at less than 5 ° /sec. The ADCP was then tilted in a different direction and a second rotation made. Based on the results from the first two rotations, calibration parameters are temporarily loaded and the instrument, tilted in a third direction is rotated once more to check the calibration. Results from each pre-deployment field calibration are shown in Table 5-4 (Figure 5-).

Table 5-4. Results from the WHOTS-11 pre-deployment ADCP compass field calibration procedure.

300 kHz (SN 7637)	Single Cycle Error (°)	Double Cycle Error (°)	Largest Double + Single Cycle Error (°)	RMS of 3rd Order and Higher + Random Error (°)	**Over all Error (°)**	Pitch Mean and Standard Deviation (°)	Roll Mean and Standard Deviation (°)
Before Calibration	2.29	0.16	2.45	0.22	**2.29**	0.28 ± 1.16	-0.43 ± 1.04
After Calibration	0.42	0.27	0.68	0.13	**0.59**	-2.01 ± 0.71	-0.29 ± 0.71

600 kHz (SN 13917)	Single Cycle Error (°)	Double Cycle Error (°)	Largest Double + Single Cycle Error (°)	RMS of 3rd Order and Higher + Random Error (°)	**Over all Error (°)**	Pitch Mean and Standard Deviation (°)	Roll Mean and Standard Deviation (°)
Before Calibration	2.80	0.45	3.25	0.17	**2.84**	1.26 ± 0.89	-0.77 ± 0.87
After Calibration	0.35	0.31	0.66	0.14	**2.76**	-16.86 ± 0.73	-0.75 ± 0.80

Post-Deployment

After the WHOTS-11 mooring was recovered, the performance of the ADCP compass was tested at the soccer field of the University of Hawai'i at Manoa on September 30th 2015 with an identical compass calibration procedure as during the pre-deployment calibration. Results from the WHOTS-11 post-deployment ADCP compass field calibration procedure are listed in Table 5-5 (Figure 5-9 and 5-10).

Table 5-5. Results from the WHOTS-11 post-deployment ADCP compass field calibration procedure

300 kHz	Single Cycle Error (°)	Double Cycle Error (°)	Largest Double + Single Cycle Error (°)	RMS of 3rd Order and Higher + Random Error (°)	**Over all Error (°)**	Pitch Mean and Standard Deviation (°)	Roll Mean and Standard Deviation (°)
After Calibration	3.38	0.34	3.72	0.18	**3.45**	0.07 ± 1.58	-0.36 ± 1.18

600 kHz	Single Cycle Error (°)	Double Cycle Error (°)	Largest Double + Single Cycle Error (°)	RMS of 3rd Order and Higher + Random Error (°)	**Over all Error (°)**	Pitch Mean and Standard Deviation (°)	Roll Mean and Standard Deviation (°)
After Calibration	2.73	0.21	2.94	0.18	**2.76**	-1.63 ± 1.39	0.09 ± 1.30

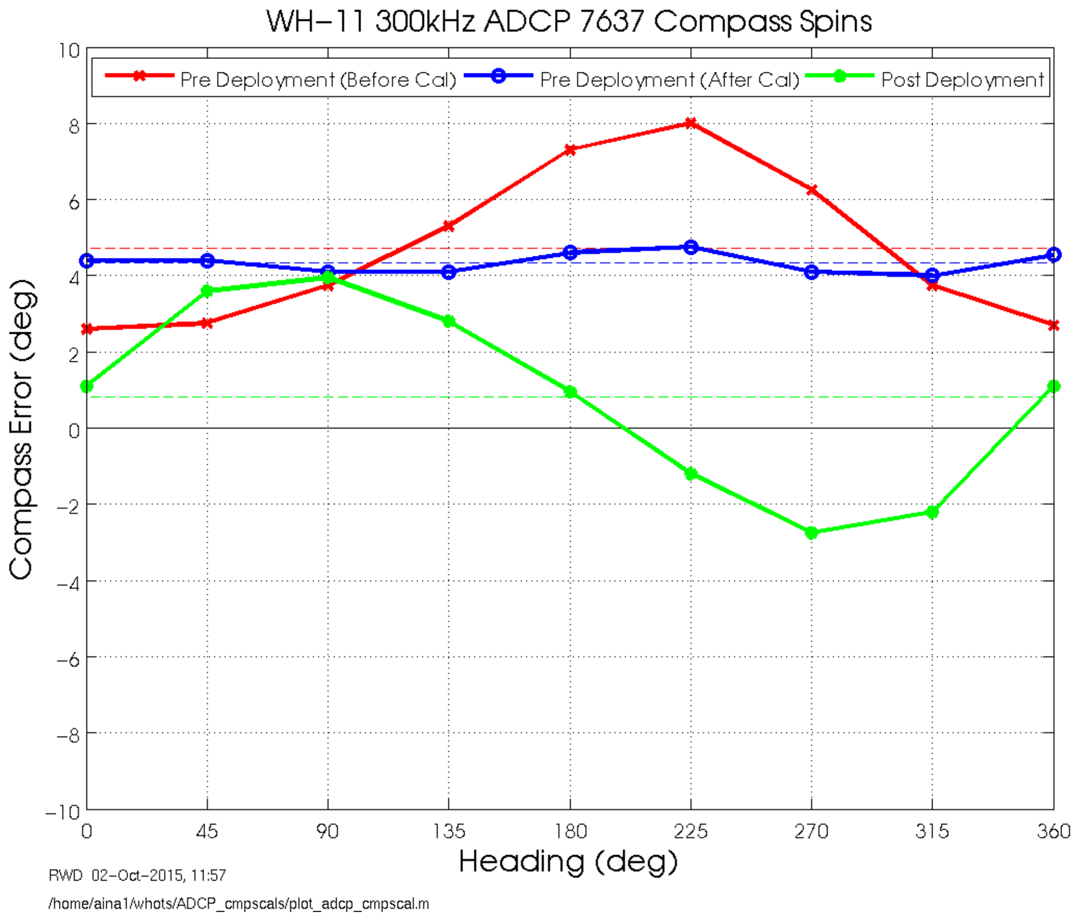

Figure 5-9. Results of the post-cruise compass calibration, conducted September 30th 2015 on ADCP SN 7637 at the University of Hawai'i at Manoa.

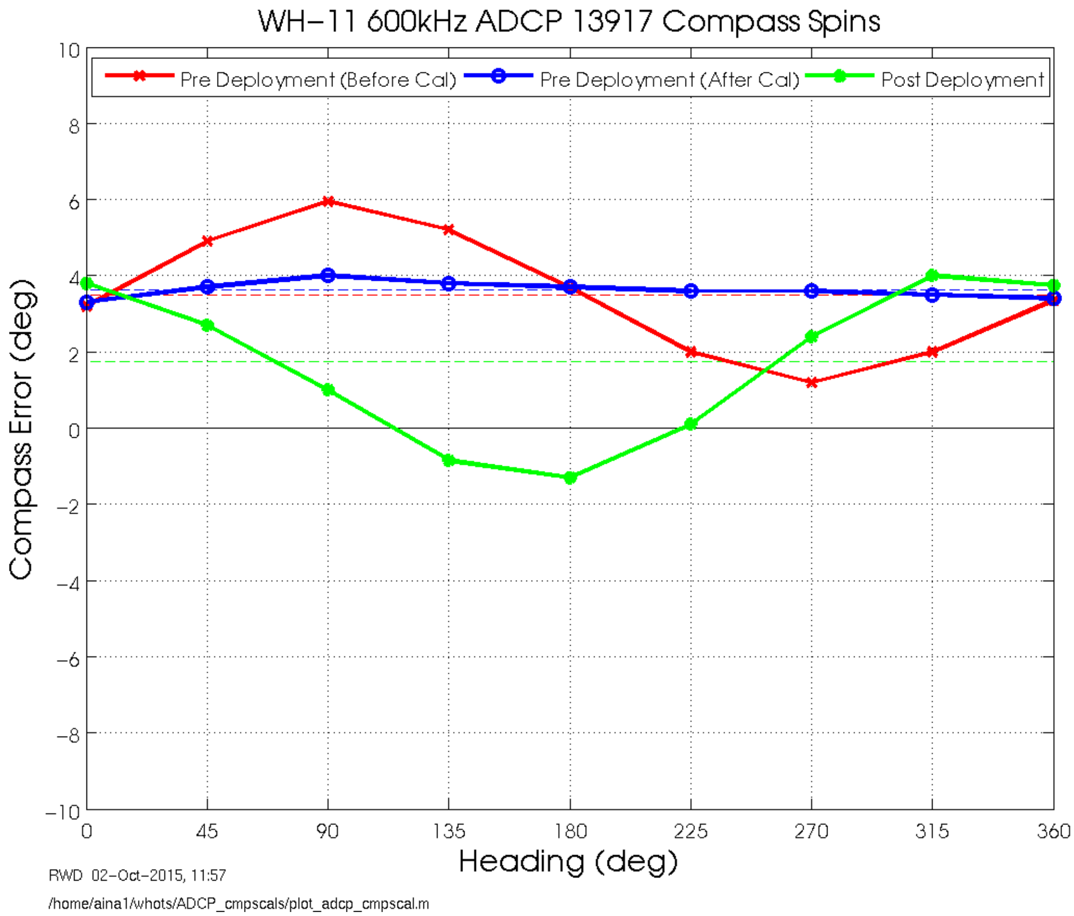

Figure 5-10. Results of the post-cruise compass calibration, conducted September 30th 2015, on ADCP SN 1825 at the University of Hawai'i at Manoa.

2. ADCP Configurations

Individual configurations for the two ADCP's on the WHOTS-11 mooring are detailed in Appendices 1 and 2. The salient differences for each of the ADCP's are summarized below.

300 kHz (125 m)

The ADCP, set to a beam frequency of 300 kHz, was configured in a burst sampling mode consisting of 40 pings per ensemble in order to resolve low-frequency wave orbital motions. The interval between each ping was 4 seconds so the ensemble length was 160 seconds. The interval between ensembles was 10 minutes. Data were recorded in earth coordinates with a heading bias of 9.47° E used. This heading bias was corrected in post-deployment processing to a heading bias of 9.75° E. False targets, usually fish, were screened by setting the threshold maximum to 70 counts. Velocity data were rejected if the difference in echo intensity among the four beams exceeded this threshold.

600 kHz (47.5m)

The ADCP, set to a beam frequency of 600 kHz, was configured in a burst sampling mode consisting of 80 pings per ensemble. The interval between each ping was 2 seconds so the ensemble length was also 160 seconds. The interval between ensembles was 10 minutes. Data were recorded in earth coordinates with a heading bias of 9.47° E used. This heading bias was corrected in post-deployment processing to a heading bias of 9.75° E. The threshold maximum was also set to 70 counts. Velocity data were rejected if the difference in echo intensity among the four beams exceeded this threshold.

3. ADCP data processing procedures

Binary files output from the ADCP were read and converted to MATLAB™ binary files using scripts developed by Eric Firing's ADCP lab (http://current.soest.hawaii.edu). The beginning of the raw data files were truncated to a time after the mooring anchor was released in order to allow time for the anchor to reach the seabed and for the mooring motions that follow the impact of the anchor on the sea floor to dissipate. The pitch, roll, and ADCP temperature were examined in order to pick reasonable times that ensured good data quality but without unnecessarily discarding too much data (Figure 5- and

Figure 5-72). Truncation at the end of the data files were chosen to be the ensemble prior to the time that the acoustic release signal was sent to avoid contamination due to the ascent of the instrument. The times of the first ensemble from the raw data, deployment and recovery time, along with the times of the truncated records of both deployments are shown in Table 5-6.

Table 5-6. ADCP record times (UTC) during WHOTS-11 deployment.

	300 kHz	600 kHz
Raw file beginning and end times	14-Jul-2014 00:00 16-Jul-2015 01:59:59	14-Jul-2014 00:00 06-Jun-2015 11:16:40
Deployment and recovery times	17-Jul-2014 02:40 in water 14-Jul-2015 16:56 anchor over 16-Jul-2014 19:45 release triggered 14-Jul-2015 23:37 on deck	17-Jul-2014 02:40 in water 14-Jul-2015 16:56 anchor over 16-Jul-2014 19:30 release triggered 15-Jul-2015 23:47 on deck
Processed data beginning and end times	17-Jul-2014 01:30 14-Jul-2015 18:40	17-Jul-2014 02:50 27-May-2015 21:36

ADCP Clock Drift

Upon recovery, the ADCP clocks were compared with the ship's time server and the difference between the two was recorded. It was found that for 300 kHz (SN 7637) ADCP the clock on the instrument was slow by 2 minutes 46 seconds. The clock on the 600 kHz (SN 13917) could not be determined, as the ADCP had stopped collecting data before recovery and could not be accurately benchmarked against a GPS clock. The last value in the quality controlled 600 kHz data set was at 27-May-2015 21:36 UTC. Past deployments of the ADCP's suggest a 9 minute difference isn't unusual. Since the drift represents just one ensemble out of a total of over 58,000, no corrections were made. However this drift may be significant if the data are used for time dependent analysis such as tidal or spectrum analysis, a drift correction needs to be applied in those cases.

Heading Bias

As mentioned in the ADCP configuration section, the data were recorded in earth coordinates. A heading bias, the angle between magnetic north and true north, can be included in the setup to obtain output data in true earth coordinates. Magnetic variation was obtained from the National Geophysical Data Center 'Geomag' calculator. (http://www.ngdc.noaa.gov/seg/geomag). For a year long deployment a constant value is acceptable because the change in declination is small, approximately -0.02° $year^{-1}$ at the WHOTS location. A heading bias of 9.47° E was entered in the setup of the WHOTS-11 ADCP's, but was corrected to 9.75° E during post-deployment processing.

Speed of sound

Due to the constant of proportionality between the Doppler shift and water speed, the speed of sound needs only be measured at the transducer head (Firing, 1991). The sound speed used by the ADCP is calculated using a constant value of salinity (35) and the temperature recorded by the transducer temperature sensor of the ADCP. Using CTD profiles close to the mooring during HOT cruises, HOT-243 to HOT-253, and from the WHOTS deployment/recovery cruises, the mean salinity at 125 dbar was 35.34 while the mean salinity at 47.5 dbar was 35.24. Mean ADCP temperature at 125 dbar was 21.52 °C and 24.65 °C at 47.5 dbar (Figure 5-8). The maximum associated mean sound velocity difference is less than 0.4 m s^{-1} which represents a change of less than 0.03%, so no correction was made.

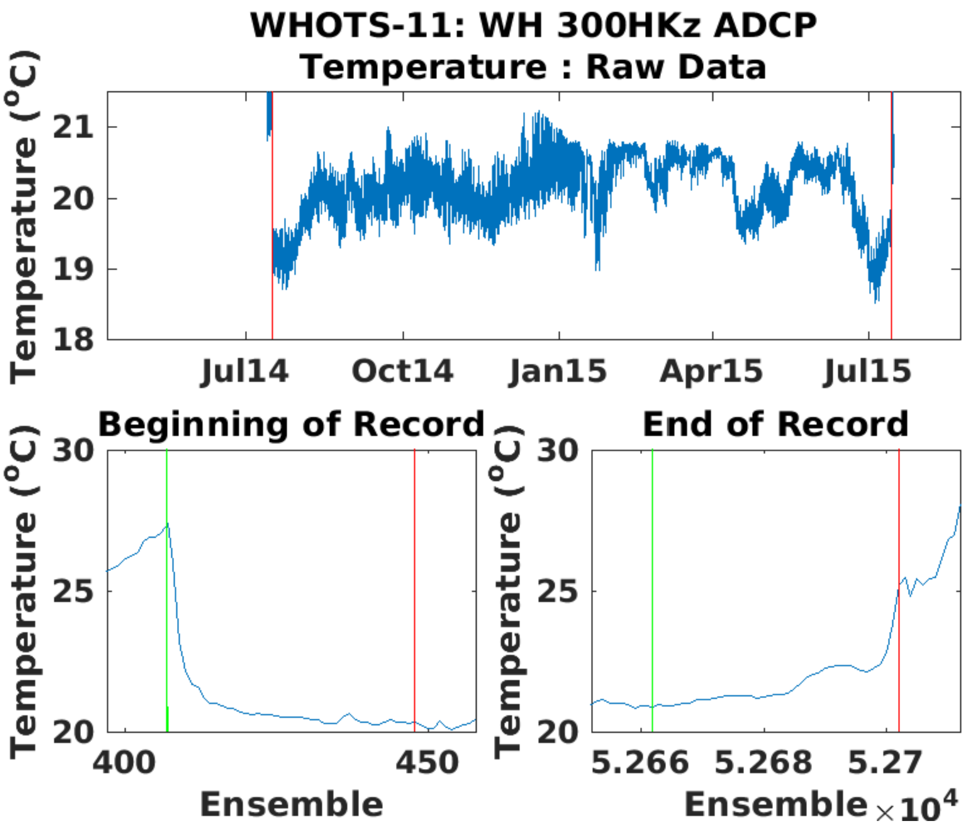

Figure 5-11. Temperature record from the 300 kHz ADCP during WHOTS-11 mooring (top panel). The bottom panel shows the beginning and end of the record with the green vertical line representing the in-water time during deployment and out-of-water time for recovery. The red line represents the anchor release and acoustic release trigger for deployment and recovery respectively.

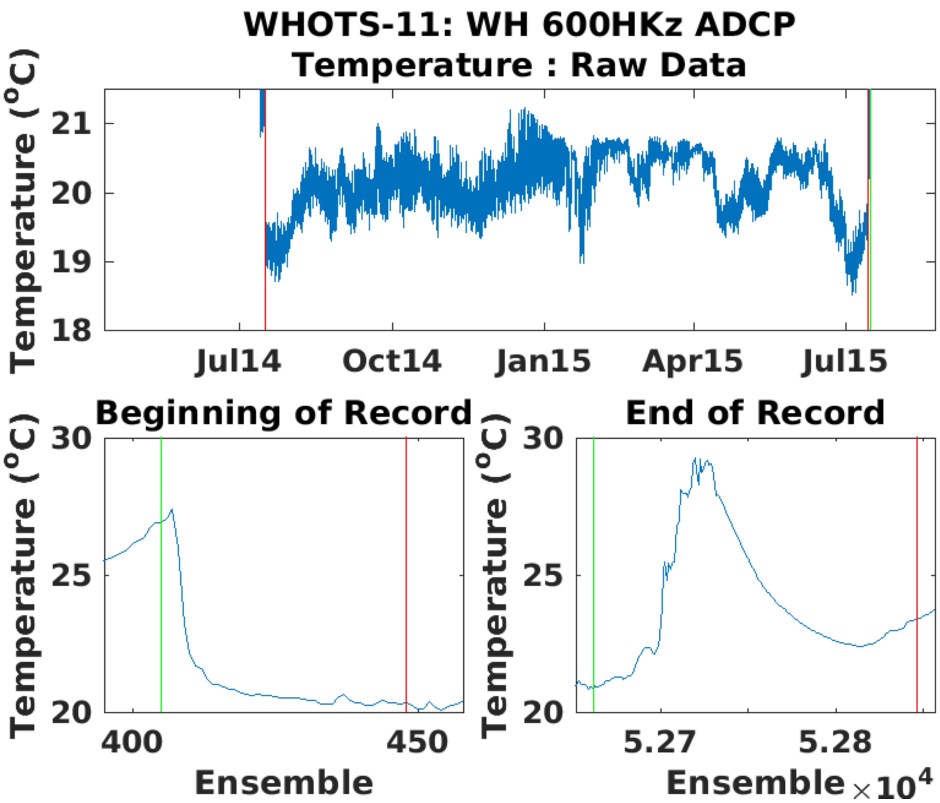

Figure 5-72. Same as Figure 5-11, but for the 600 kHz ADCP.

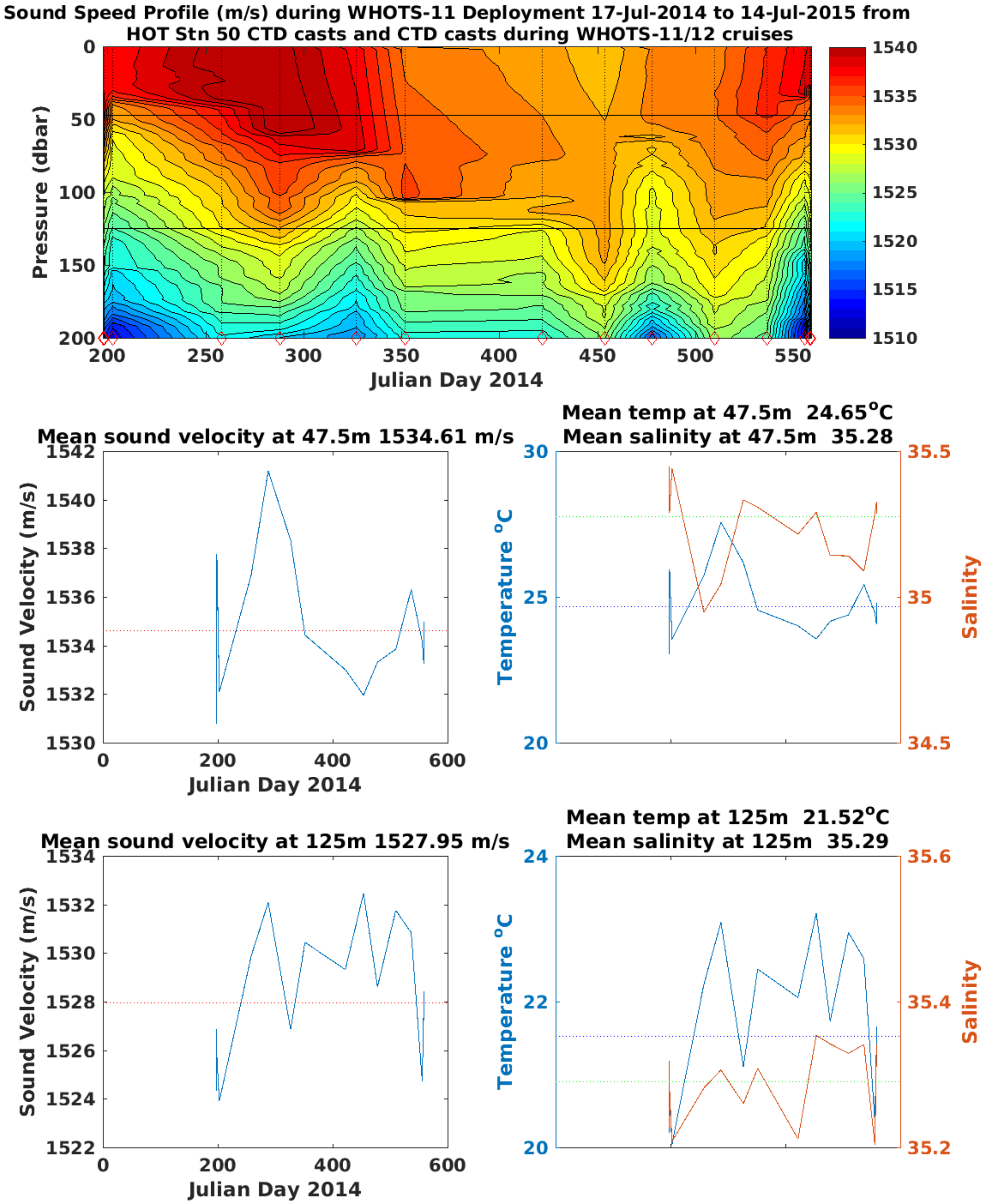

Figure 5-83. Sound speed profile (top panel) during the deployment of the WHOTS-11 mooring from 2 dbar CTD data taken during regular HOT cruises and CTD profiles taken during the WHOTS-12 recovery/deployment cruise (individual casts marked with a red diamond). The bottom left panels show the sound velocity at the depth of the ADCP's (47.5 m and 125 m), with the mean sound velocity indicated with a red line. The lower right panels show the temperature and salinity at each ADCP depth for the time series with the mean temperatures indicated with blue lines and mean salinity indicated with green lines.

Quality Control

Quality control of the ADCP data involved the thorough examination of the velocity, instrument orientation and diagnostic fields to develop the basis of the QC flagging procedures. Details of the methods used can be found in the WHOTS Data Report 1 (Santiago-Mandujano et al., 2007). The following QC procedures were applied to the WHOTS-11 deployment ADCP data.

1) The first bin (closest to the transducer) is sometimes corrupted due to what is known as ringing. A period of time is needed for the sound energy produced during a transmit pulse at the transducer to dissipate before the ADCP is able to properly receive the returned echoes. The blanking interval is used to prevent useless data from being recorded. If it is too short, signal returns can be contaminated from the lingering noise from the transducer. The default value for the blanking interval, (expressed as a distance) of 1.76 m was used for the 300 kHz ADCP, whereas an interval of 0.88 m was used for the 600 kHz ADCP. Thus bin 1 was flagged and replaced with Not a Number (NaN) in the quality controlled dataset (Figure 5-94).

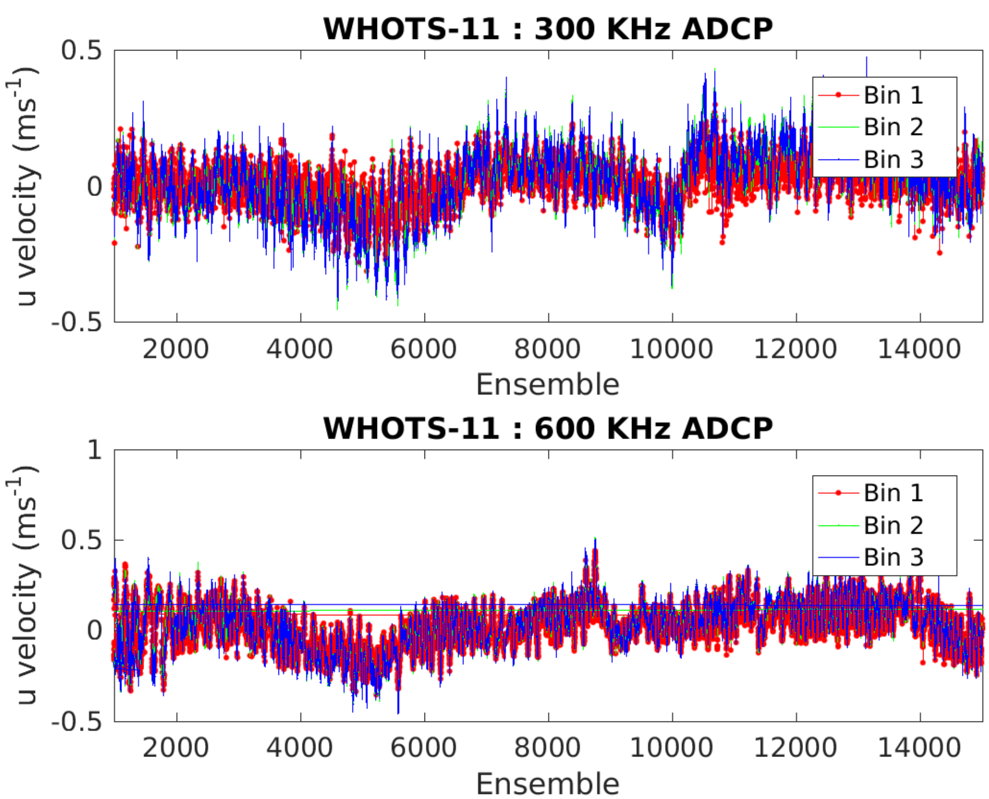

Figure 5-94. Eastward velocity component for the 300 kHz (top panel) and the 600 kHz (bottom panel) ADCPs showing the incoherence between depth 1 (red) and bins 2 (green) and 3 (blue).

2) For an upward-looking ADCP with a beam angle of 20° within range of the sea surface, the upper 6% of the depth range is contaminated with sidelobe interference (RDI, 1996). This is a result of stronger signal reflection from the sea surface (than from scatterers) overwhelming the sidelobe suppression of the transducer. Data are flagged using echo intensity (a measure of the strength of the return signal) from each beam to determine when the signal is contaminated with reflection from the sea surface. In practice, the majority of the data within the upper 4 bins (~14% of the vertical range) were flagged. These upper 4 bins range from about 15 m up to the sea surface.

3) The use of four beams (along with instrument orientation) to resolve currents into their component earth-referenced velocities provides us with a second estimate of the vertical velocity. The scaled difference between these estimates is defined as the error velocity and it is useful for assessing data quality. Error velocities with an absolute magnitude greater than 0.15 m s^{-1} (a value comparable to the standard deviation of observed horizontal velocities) were flagged and removed.

4) An indication of data quality for each ensemble is given by the "percent good" data indicator which accompanies each individual beam for each individual bin. The use of the percent good indicator is determined by the coordinate transformation mode used during the data collection. With profiles transformed into earth coordinates (as in the case of the WHOTS-11 deployment) the percent good fields show the percentage of data that was made using 4 and 3 beam solutions in each depth cell within an ensemble, and the percentage that was rejected as a result of failing one of the criteria set during the instrument setup (see Appendix 1: WHOTS-11 300 kHz ADCP Configuration). Data were flagged when data in each depth cell within an ensemble made from 3 or 4 beam solutions was 20% or less.

5) Data were rejected using correlation magnitude, which is the pulse-to-pulse correlation (in ping returns) for each depth cell. If anyone beam had a correlation magnitude of 20 counts or less, that data point was flagged.

6) Histograms of raw vertical velocity data and partially cleaned data from the ADCP [see Figure 5-105 and 5-16 and the WHOTS Data Report 1 (Santiago-Mandujano et al., 2007)] showed vertical velocities larger than expected, some exceeding 1 m s^{-1}. Recall that the instruments' burst sampling (4-second intervals for the 300 kHz and 2-second intervals for the 600 kHz, for 160 seconds every 10 minutes) was designed to minimize aliasing by occasional large ocean swell orbital motions (Section 3), and therefore are not the source of these large speeds in the data. These large vertical speeds are possibly fish swimming in the beams based on the histograms of the partially cleaned data; depth cells with an absolute value of vertical velocity greater than 0.3 m s^{-1} were flagged.

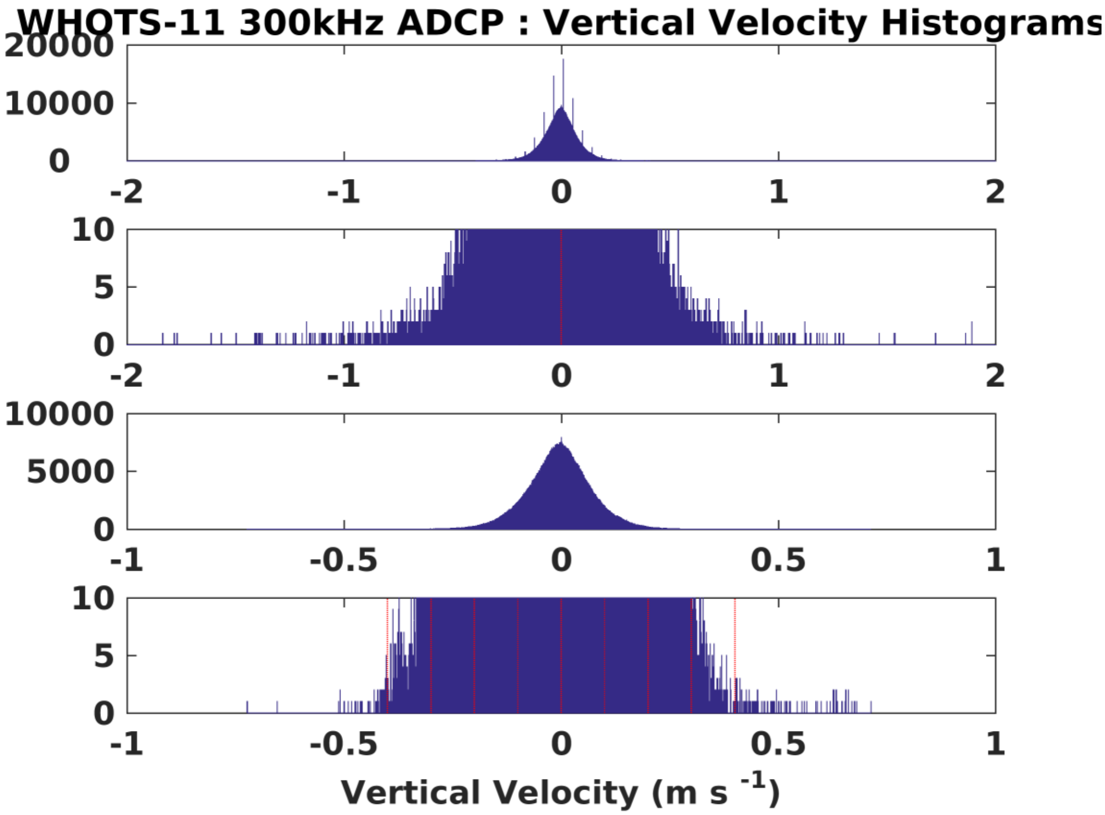

Figure 5-105. Histogram of vertical velocity of the 300 kHz ADCP for raw data (top panel) and enlarged for clarity (upper middle panel), and for partial quality controlled data (lower middle panel) and enlarged for clarity (bottom).

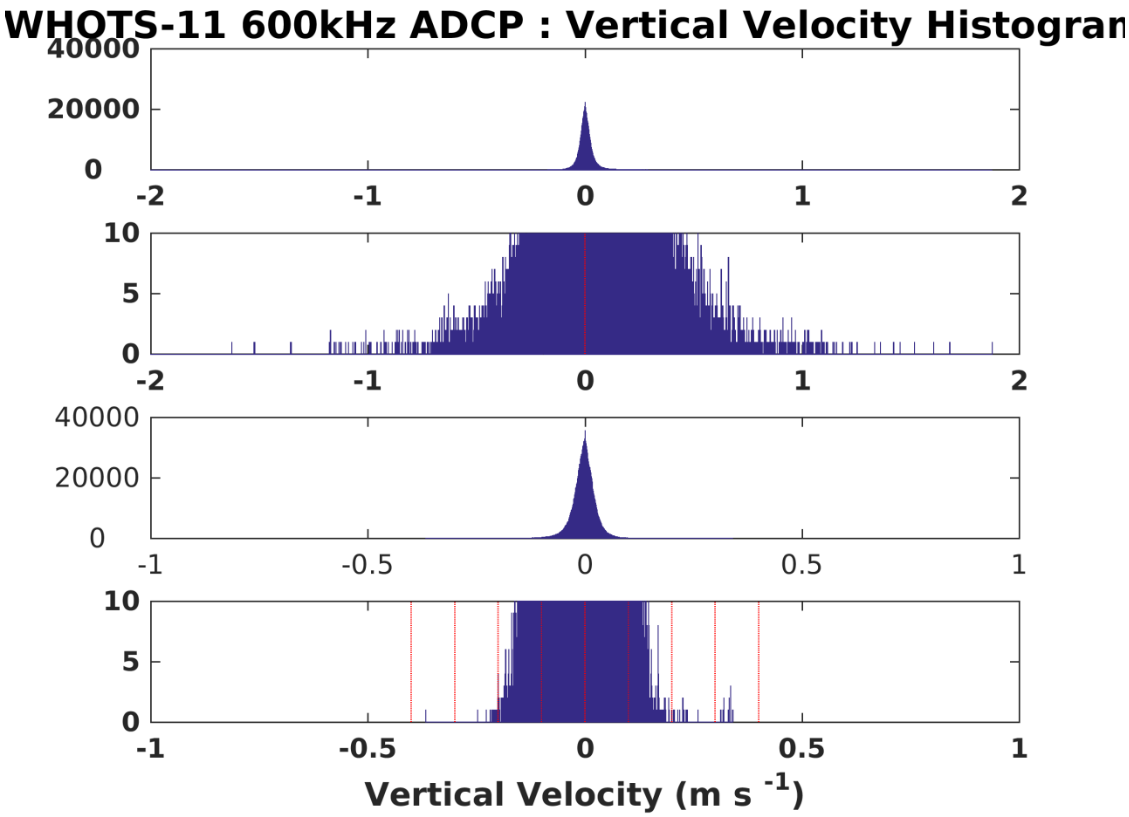

Figure 5-116. Histogram of vertical velocity of the 300 kHz ADCP for raw data (top panel) and enlarged for clarity (upper middle panel), and for partial quality controlled data (lower middle panel) and enlarged for clarity (bottom).

7) A quality control routine known as 'edgers' identifies outliers in surface bins using a five point median differencing method. The median velocity from surface bins was calculated for each ensemble, and then a five point running median of the surface bin median was calculated. This was then compared to individual velocity observations in the surface bins, and those differing by greater than 0.48 m/s were flagged.

8) A 5-pole low pass Butterworth filter with a cutoff frequency of 1/4 cycles/hour was used upon the length of the time-series to isolate low frequency flow for each bin independently. The low frequency flow is then subtracted giving a time series of high frequency velocity component fluctuations for each bin. Data points were considered outliers when their values exceeded four standard deviations from the mean (for each bin) and were removed.

9) A median residual filter used a 7-point (70 minute) median differencing method to define velocity fluctuations. A 7-point running median is calculated for each bin independently and the result is subtracted out giving time series of fluctuations relative to the running median. Outliers greater than four standard deviations from the mean of the 7 points are flagged and removed for each bin.

10) Meticulous verification of all the quality control routines was performed through visual inspections of the quality controlled velocity data. Two methods were utilized; time-series of u and v components for multiple bins were evaluated as well as individual vertical profiles. The time-series methodology involved inspecting u and v components separately, five bins at a time, over 600 ensembles (100 hours). Any instance showing one bin behaving erratically from the other four bins was investigated further. If it seemed that there could be no reasonable rationale for the erratic points from the identified bin, the points were flagged [see **Error! Reference source not found.**5 and **Error! Reference source not found.** and the WHOTS Data Report 1 (Santiago-Mandujano et al., 2007)]. The intent of the vertical inspection of vertical profiles of the u and v components was to find entire profiles that were not aligned with neighboring profiles. Thirty u and v profiles were stacked at a time and were visually inspected for any anomalous data.

C. Vector Measuring Current Meter (VMCM)

Vector measuring current meters (VMCM) were deployed on the WHOTS-11 mooring at depths of 10 m and 30 m. The compass from both instruments did not record data during the deployment, therefore the current direction is not available. VMCM data were processed by the WHOI/UOP group. A copy of the processing report is in Appendix 3 in Section 3.h. VMCM record times are shown in Table 5-7.

Table 5-7. Record times (UTC) for the VMCMs at 10 m and 30 m during the WHOTS-11 deployment

	WHOTS-11	
	VMCM062	VMCM083
Deployment and recovery times	16-Jul-2014 18:42 15-Jul-2015 01:31	16-Jul-2014 18:16 15-Jul-2015 01:42
Processed file beginning and end times	17-Jul-2014 04:10 14-Jul-2015 16:55	17-Jul-2014 04:10 14-Jul-2015 16:55

Daily (24 hour) moving averages of quality controlled 600 kHz ADCP data are compared to VMCM current speed data interpolated to the ADCP ensemble times in the top panels of

Figure 5-127 and18, and the difference is shown in the middle panels. The absolute value of the mean difference plus or minus one standard deviation is shown at the top of the middle panel. Speeds are not compared if greater than 80% of the ADCP data within a 24 hour average was flagged. The absolute value of mean current speed differences for the VMCMs at 10 and 30 m had a mean of 3 cm/s, with standard deviations of 3 cm/s. The VMCM data does not appear to degrade over time for any deployment. Propeller fouling would dampen measured VMCM velocity magnitudes, but a decrease in VMCM velocity magnitude compared to ADCP velocity magnitude with time is not observed.

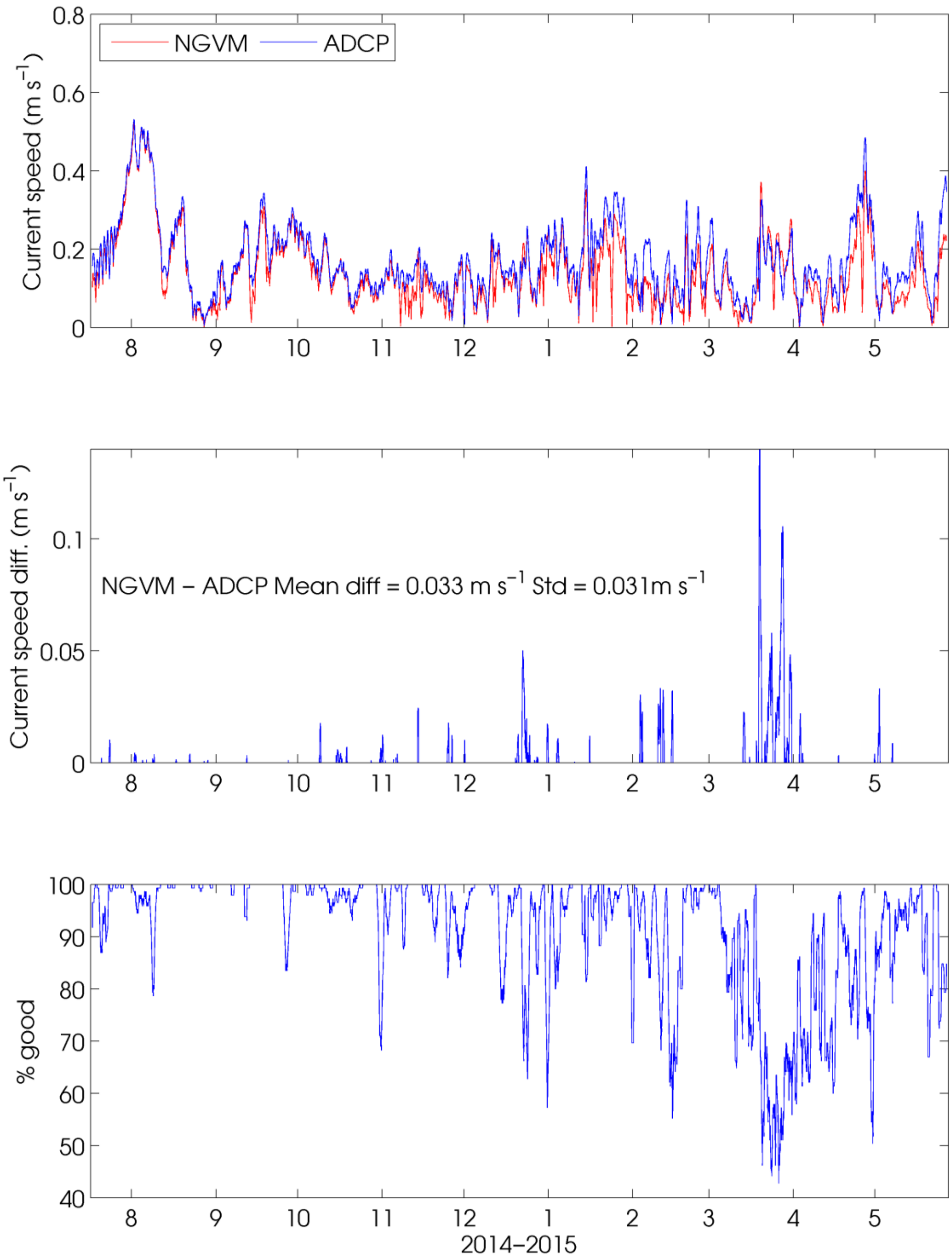

Figure 5-127. A comparison of 10 m VMCM and ADCP U current speeds for WHOTS-11. The top panel shows 24 hour moving averages of VMCM speed at 10 m depth (red) and ADCP U speed (blue) from the nearest depth bin to 10 m. The middle panel shows the difference, and the bottom panel shows the percentage of ADCP data within the moving average not flagged by quality control methods.

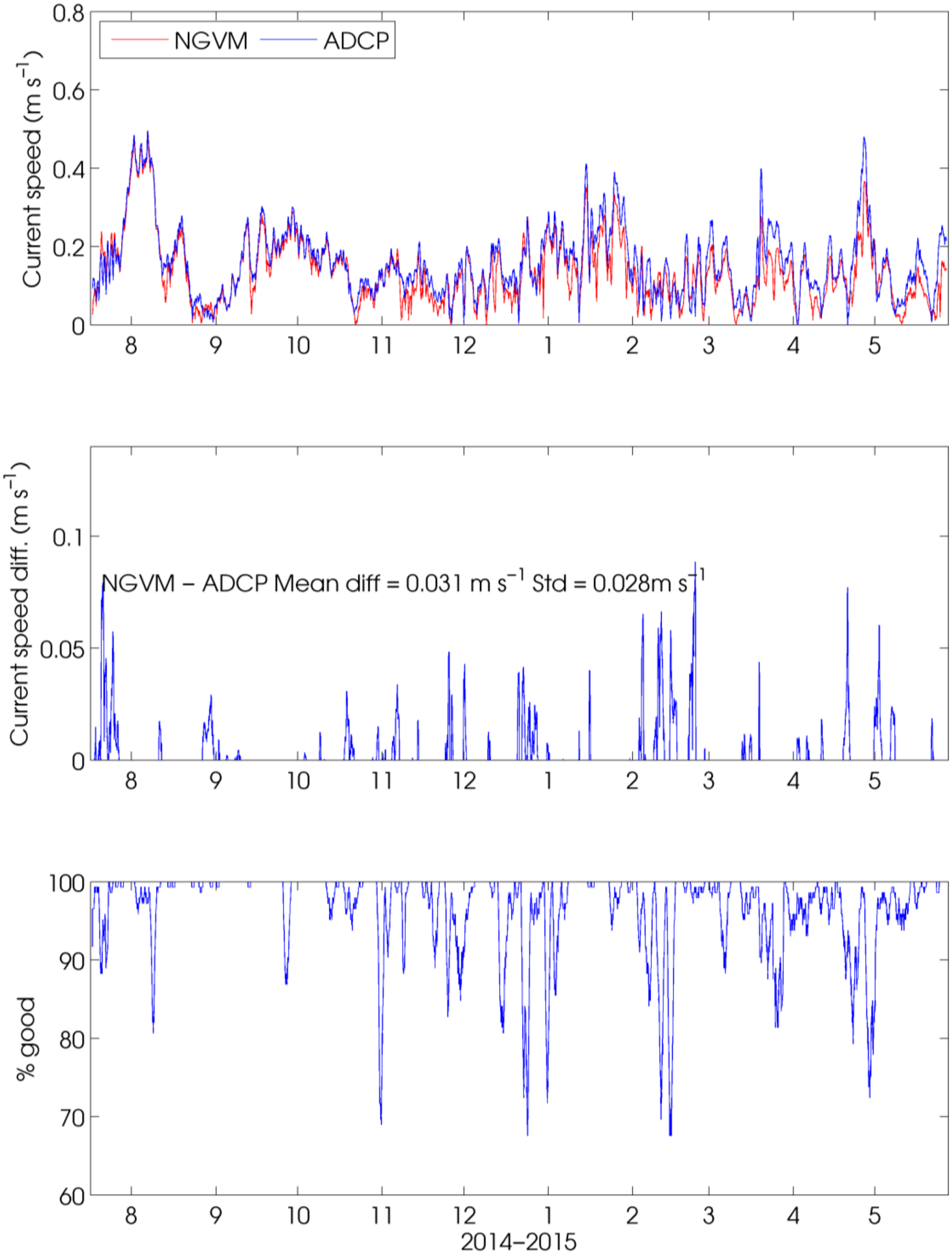

Figure 5-138. Same as in

Figure 5-127 but for the 30 m VMCM.

D. Global Positioning System Receiver and ARGOS Positions

Xeos Global Positioning System receiver (IMEI 300 340 1370 198) and ARGOS beacon SN7580 were attached to the tower top of the buoy during the WHOTS-11 deployment. Data returns from the receivers were high (Table 5-8). Both instruments functioned until recovery

Table 5-8. GPS and ARGOS record times (UTC) during WHOTS-11

WHOTS-11	Xeos GPS	ARGOS
Raw file beginning and end times	17-Jul-2014 04:33:42 14-Jul-2015 16:45:45	17-Jul-2014 05:04:00 14-Jun-2015 03:53:00

ARGOS positions were available during the WHOTS-11 deployment and they provided additional information on the buoy's motion. ARGOS data were recorded at 10 minutes intervals, although there are some small gaps at repeated times present in the records. Samples taken before mooring deployment were eliminated. Data were screened for points that were greater than 2.5 nautical miles from the surveyed anchor positions for each deployment which was considered to be the buoy watch circle radius. The velocity magnitude was calculated and positions that resulted in speeds greater than 1 m s^{-1} were removed. Data were interpolated onto a regular time grid in order to compute spectra.

For comparison,

Figure 5- shows the ARGOS buoy's positions together with the GPS positions during the WHOTS-11 deployment. The standard deviation of the difference between these two records is about 900 m.

The ARGOS positions of the WHOTS-11 buoy for the duration of the deployment are in

Figure 5-140, and shows the color-coded positions according to their data quality. The data quality is determined by its distance from the satellite track. Data of a better quality have a higher flag number: 3 is for a distance less than 150 m, 2 is for a distance between 150 and 350 m, and 1 is for a distance between 350 and 1000 m. For the duration of the deployment, the buoy had a mean position of about 1.5 km from the anchor, with a standard deviation of about 600 m.

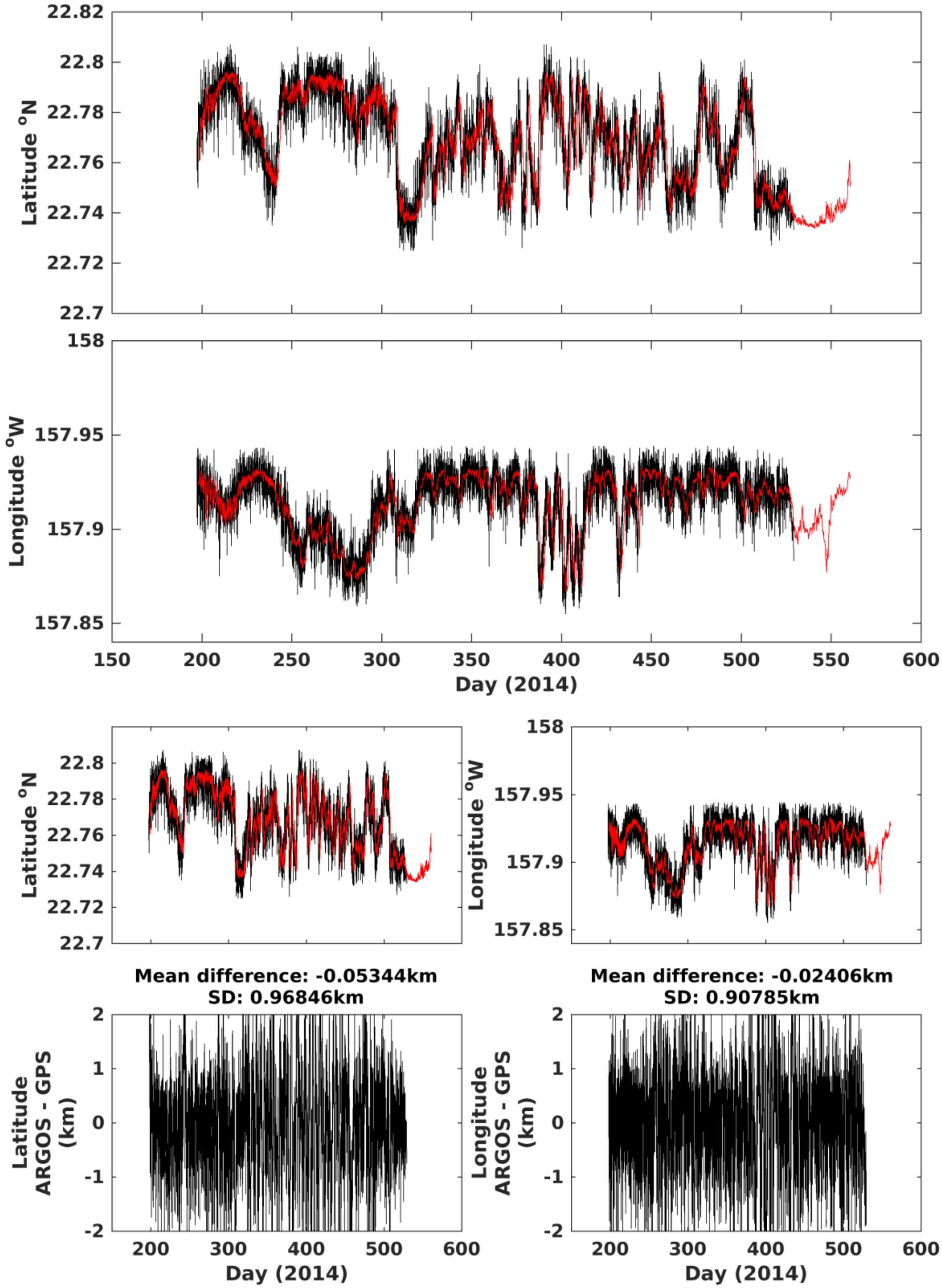

Figure 5-19. WHOTS-11 buoy position from ARGOS data (black line), and from GPS data (red line). The top and two middle panels show the latitude and longitude of the buoy. The bottom panel shows the difference between the GPS positions and the ARGOS positions interpolated to the GPS times.

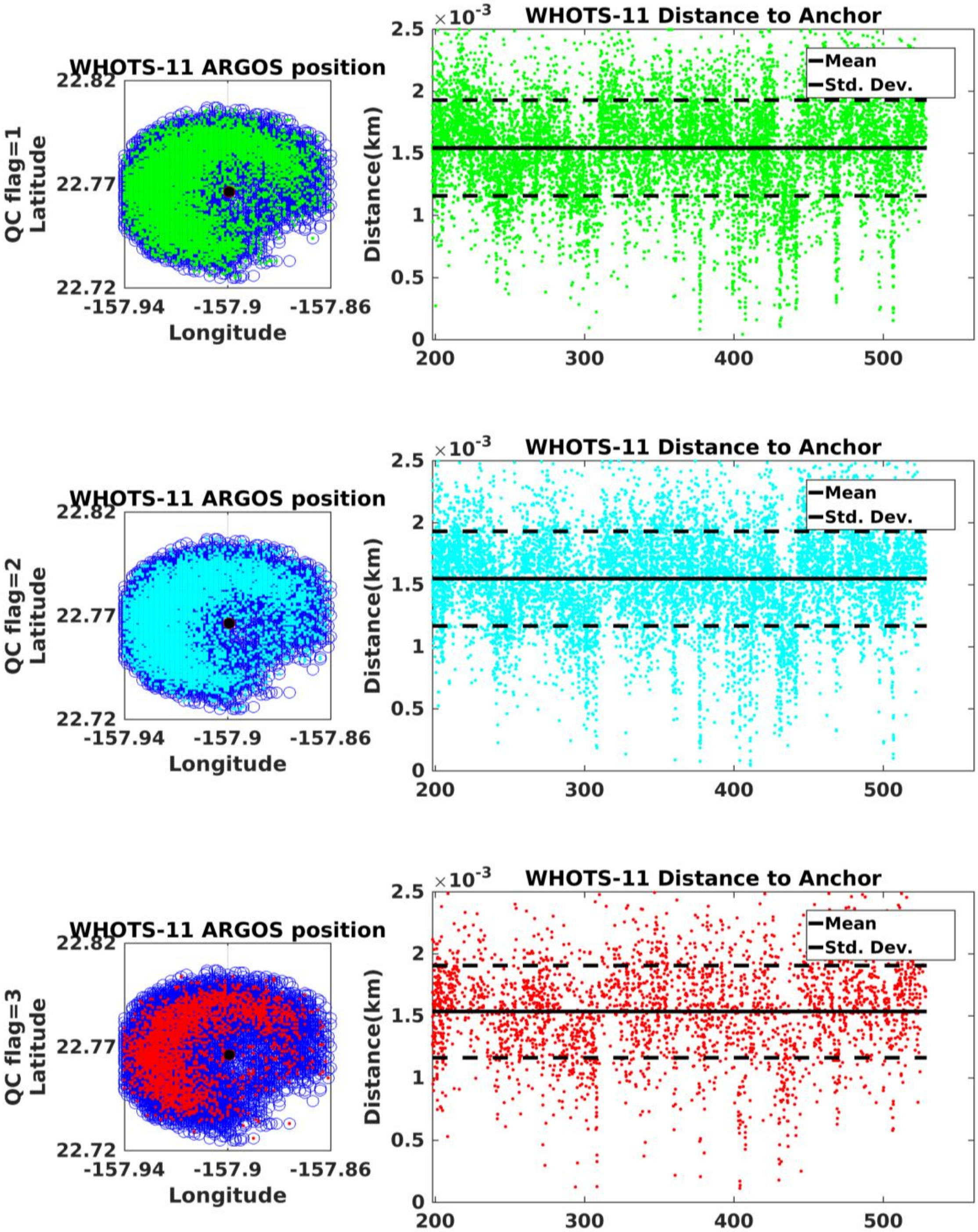

Figure 5-140. WHOTS-11 buoy ARGOS positions (circles, left panels), and distance from its anchor (dots, right panels). The data are colored according to their quality control flag, 1: green, 2: light blue, 3: red. The black circle in the center of the left side panels is the location of the mooring's anchor. The black line in the right panel plots is the mean distance between the buoy and its anchor, and the dashed line is the mean plus minus one standard deviation.

6. Results

During the WHOTS-11 cruise (WHOTS-11 mooring deployment), Station ALOHA was under the influence of the eastern North Pacific high pressure system, and the associated east-northeasterly trade winds. Conditions were favorable for deployment of the WHOTS-11 mooring on 16 July, with 15-18 kt ENE winds. Weather conditions remained favorable during 17-19 July, with ENE wind speeds of 17 kts with occasional higher gusts. Tropical storm Wali started developing SE of Hilo, but weakened to below tropical storm status before reaching the islands. However Wali did cause overcast conditions and a few showers during the WHOTS-10 mooring recovery on 20 July causing an apparent drop in the sea surface salinity as indicated by the thermosalinograph record (Figure 6-13). Winds intensified to 20- 25 kts, with swells in the 8-10 ft range in the morning of the mooring recovery on 20 July, only to decrease to less than 10 kts soon after, and for the rest of the day. Winds were from the east in the 18-20 kt range on the morning of 22 July, but intensified to 25-40 kts with occasional higher gusts (up to 45 kts) for the rest of the day, causing the cancellation of additional CTD casts that were planned for that day. Near-surface currents were slightly westward during transit near Station ALOHA, turning NNEward at about 0.2 m/s during the WHOTS-11 mooring deployment, and fluctuating from NEward to NWward the rest of the cruise. There were no obvious cyclonic or anti-cyclonic eddies present, although a combination of internal semidiurnal and diurnal tides, along with near-inertial oscillations, were noticeable especially in vertical shear. CTD casts conducted near the moorings (**Error! Reference source not found.** through **Error! Reference source not found.**), displayed a subsurface salinity maximum at 50 dbar.

During the WHOTS-12 cruise, (WHOTS-11 mooring recovery), Station ALOHA was under the influence of east-northeasterly trade winds. In addition, the remnants of Tropical Storm Ela were moving northwestward to the north of the islands, bringing hot and humid conditions (relative humidity about 96% as measured by the WHOTS buoy's instruments). Conditions during the WHOTS-12 deployment on July 11th-12th were marginal, with nearly 20 kt NE winds and 5-6 ft waves from the NE. Weather conditions were favorable on July 12th through 14th, with NE wind speeds of 15-20 kt with occasional higher gusts. Winds were 18 kt from the east on July 14th -15th during the WHOTS-11 recovery, and remained in the 15-17 kt range on July 15th -16th.

Near-surface currents were nearly 0.5 m s^{-1} SSWward for the duration of the WHOTS-12 cruise. There were no obvious cyclonic or anti-cyclonic eddies present, although a combination of internal semidiurnal and diurnal tides, along with near-inertial oscillations, were noticeable. CTD casts conducted near the moorings (**Error! Reference source not found.** through **Error! Reference source not found.**), displayed a broad subsurface salinity maximum between 40 and 120 dbar.

The temperature MicroCAT records during the WHOTS-11 deployment (Figure 6- through Figure 6-) show obvious seasonal variability in the upper 100 m, and a sudden drop during July 2015, apparent below 25 m, but more obvious in the deeper instruments. The salinity records (Figure 6- through Figure 6-23) do not show an obvious seasonal cycle, but it shows an increase between November 2014 and May 2015, and two instances of salinity decrease during August 2014 and May 2015 by the instruments located above 65 m.

Figure 6- and
Figure 6-33 show contours of the WHOTS-11 MicroCAT data in context with data from the previous 10 deployments. The seasonal cycle is obvious in the temperature record, with record temperatures (higher than 26 °C) in the summer of 2004 and in the summer of 2014. Salinities in the subsurface salinity maximum were relatively low during the first 6 years of the record, only to increase drastically after 2008, with some episodes of lower salinity in mid-2011, early 2012, early 2013, and mid-2014. The salinity maximum extended to near the surface during some instances in early 2010, 2011, late 2012-early 2013, during February-March 2013, and early 2015. When plotted in σ_θ coordinates (
Figure 6-33), the salinity maximum seems to be centered roughly between 24 and 24.5 $\sigma_{\theta.}$

Records from the WHOTS-11 SeaCATs (Figure 6-32) deployed near the bottom of the mooring (4671 m) detected temperature and salinity changes related to episodic ‘cold events’ apparently caused by bottom water moving between abyssal basins (Lukas et al., 2001). These events are being monitored by instruments at the ALOHA Cabled Observatory (ACO, Howe et al., 2011), a deep water observatory located at the bottom of Station ALOHA (about 6 nautical miles west from the WHOTS-11 anchor), since June 2011. Figure 6-32 shows temperature and salinity records from the WHOTS-11 SeaCATs superimposed on the ACO data. The SeaCAT data agreed with the sudden temperature decrease and the salinity increase registered by ACO instruments in November 2014 during a ‘cold event’ episode. The instruments also show the gradual return to temperature and salinity values observed before the event.

Figure 6- through
Figure 6-38 show time series of the zonal, meridional, and vertical currents recorded with the moored ADCPs during the WHOTS-12 deployment, and Figure 6- shows the currents at 10 and

30 m collected by the VMCMs. Figure 6- through

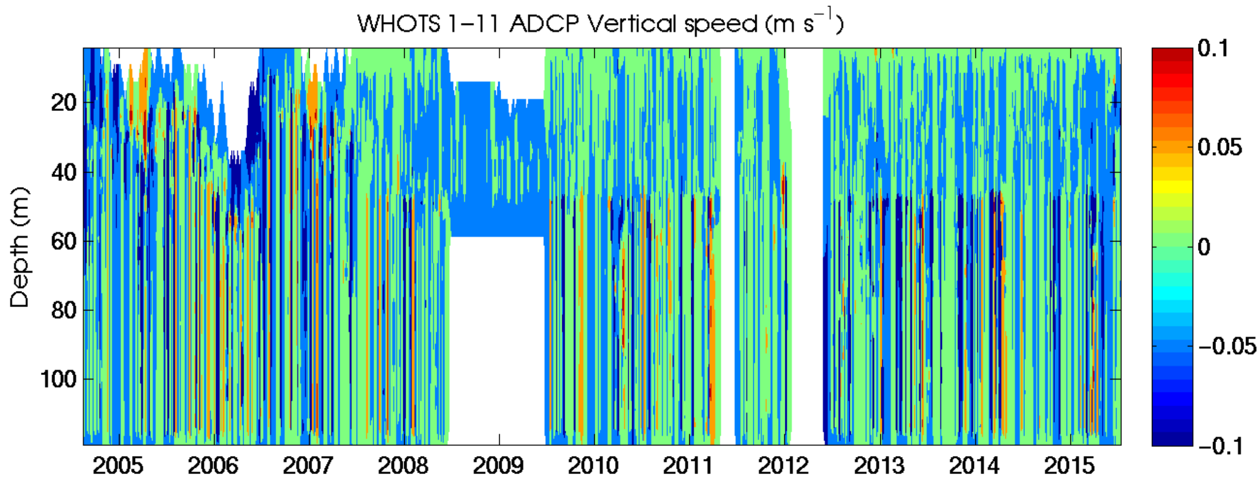

Figure 6-35 show contours of the ADCP current components in context with data from the previous deployments. In spite of the gaps in the data, an obvious variability is seen in the zonal and meridional currents, apparently caused by passing eddies. On top of this variability there have been periods of intermittent positive or negative zonal currents, for instance during 2007-

2008. The contours of vertical current component (

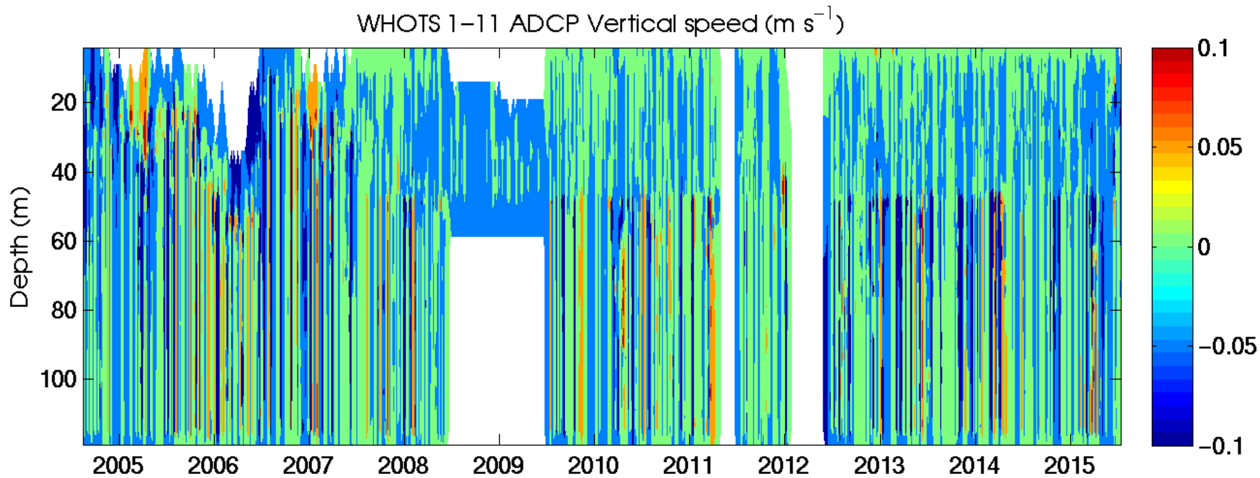

Figure 6-35) show a transition in the magnitude of the contours near 47 m, indicating that the 300 kHz ADCP located at 126 m moves more vertically than the 600 kHz ADCP located at 47.5 m.

A comparison between the moored ADCP data and the shipboard ADCP data obtained during the WHOTS-11 cruise (during the WHOTS-11 mooring deployment) is shown in Figure 6-39 and Figure 6-. Similar comparison during the WHOTS-12 cruise (WHOTS-11 mooring recovery) is shown in Figure 6-40a and Figure 6-40b. Some of the differences seen especially in the zonal component may be due to the mooring motion, which was not removed from the data.

Comparisons between the shipboard ADCP from HOT cruises and the mooring data are compiled in Table 6-1, and shown in Figure 6-4 through **Error! Reference source not found.**. The correlation coefficient from these comparisons is higher than 0.6 for the majority of the cruises.

The motion of the WHOTS-11 buoy was registered by the Xeos-GPS receiver, and its positions are plotted in Figure 6-58. The buoy was located west of the anchor for the majority of the deployment, except during September-October 2014, and for short periods in February 2015 when it was east of it. Power spectrum of these data (Figure 6-55) shows extra energy at the inertial period (~31 hr). Combining the buoy motion with the tilt (a combination of pitch and roll) from the ADCP data (Figure 6-56), showed that the tilt increased as the buoy distance from the anchor increased. This was expected since the inclination of the cable increases as the buoy moves away from the anchor.

A. CTD Profiling Data

Profiles of temperature, salinity and potential density (σ_θ) from the casts obtained during the WHOTS-11 deployment cruise are presented in **Error! Reference source not found.**1 through **Error! Reference source not found.**6, together with the results of bottle determination of salinity. Figure 6-7 through

Figure 6-12 are the results of the CTD profiles during the WHOTS-12 cruise.

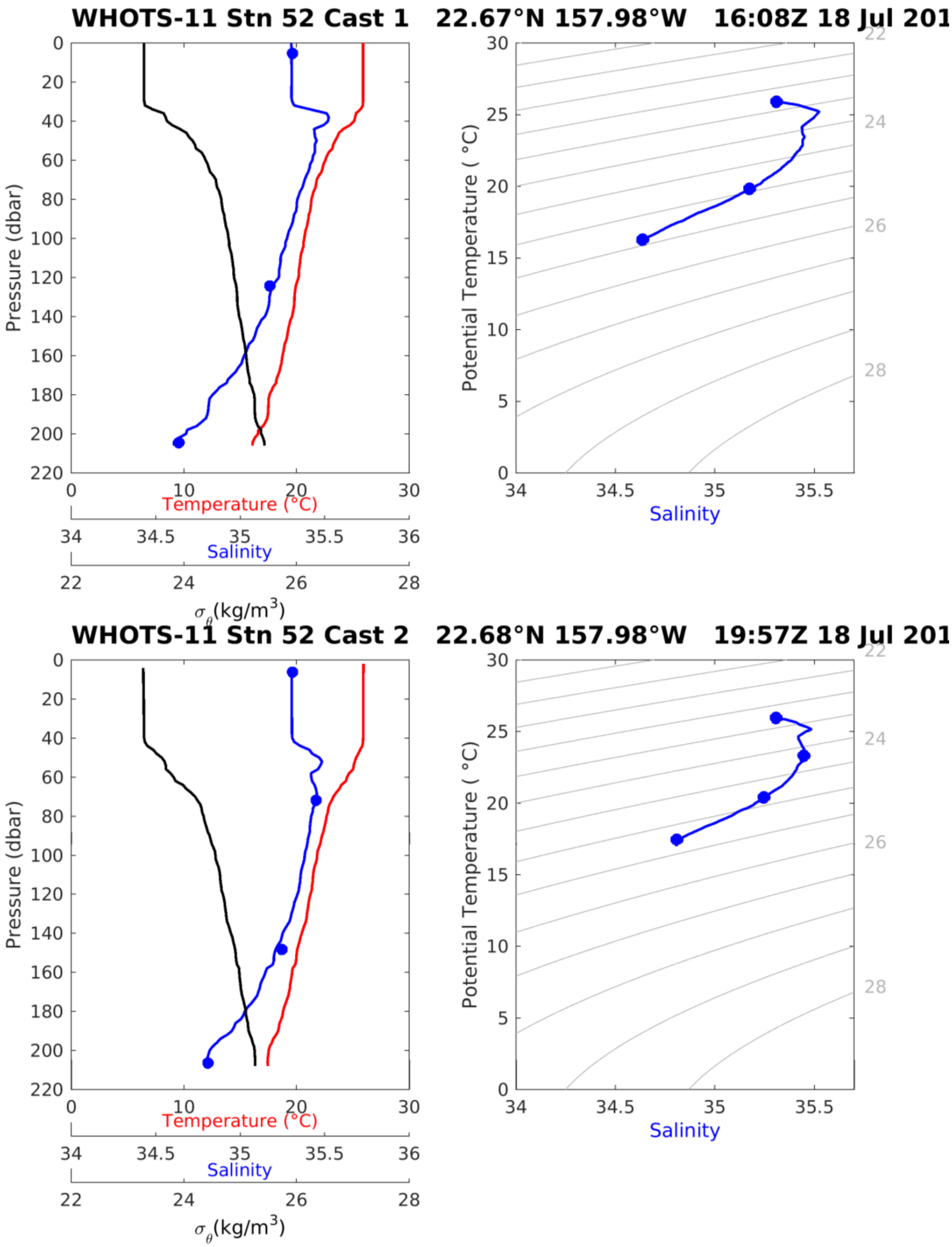

Figure 6-1. [Left panels] Profiles of CTD temperature, salinity, and potential density (σ_θ) as a function of pressure, including discrete bottle salinity samples (when available) for station 52 cast 1 (top left) and cast 2 (bottom left) during the WHOTS-11 cruise.
[Right panels] Profiles of CTD salinity as a function of potential temperature, including discrete bottle salinity samples (when available) for station 52 cast 1 (top right) and cast 2 (bottom right) during the WHOTS-11 cruise.

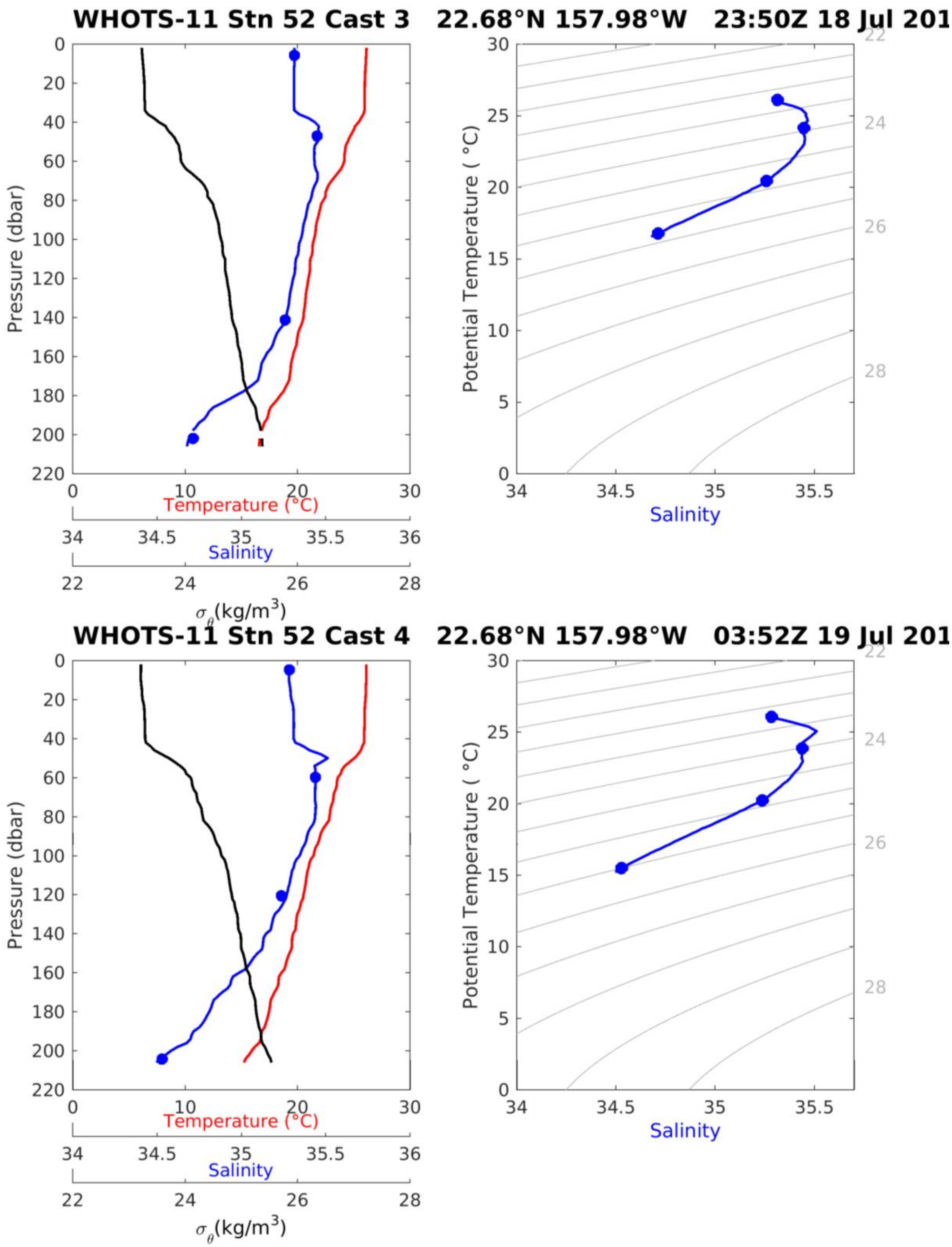

Figure 6-2. [Upper panels] Same as in Figure 6-1, but for station 52, cast 3.
[Lower panels] Same as in Figure 6-1, but for station 52, cast 4.

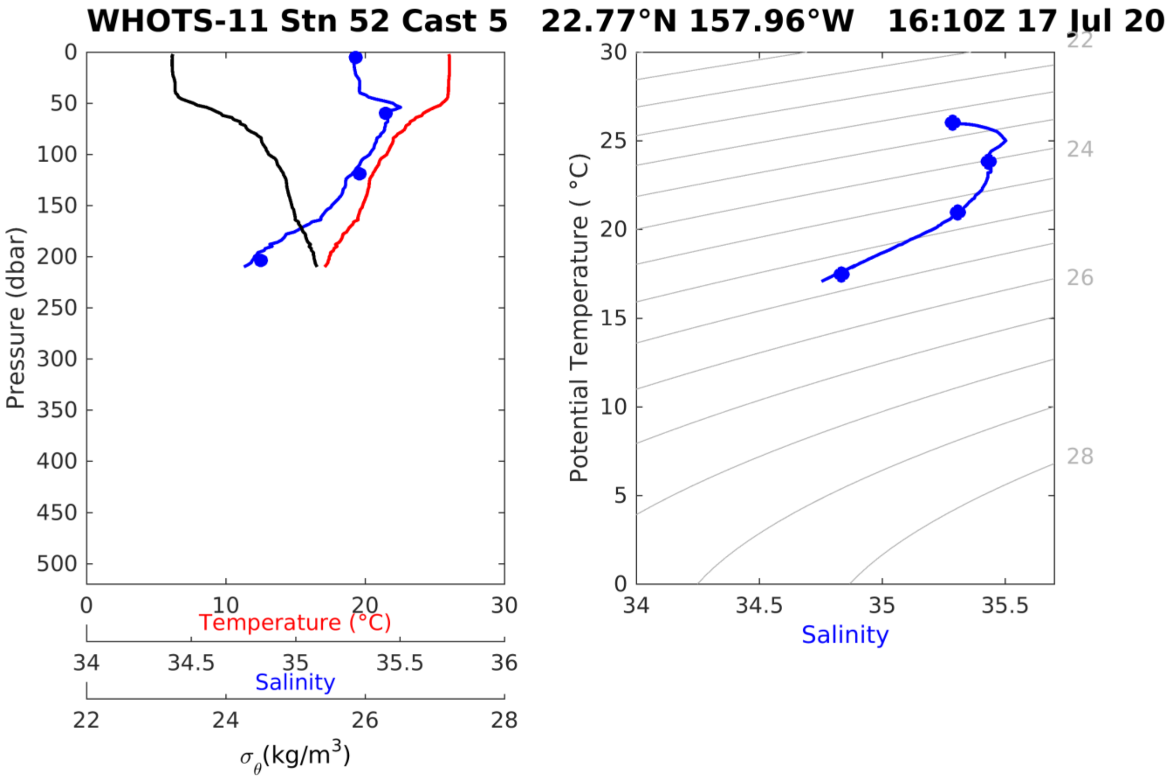

Figure 6-3. Same as in Figure 6-1, but for station 52, cast 5.

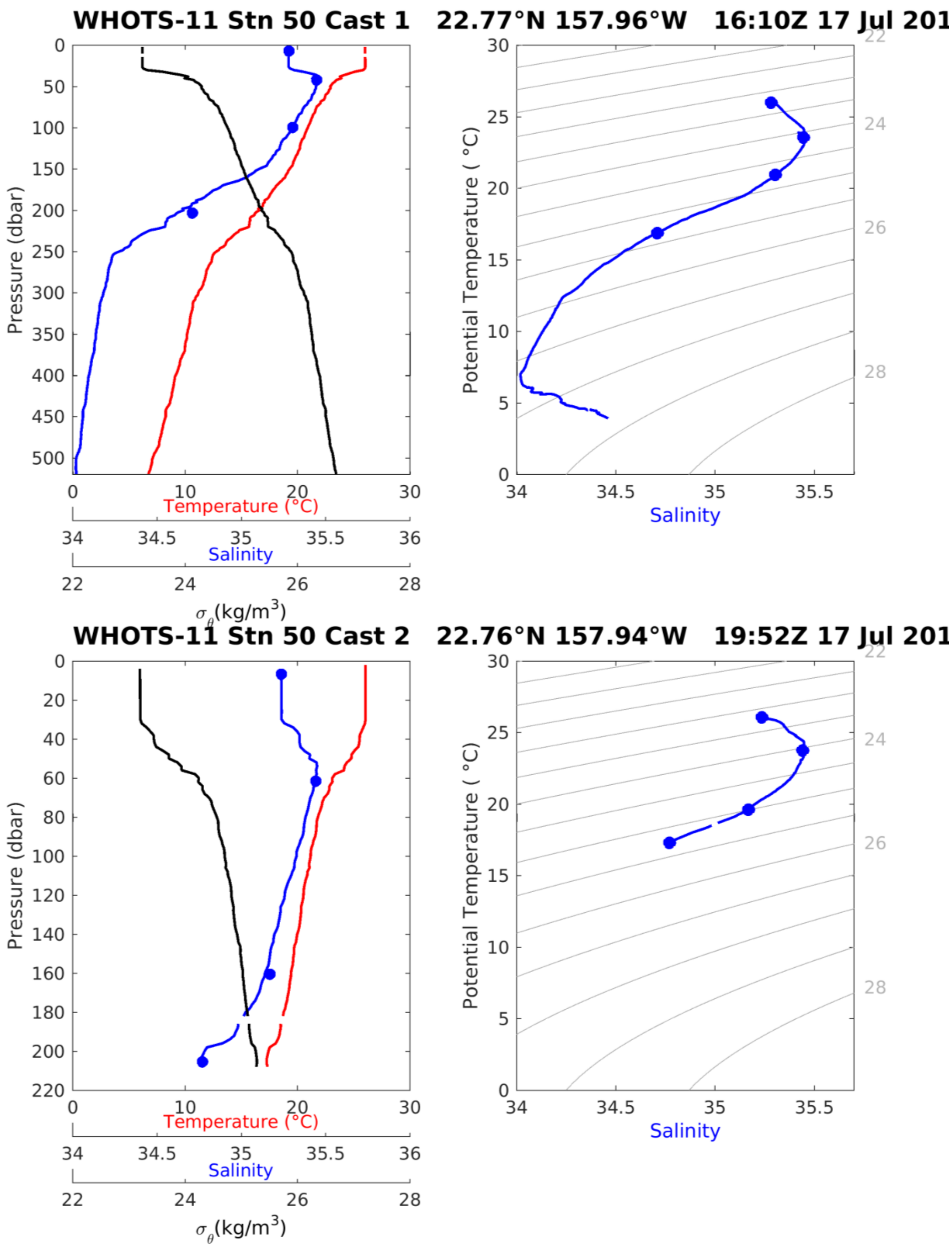

Figure 6-4 [Upper panels] Same as in Figure 6-1, but for station 50 cast 1.
[Lower panels] Same as in Figure 6-1, but for station 50 cast 2.

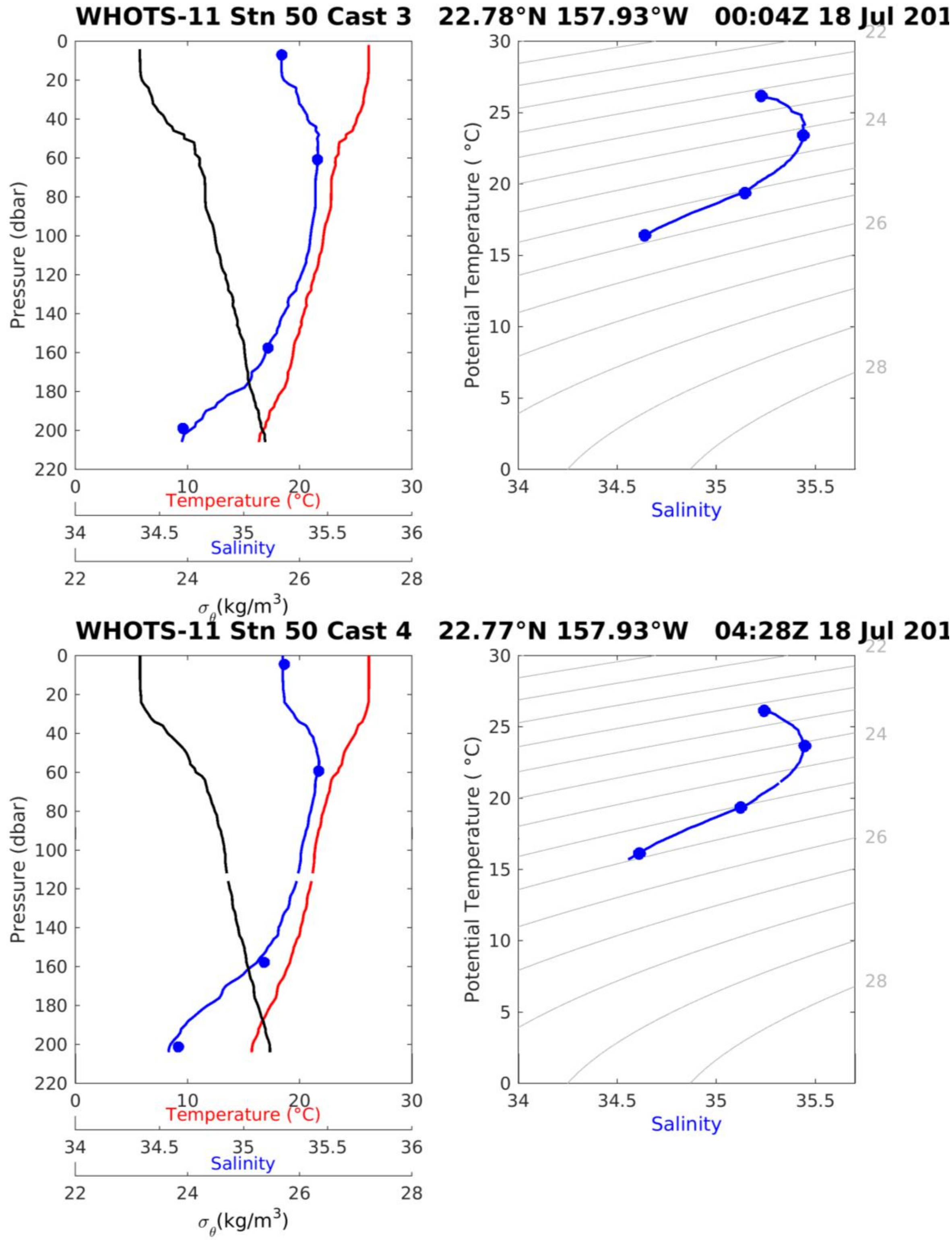

Figure 6-5. [Upper panels] Same as in Figure 6-1, but for station 50 cast 3.
[Lower panels] Same as in Figure 6-1, but for station 50 cast 4.

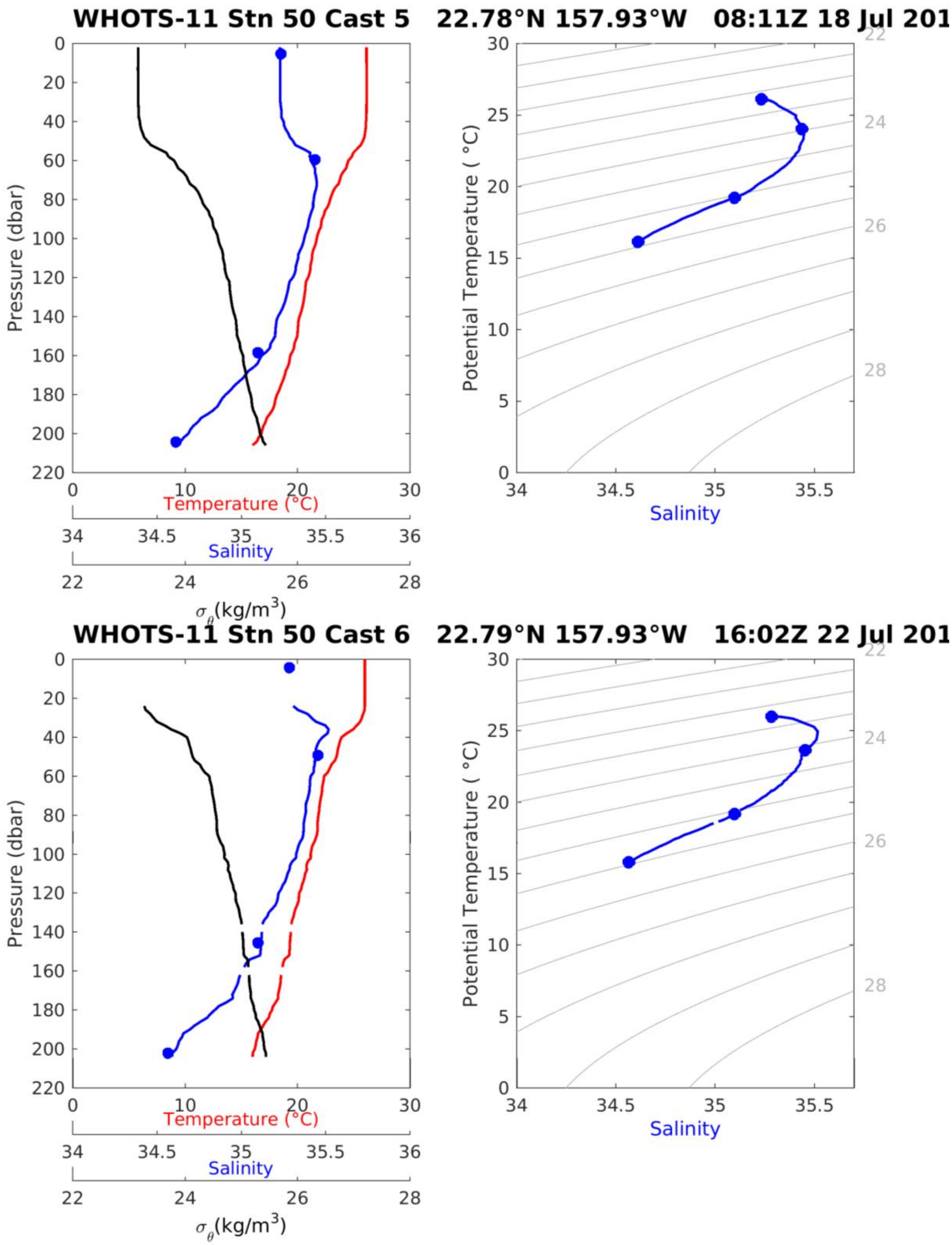

Figure 6-6 [Upper panels] Same as in Figure 6-1, but for station 50 cast 5.
[Lower panels] Same as in Figure 6-1, but for station 50 cast 6.

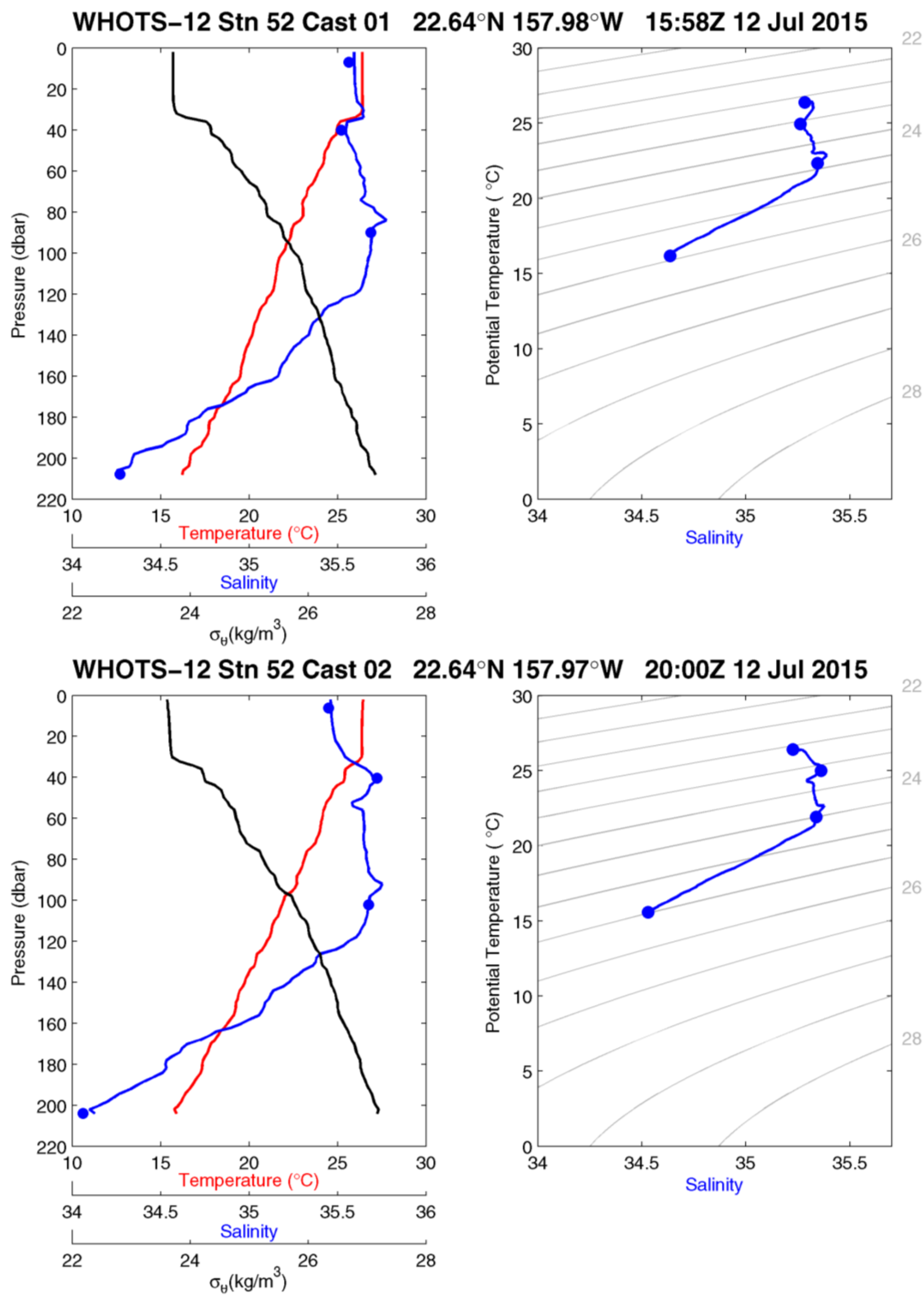

Figure 6-7. [Left panels] Profiles of CTD temperature, salinity, and potential density (σ_θ) as a function of pressure, including discrete bottle salinity samples (when available) for station 52 cast 1 (top left) and cast 2 (bottom left) during the WHOTS-12 cruise.
[Right panels] Profiles of CTD salinity as a function of potential temperature, including discrete bottle salinity samples (when available) for station 52 cast 1 (top right) and cast 2 (bottom right) during the WHOTS-12 cruise.

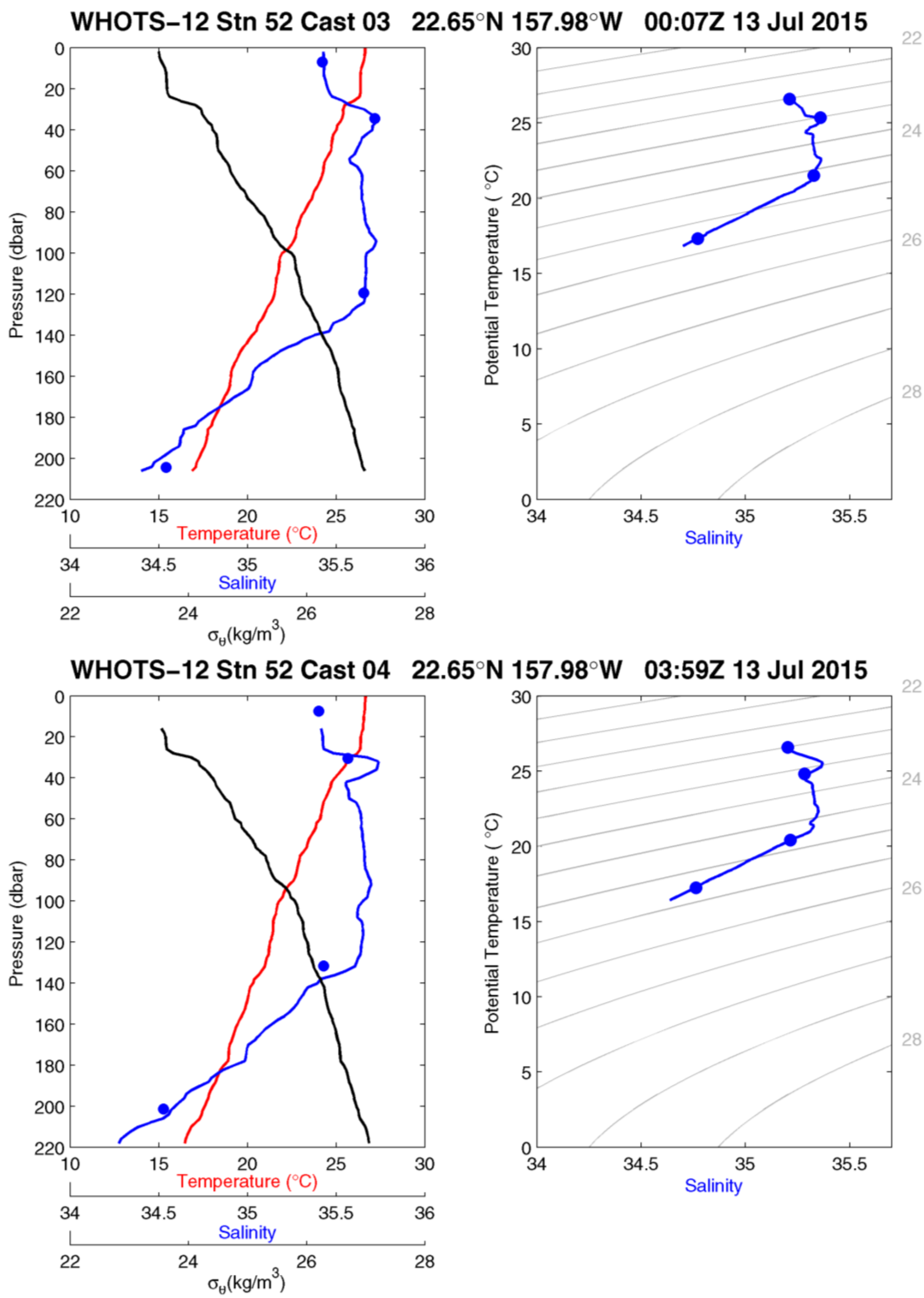

Figure 6-8. [Upper panels] Same as in Figure 6-7, but for station 52, cast 3.
[Lower panels] Same as in Figure 6-7, but for station 52, cast 4.

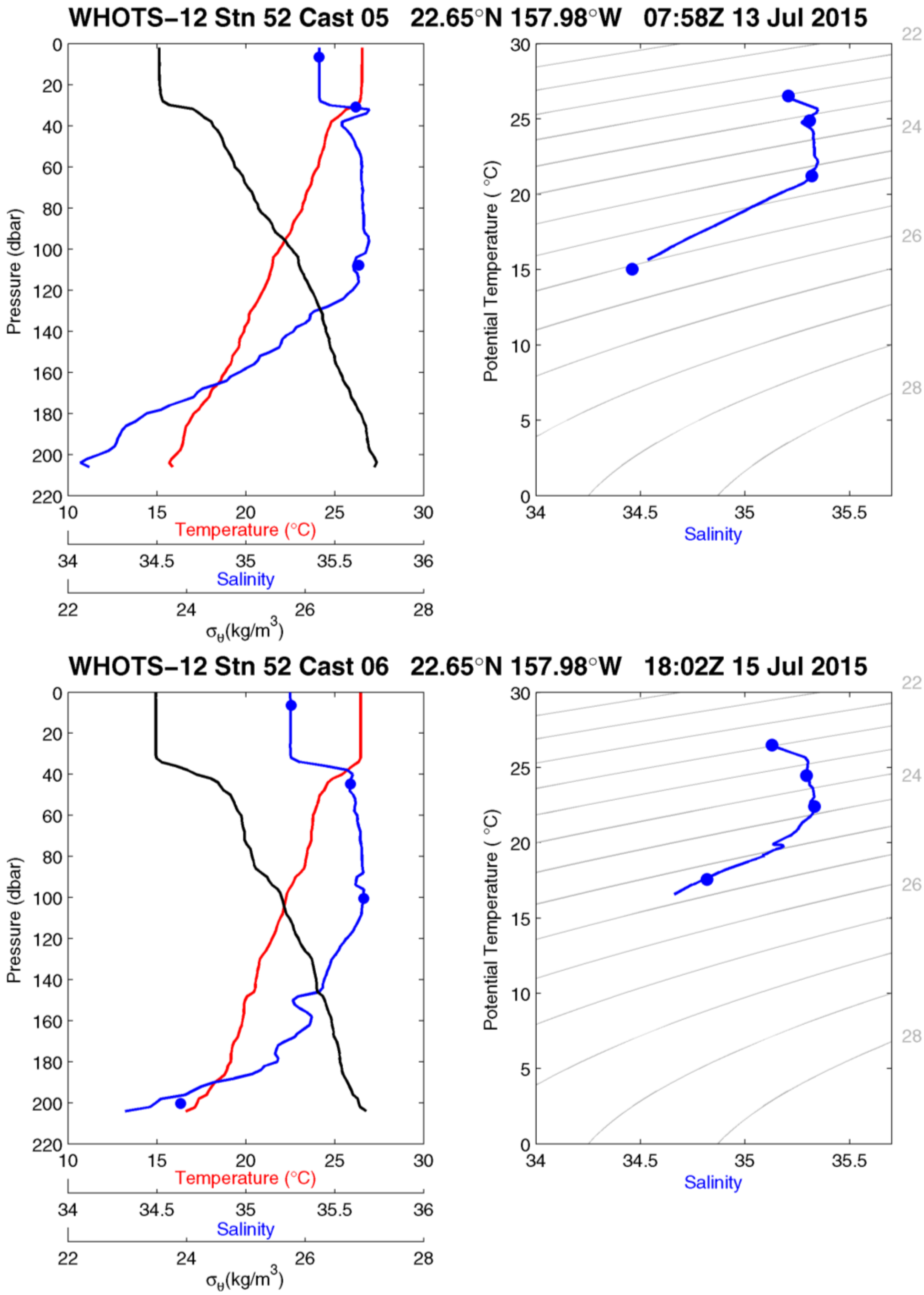

Figure 6-9. [Upper panels] Same as in Figure 6-7, but for station 52, cast 5.
[Lower panels] Same as in Figure 6-7, but for station 52, cast 6.

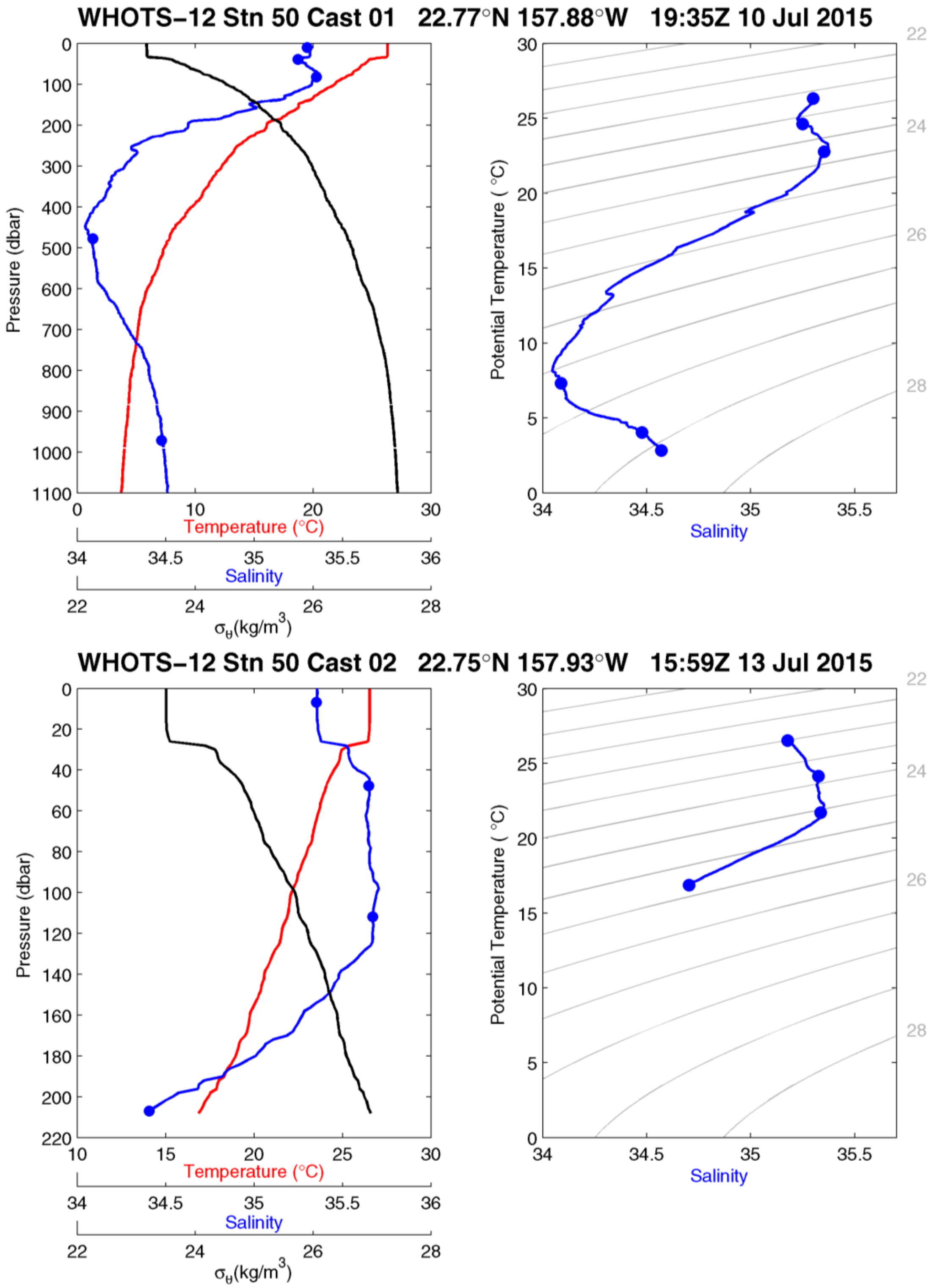

Figure 6-10. [Upper panels] Same as in Figure 6-7, but for station 50 cast 1.
[Lower panels] Same as in Figure 6-7, but for station 50 cast 2.

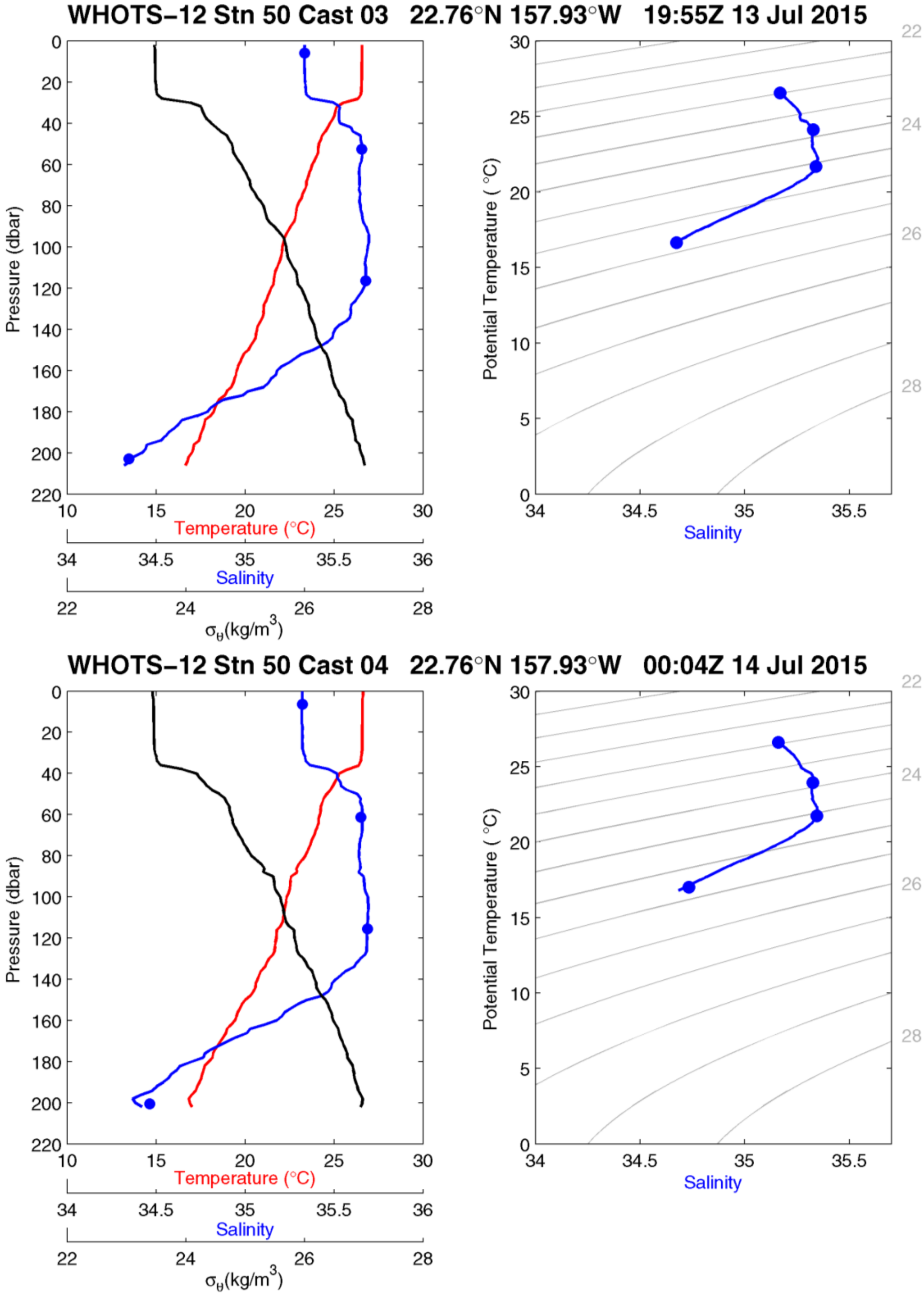

Figure 6-11. [Upper panels] Same as in Figure 6-7, but for station 50 cast 3.
[Lower panels] Same as in Figure 6-7, but for station 50 cast 4.

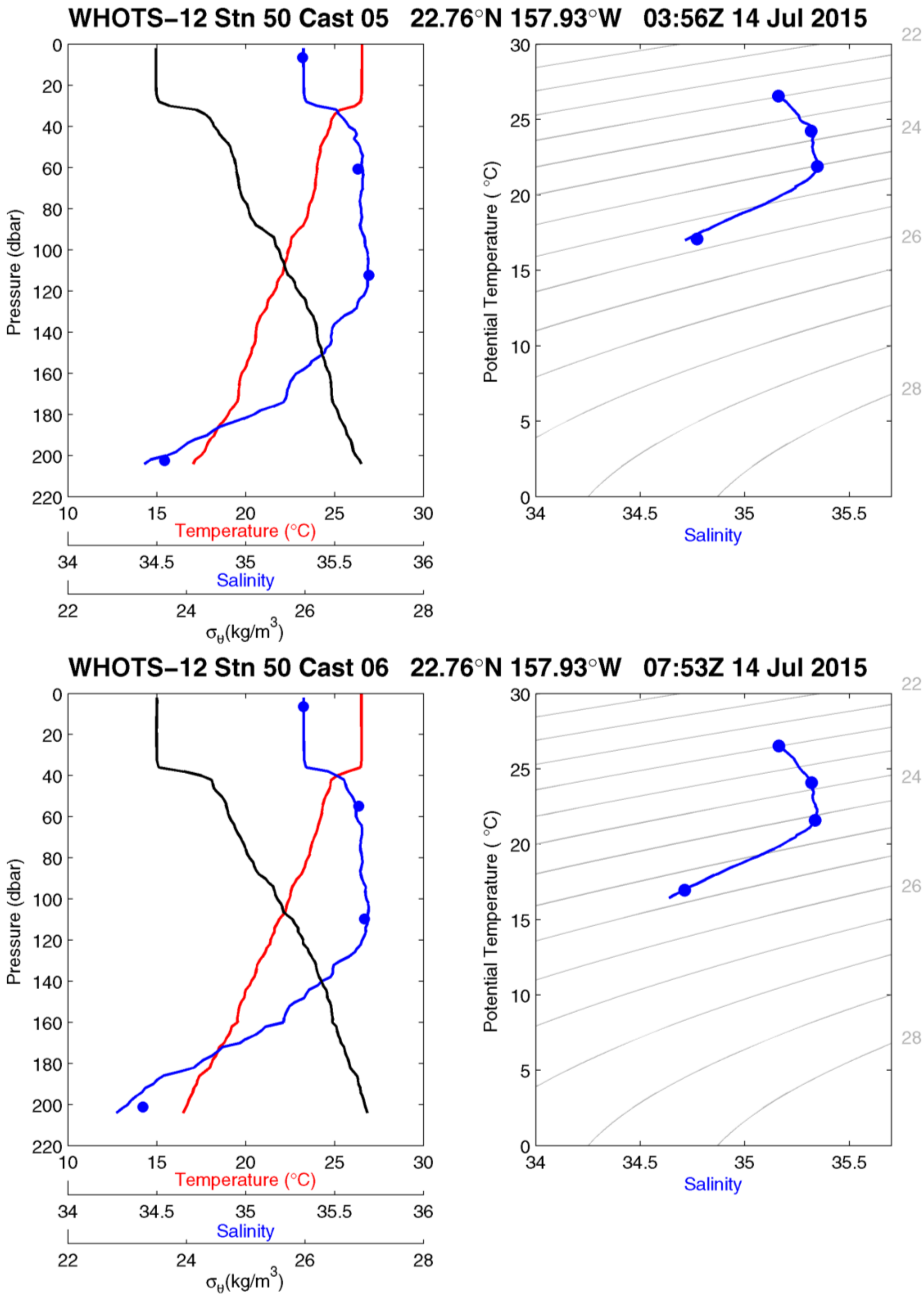

Figure 6-12. [Upper panels] Same as in Figure 6-7, but for station 50 cast 5.
[Lower panels] Same as in Figure 6-1, but for station 50 cast 6.

B. Thermosalinograph Data

Underway measurements of near surface temperature and near surface salinity from thermosalinograph system and navigational data for the WHOTS-11 cruise are presented in

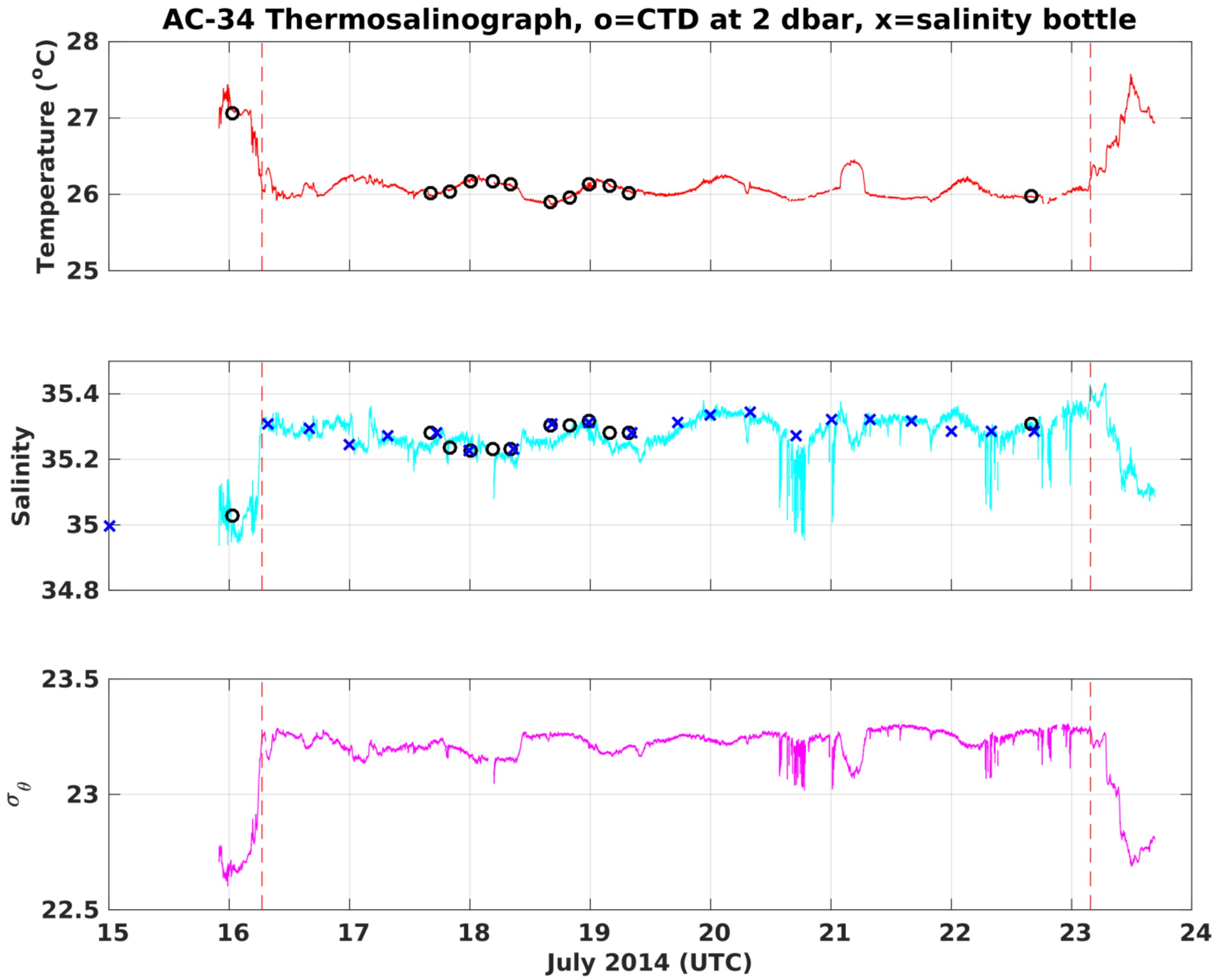

Figure 6-13a and 6-13b, respectively. The corresponding thermosalinograph data during the WHOTS-12 cruise are shown in Figures and Figure 6-a and 6-14b.

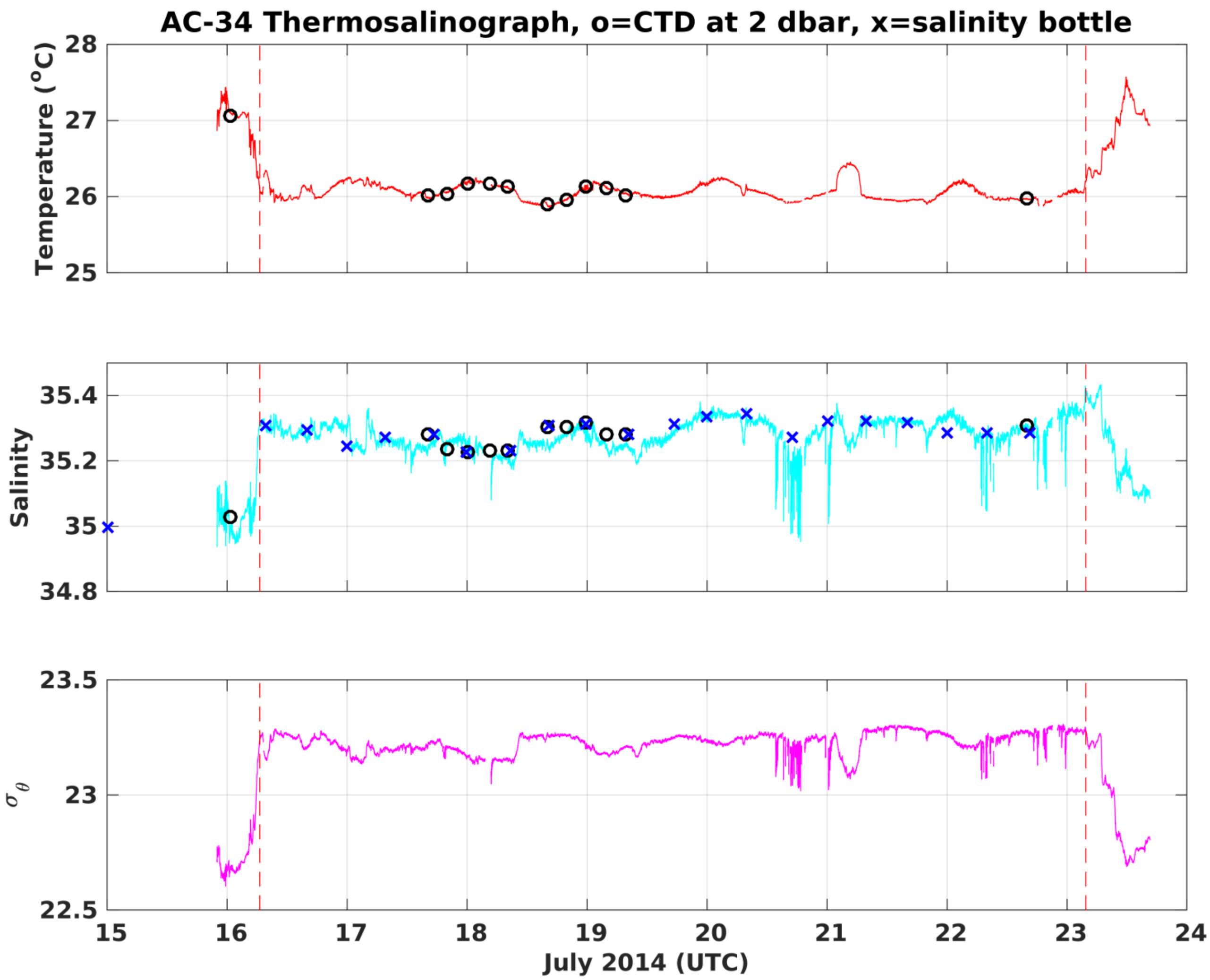

Figure 6-13a. Final processed temperature (upper panel), salinity (middle panel) and potential density (σ_θ) (lower panel) data from the continuous underway system on board the R/V Hi'ialakai during the WHOTS-11 cruise. Temperature and salinity taken from 6-dbar CTD data (circles) and salinity bottle sample data (crosses) are superimposed. The dashed vertical red line indicates the period of occupation of Station ALOHA and the WHOTS site.

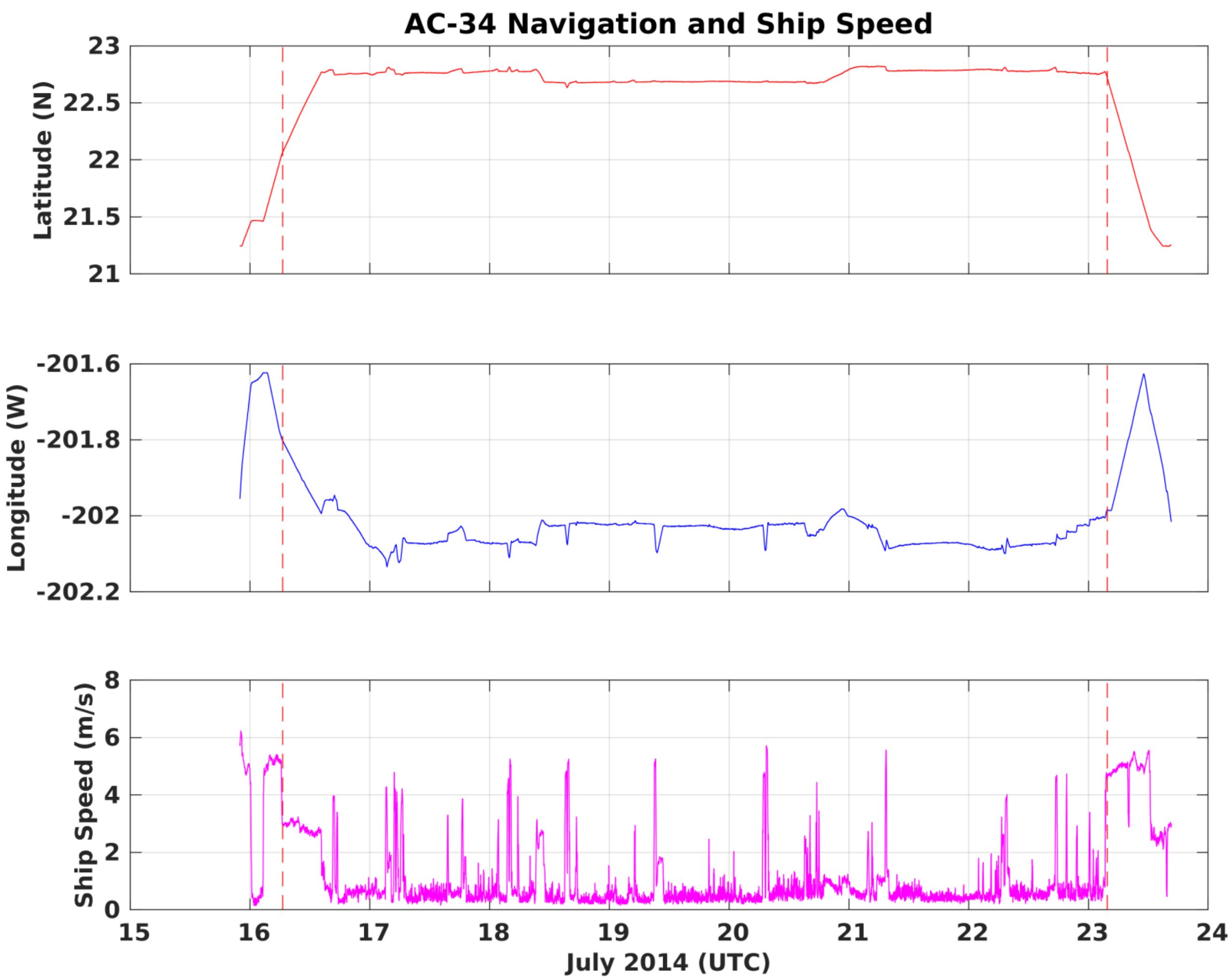

Figure 6-13b. Timeseries of latitude (upper panel), longitude (middle panel), and ship's speed (lower panel) during the WHOTS-11 cruise.

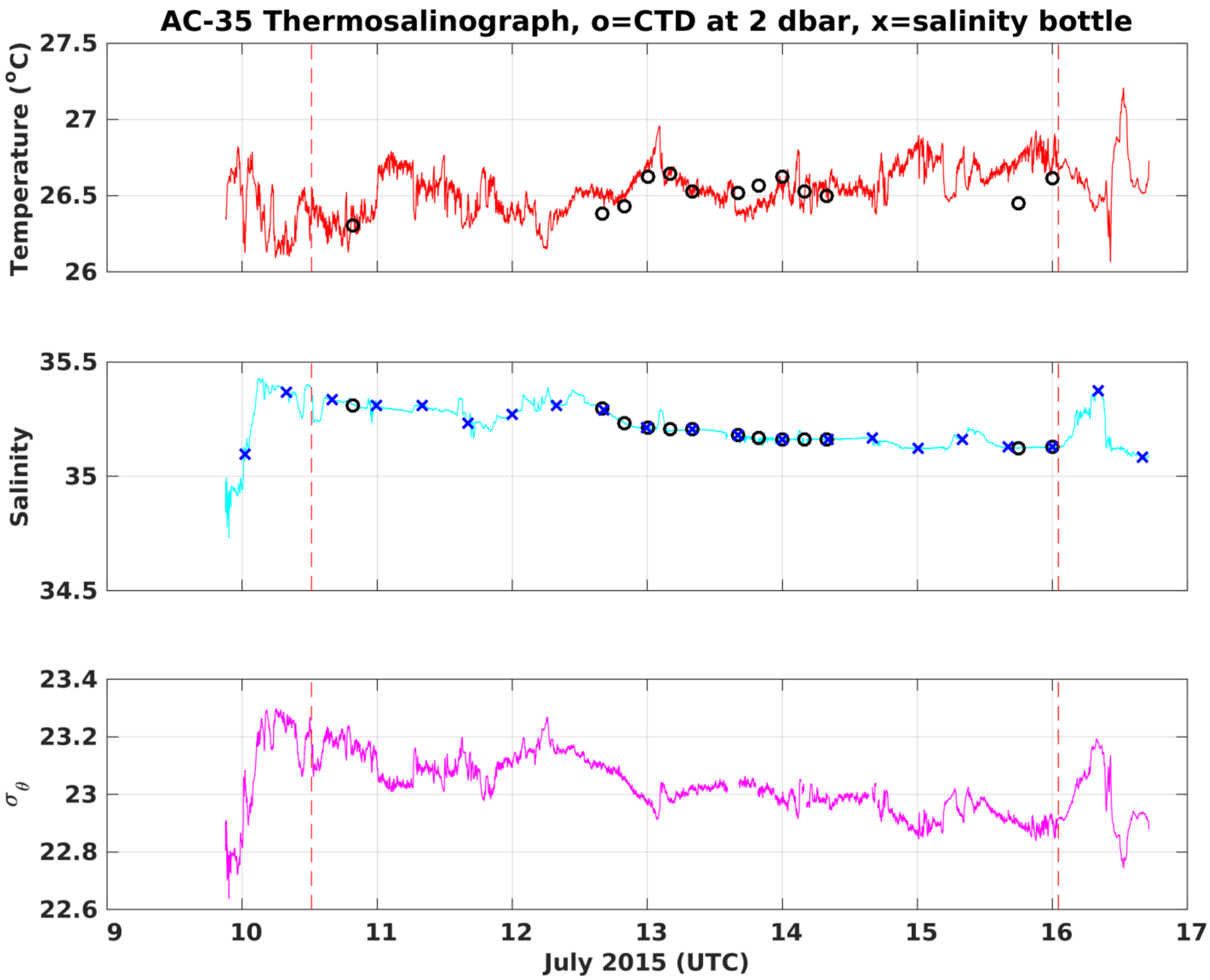

Figure 6-24a. Final processed temperature (upper panel), salinity (middle panel) and potential density (σ_θ) (lower panel) data from the continuous underway system on board the R/V Hi'ialakai during the WHOTS-12 cruise. Temperature and salinity taken from 6-dbar CTD data (circles) and salinity bottle sample data (crosses) are superimposed. The dashed vertical red line indicates the period of occupation of Station ALOHA and the WHOTS site.

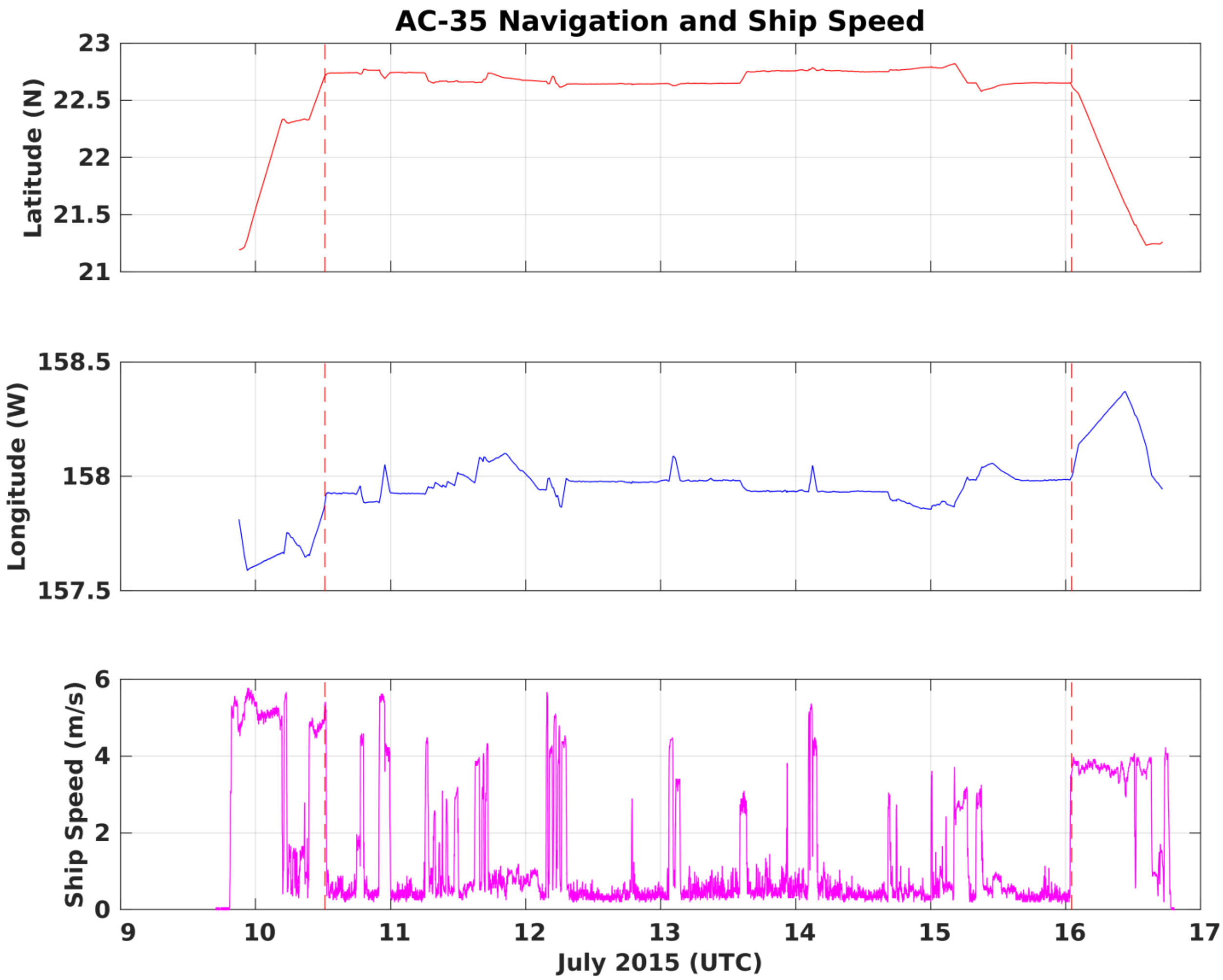

Figure 6-14b. Timeseries of latitude (upper panel), longitude (middle panel), and ship's speed (lower panel) during the WHOTS-12 cruise.

C. MicroCAT/SeaCAT Data

The temperature measured by MicroCATs during the mooring deployment is presented in Figure 6-15 to Figure 6-23 for each of the depths where the instruments were located. The salinity is plotted in Figure 6-20 to Figure 6-284. The potential density (σ_θ) is plotted in Figure 6-5 to Figure 6-289.

Contoured plots of temperature and salinity as a function of depth are presented in Figure 6-30; and contoured plots of potential density (σ_θ) as a function of depth, and of salinity as a function of σ_θ are in

Figure 6-33.

The potential temperature and salinity measured by the deep SeaCATs during the mooring deployment are shown in Figure 6-32. Also shown in the plot are the potential temperature and salinity data obtained with a MicroCAT (SBE-37) installed in the ALOHA Cabled Observatory, about 6 nautical miles west from the WHOTS-11 anchor, the instrument is located 2 m above the bottom.

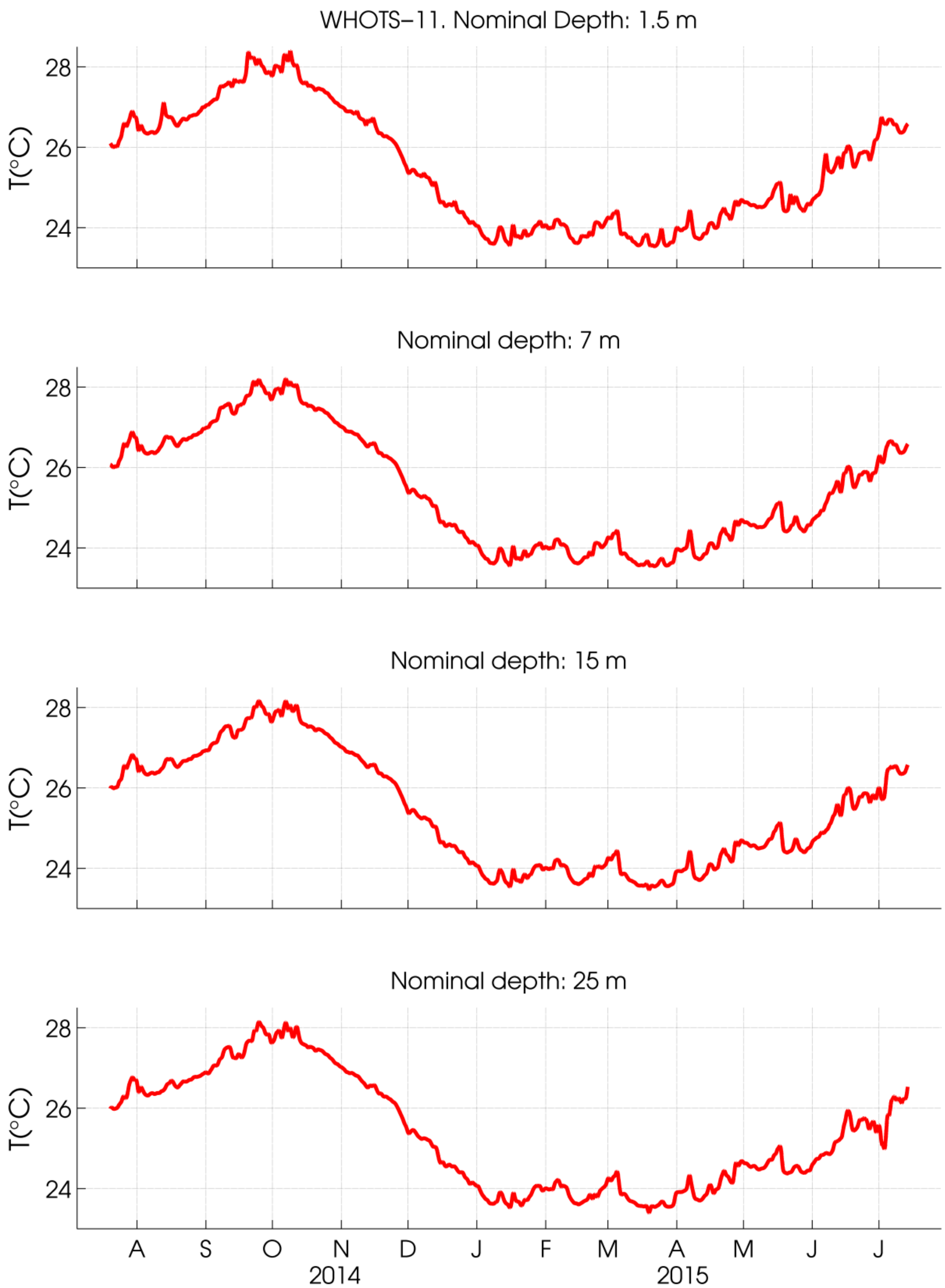

Figure 6-15. Temperatures from MicroCATs during WHOTS-11 deployment at 1.5, 7, 15, and 25 m.

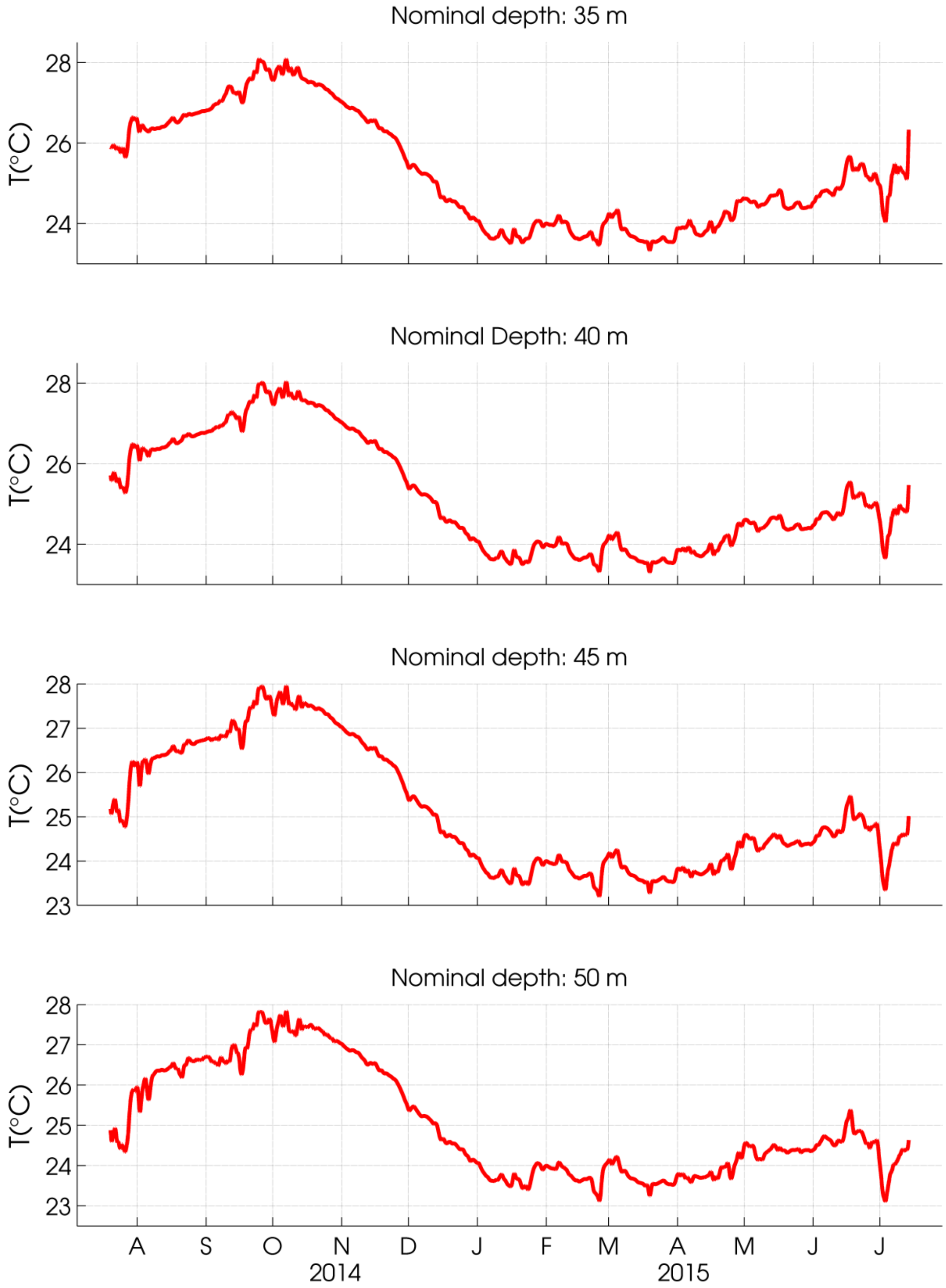

Figure 6-16. Same as in Figure 6-5, but at 35, 40, 45, and 50 m.

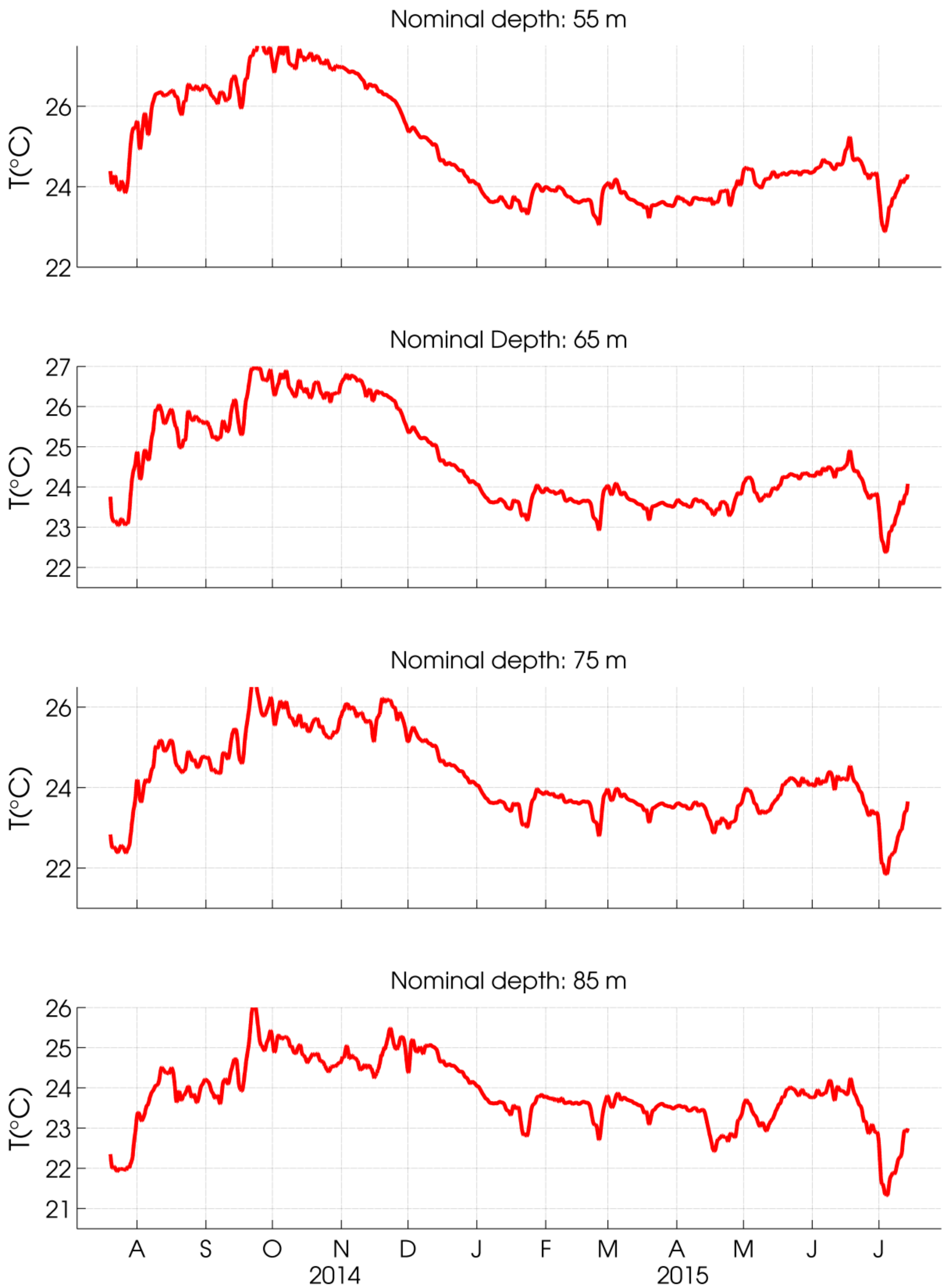

Figure 6-17. Same as in Figure 6-5, but at 55, 65, 75, and 85 m.

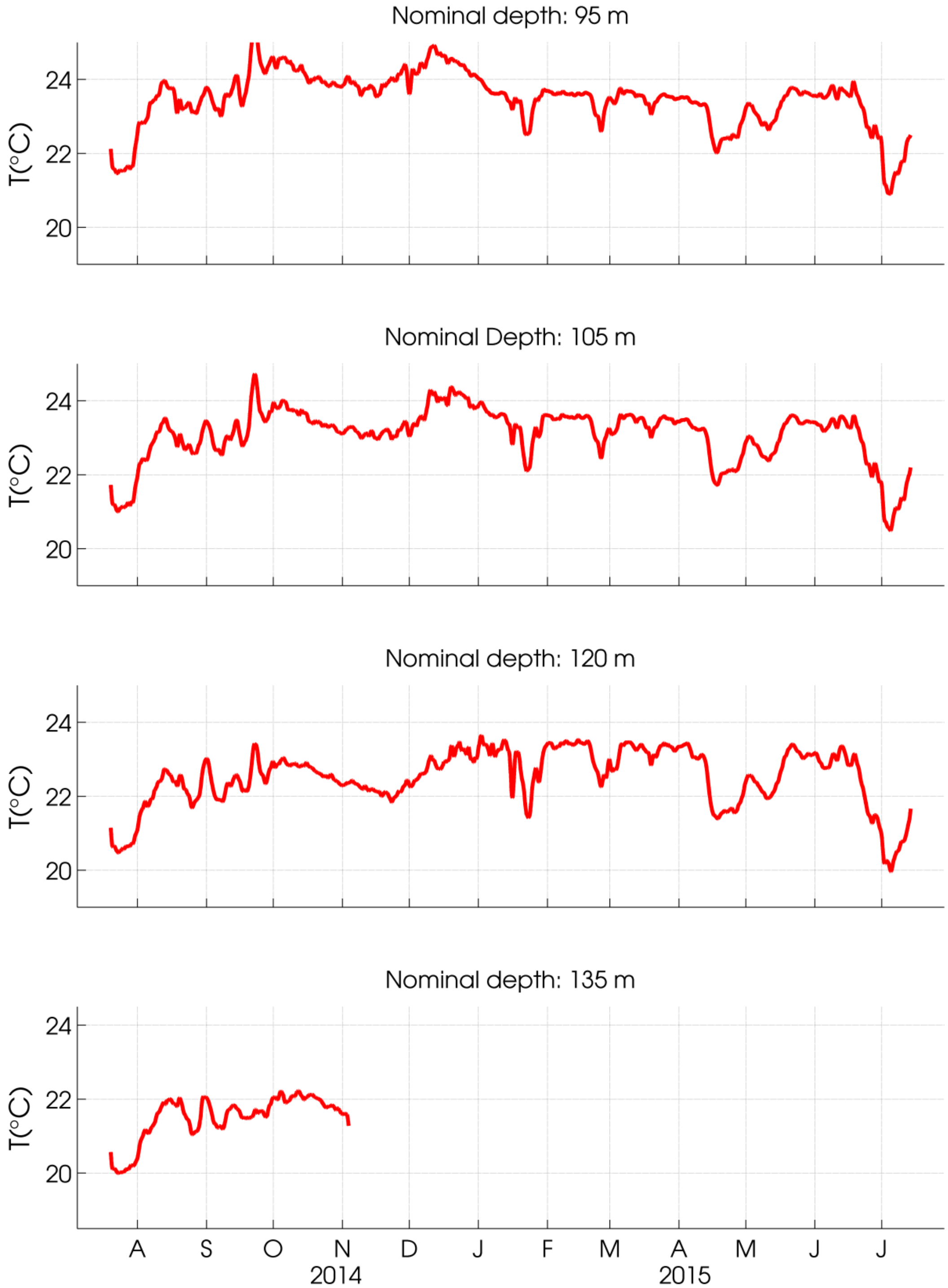

Figure 6-18. Same as in Figure 6-5, but at 95, 105, 120, and 135 m.

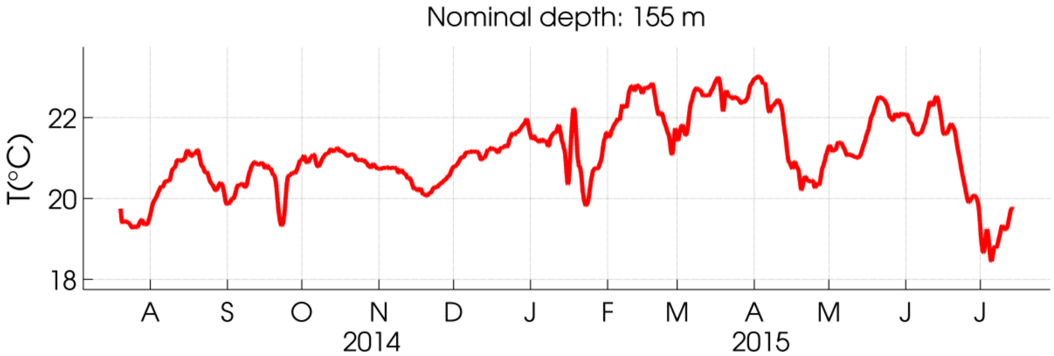

Figure 6-19. Same as in Figure 6-5, but at 155 m.

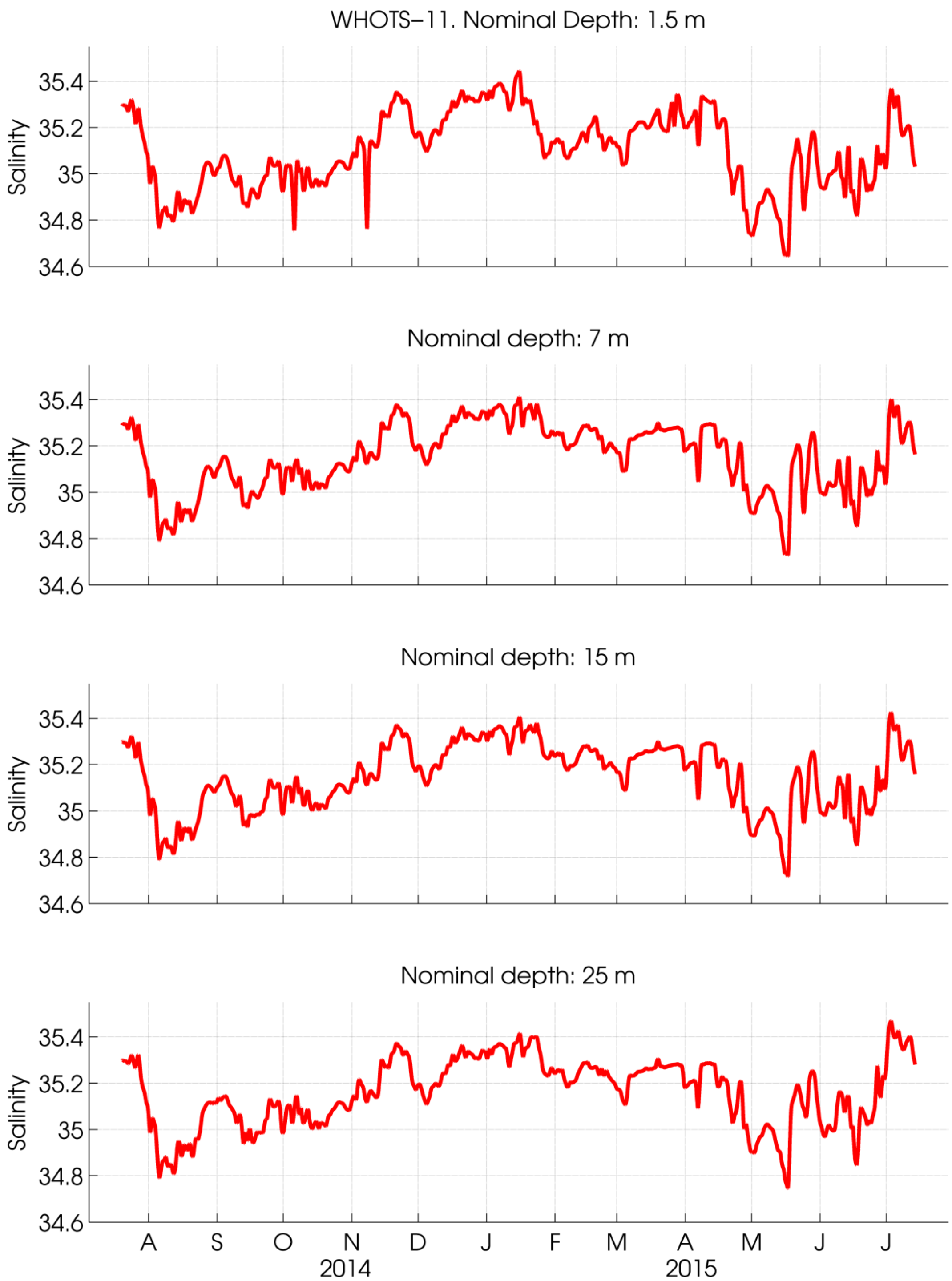

Figure 6-20. Salinities from MicroCATs during WHOTS-11 deployment at 1.5, 7, 15, and 25 m.

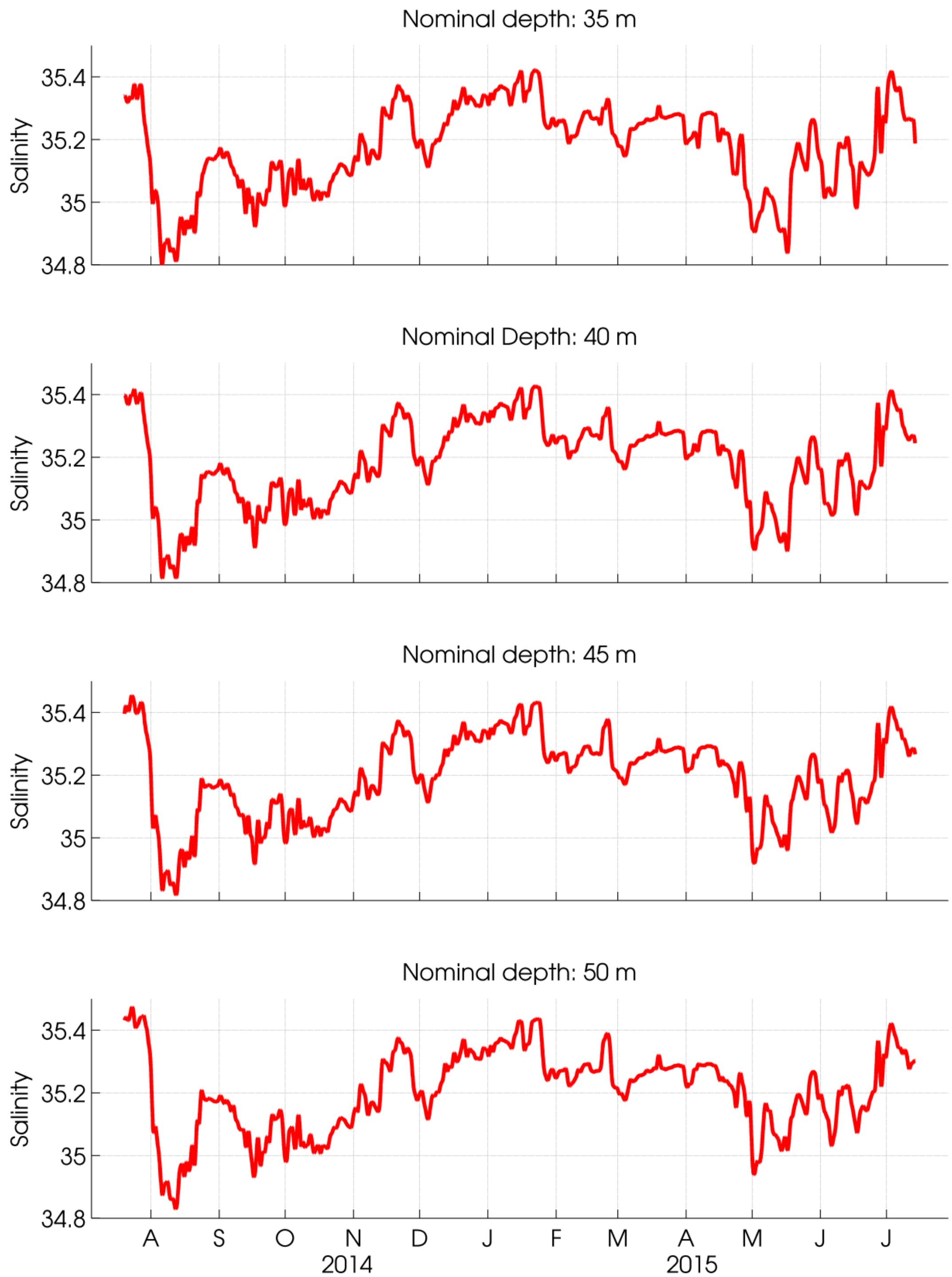

Figure 6-21. Same as in Figure 6-20, but at 35, 40, 45, and 50 m.

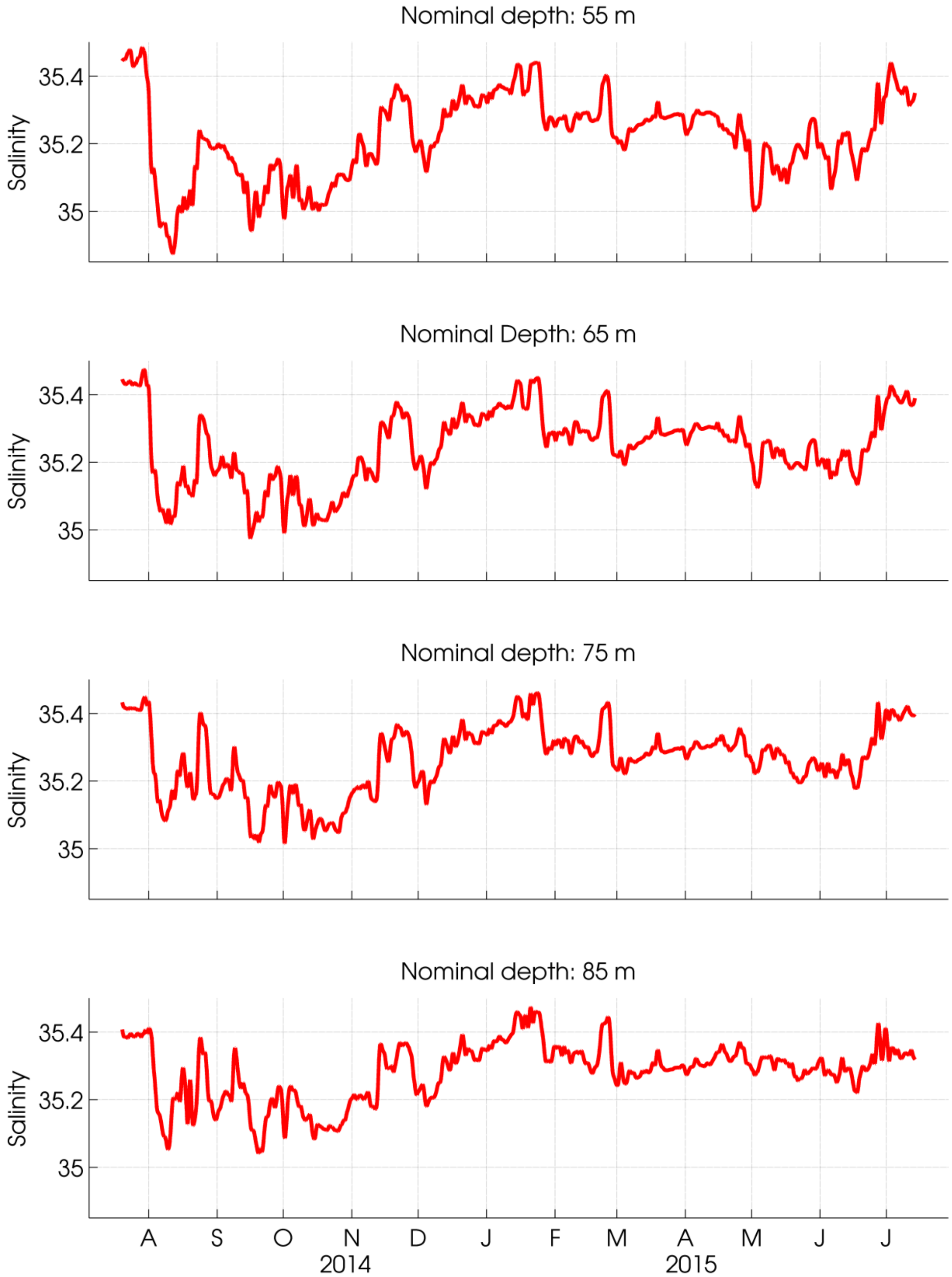

Figure 6-22. Same as in Figure 6-20, but at 55, 65, 75, and 85 m.

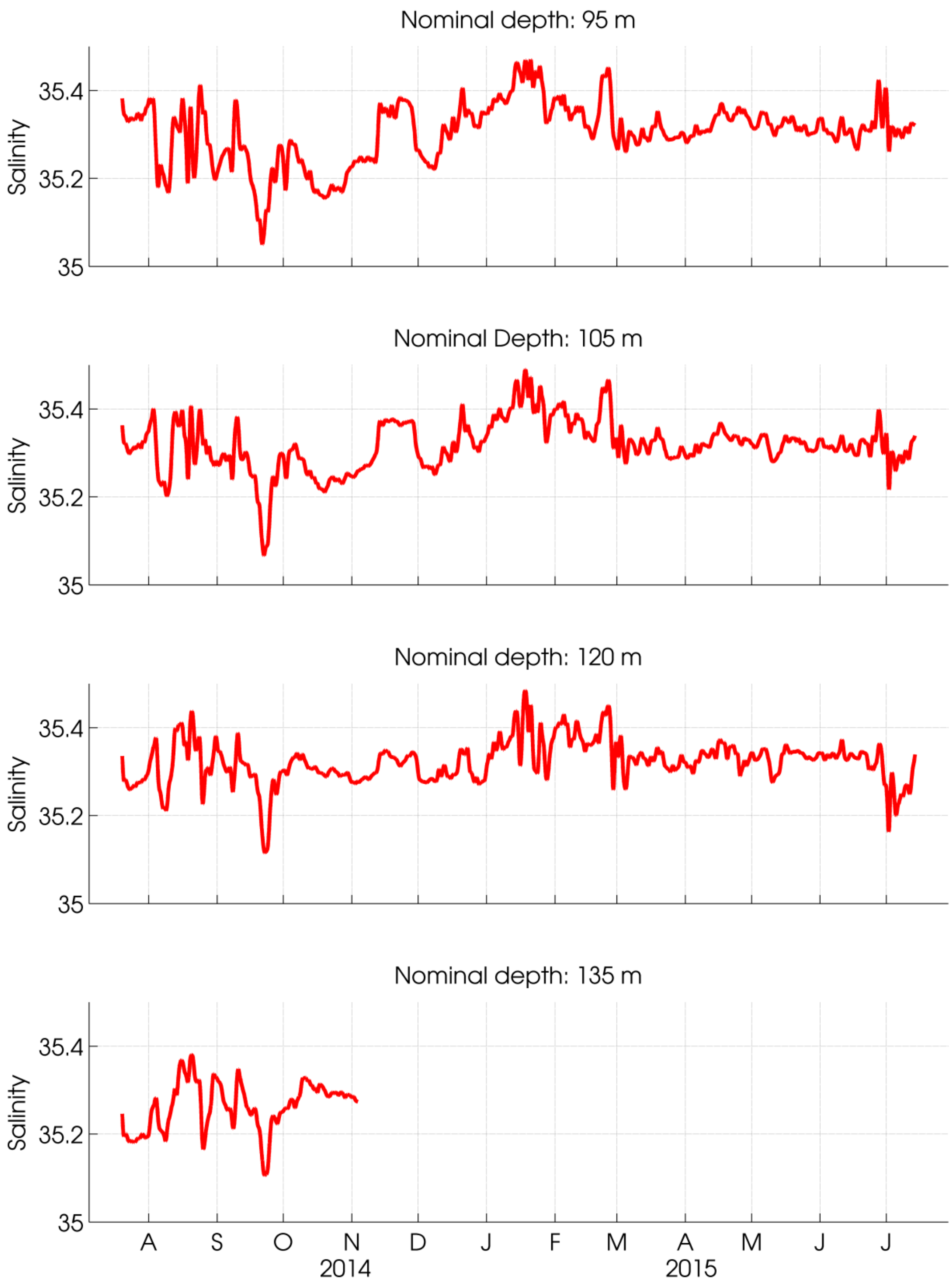

Figure 6-23. Same as in Figure 6-20, but at 95, 105, 120, and 135 m.

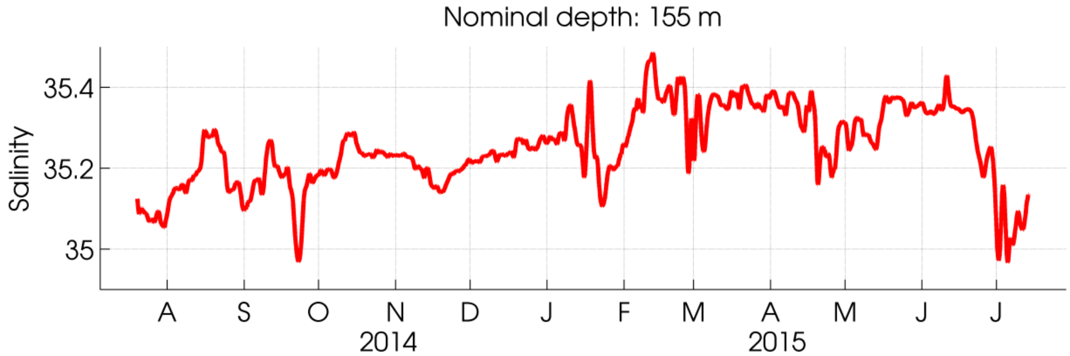

Figure 6-24. Same as in Figure 6-20, but at 155 m.

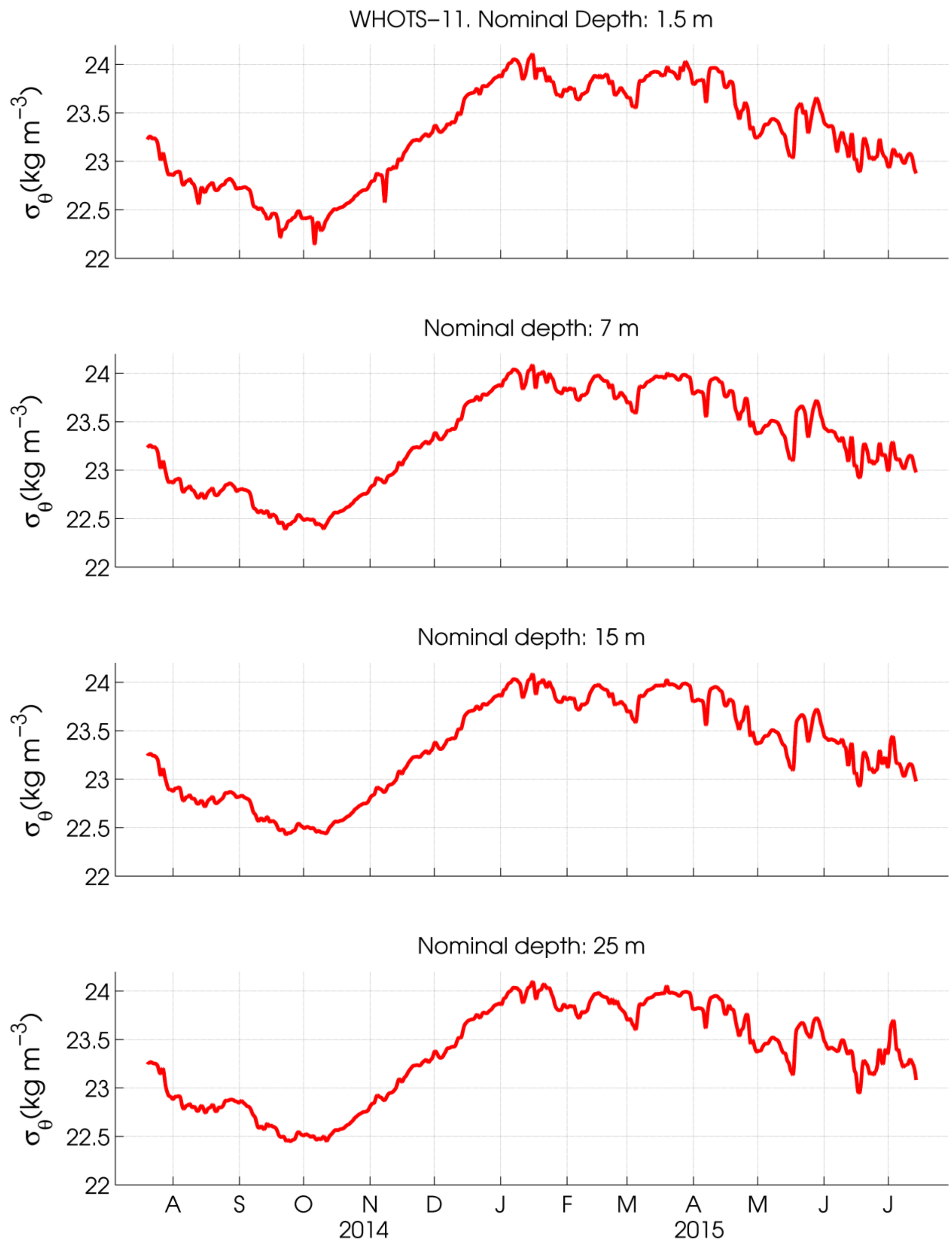

Figure 6-25. Potential densities (σ_θ) from MicroCATs during WHOTS-11 deployment at 1.5, 7, 15, and 25 m.

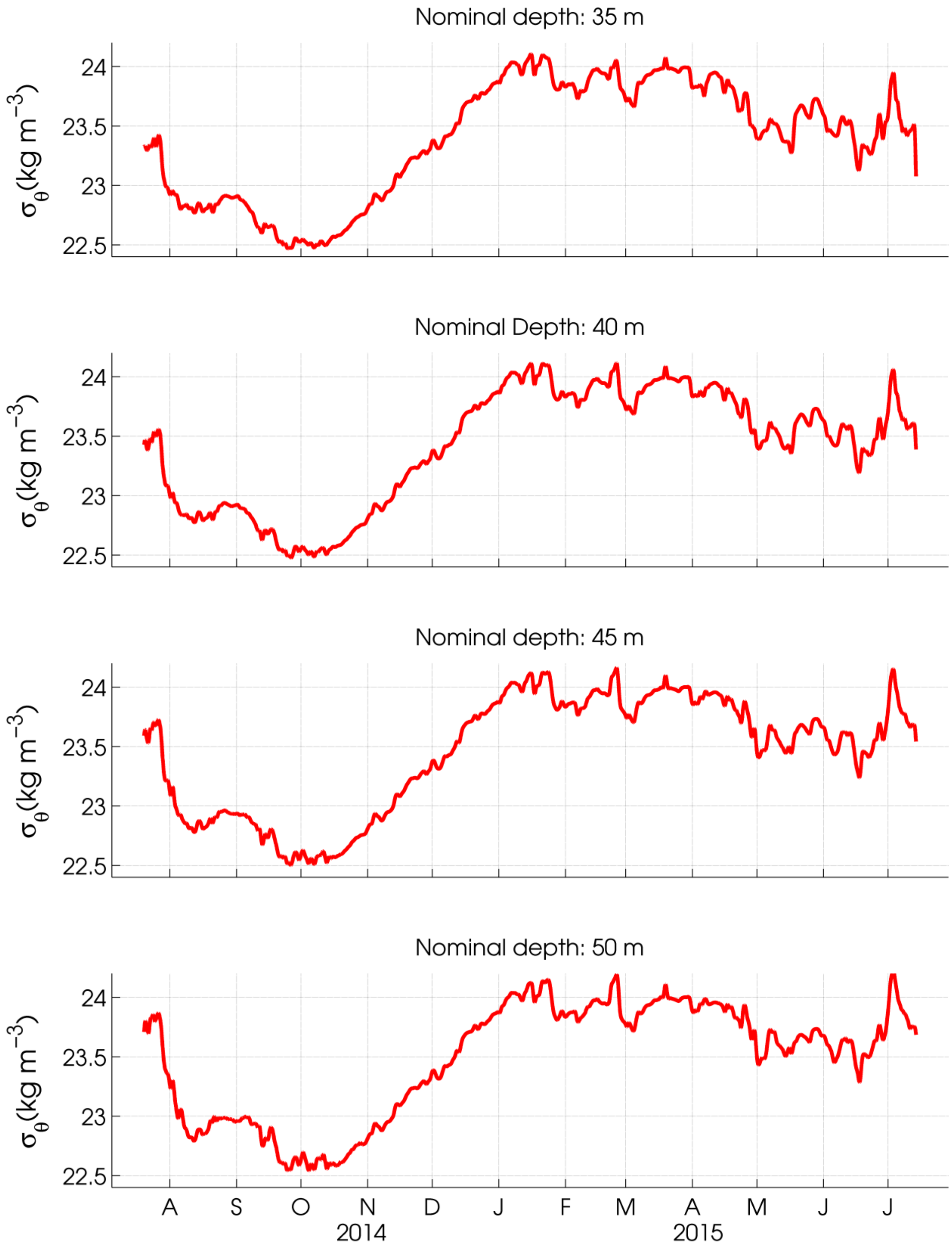

Figure 6-26. Same as in Figure 6-25, but at 35, 40, 45, and 50 m.

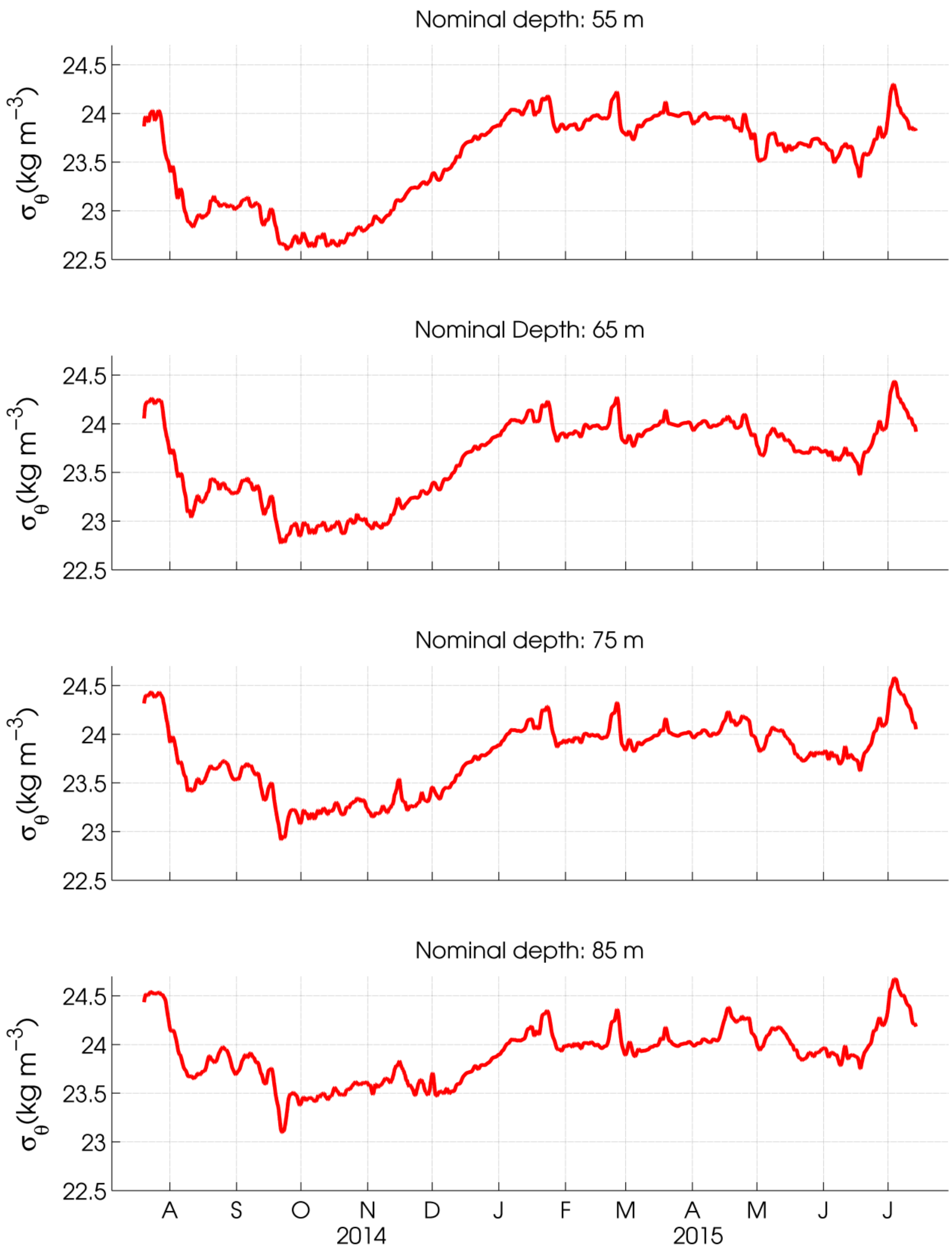

Figure 6-27 Same as in Figure 6-25, but at 55, 65, 75, and 85 m.

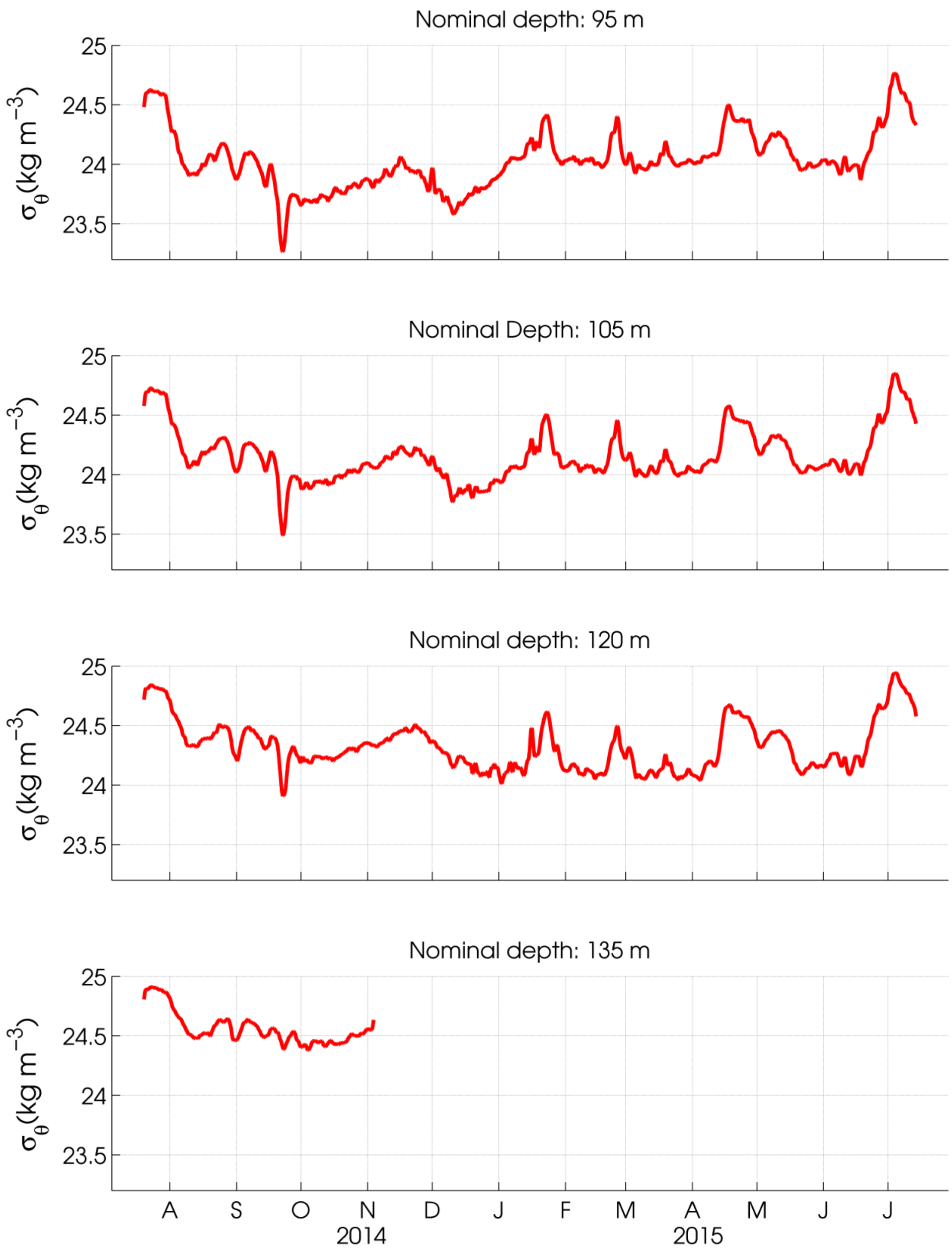

Figure 6-28. Same as in Figure 6-25, but at 95, 105, 120, and 135 m.

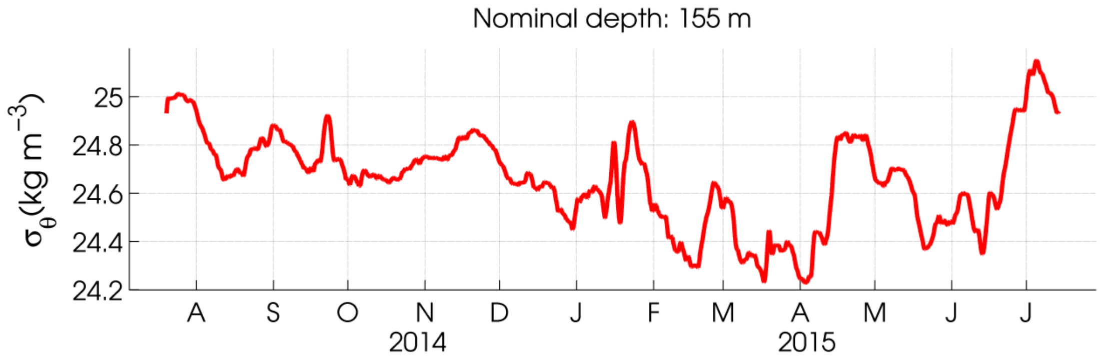

Figure 6-29. Same as in Figure 6-25, but at 155 m.

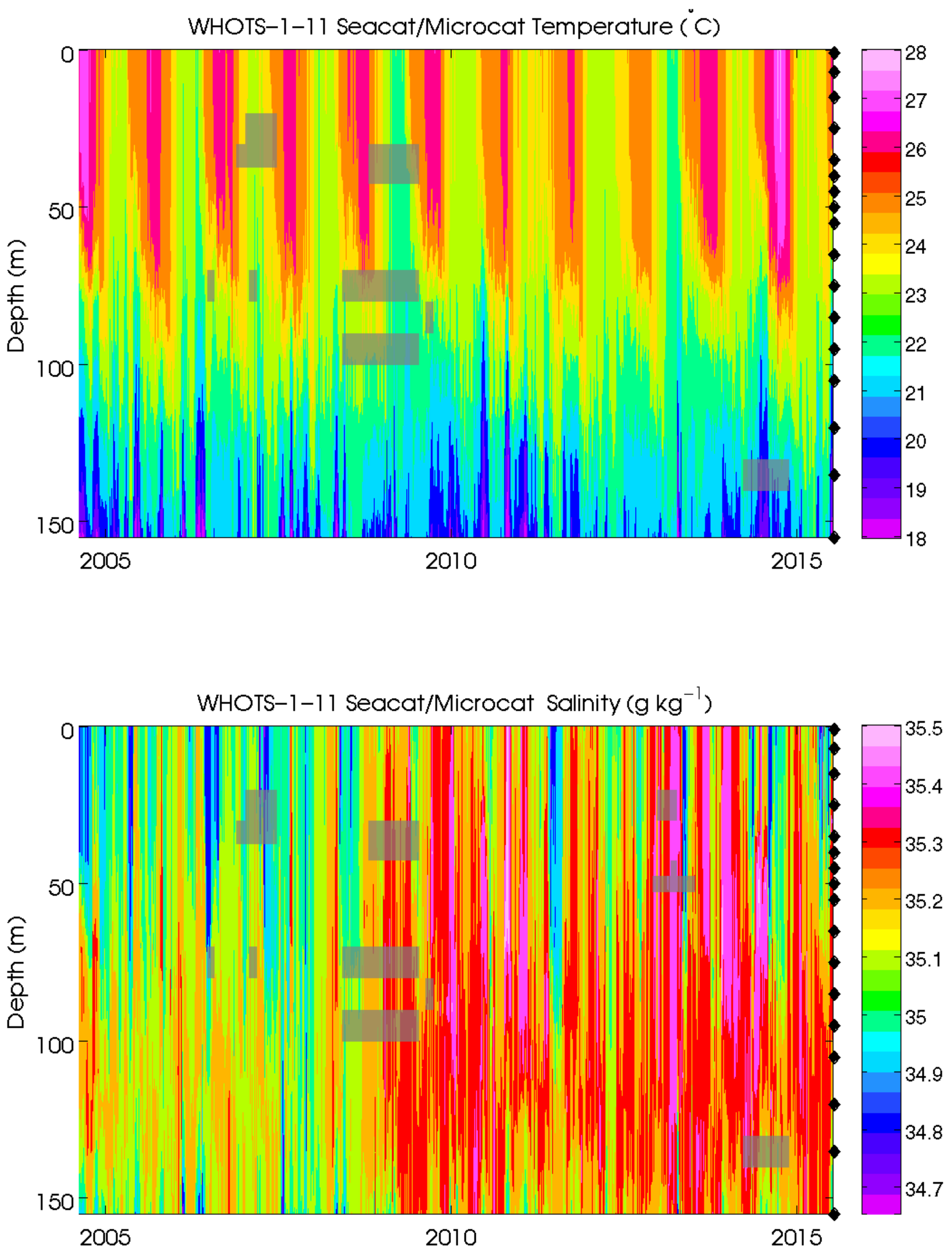

Figure 6-30. Contour plots of temperature (upper panel), and salinity (lower panel) versus depth from SeaCATs/ MicroCATs during WHOTS-1 through WHOTS-11 deployments. The shaded areas indicate missing data. The diamonds along the right axis indicate the instruments depths.

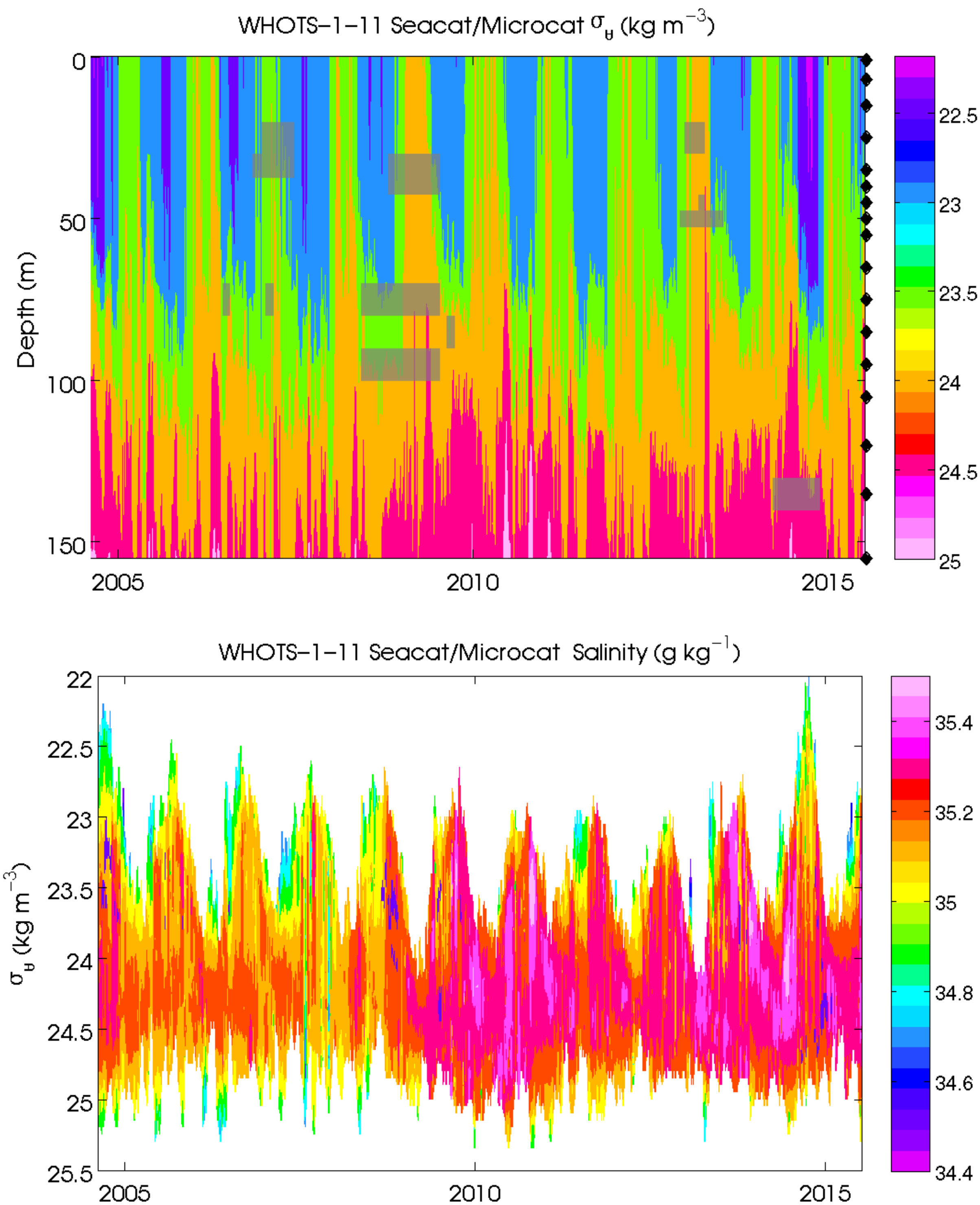

Figure 6-33. Contour plots of potential density (σ_θ , upper panel), versus depth, and of salinity versus σ_θ (lower panel) from SeaCATs/MicroCATs during WHOTS-1 through WHOTS-11 deployments. The shaded areas indicate missing data. The diamonds along the right axis in the upper figure indicate the instruments depths.

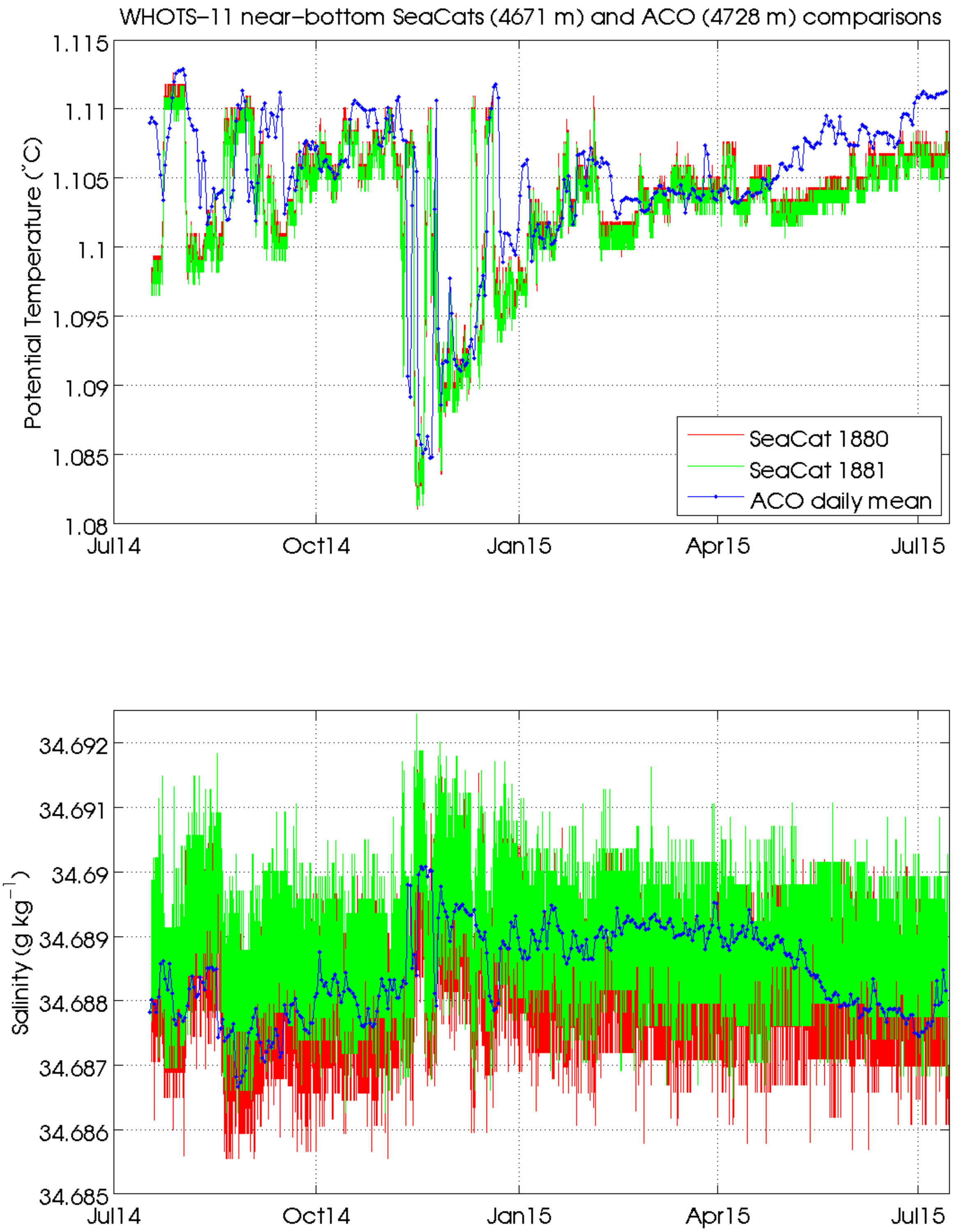

Figure 6-32 Potential temperature (upper panel) and salinity (lower panel) time-series from the ALOHA Cabled Observatory (ACO) sensors and from the WHOTS-11 SeaCATs 1880 and 1881.

D. Moored ADCP Data

Contoured plots of smoothed horizontal and vertical velocity as a function of depth during the mooring deployments 1 through 11 are presented in Figure 6- through

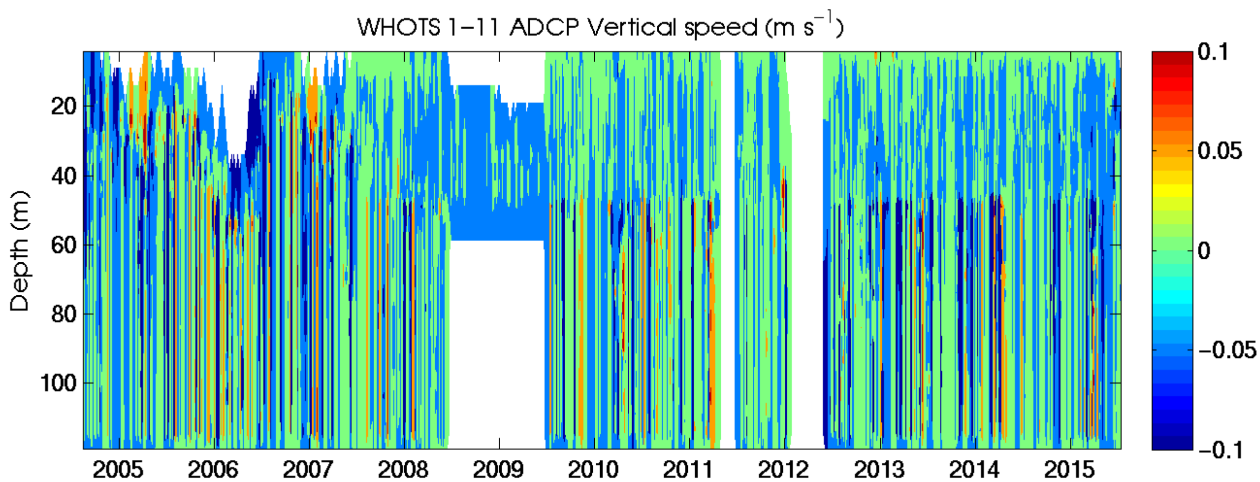

Figure 6-35. A staggered time-series of smoothed horizontal and vertical velocities are shown in Figure 6-36 through

Figure 6-38. Smoothing was performed by applying a daily running mean to the data and then interpolating the data on to an hourly grid.

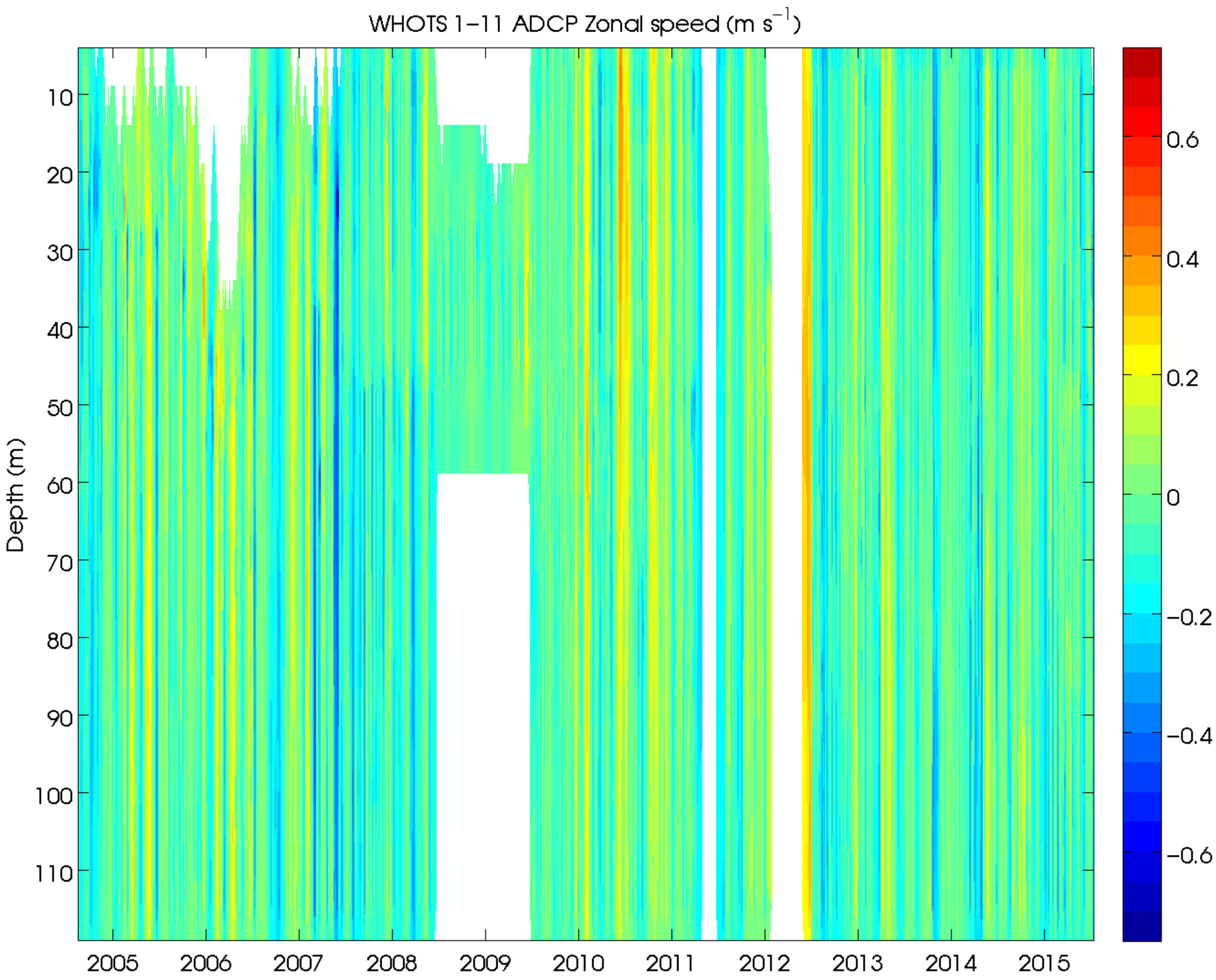

Figure 6-33. Contour plot of east velocity component (m s^{-1}) versus depth and time from the moored ADCPs from the WHOTS-1 through -11 deployments.

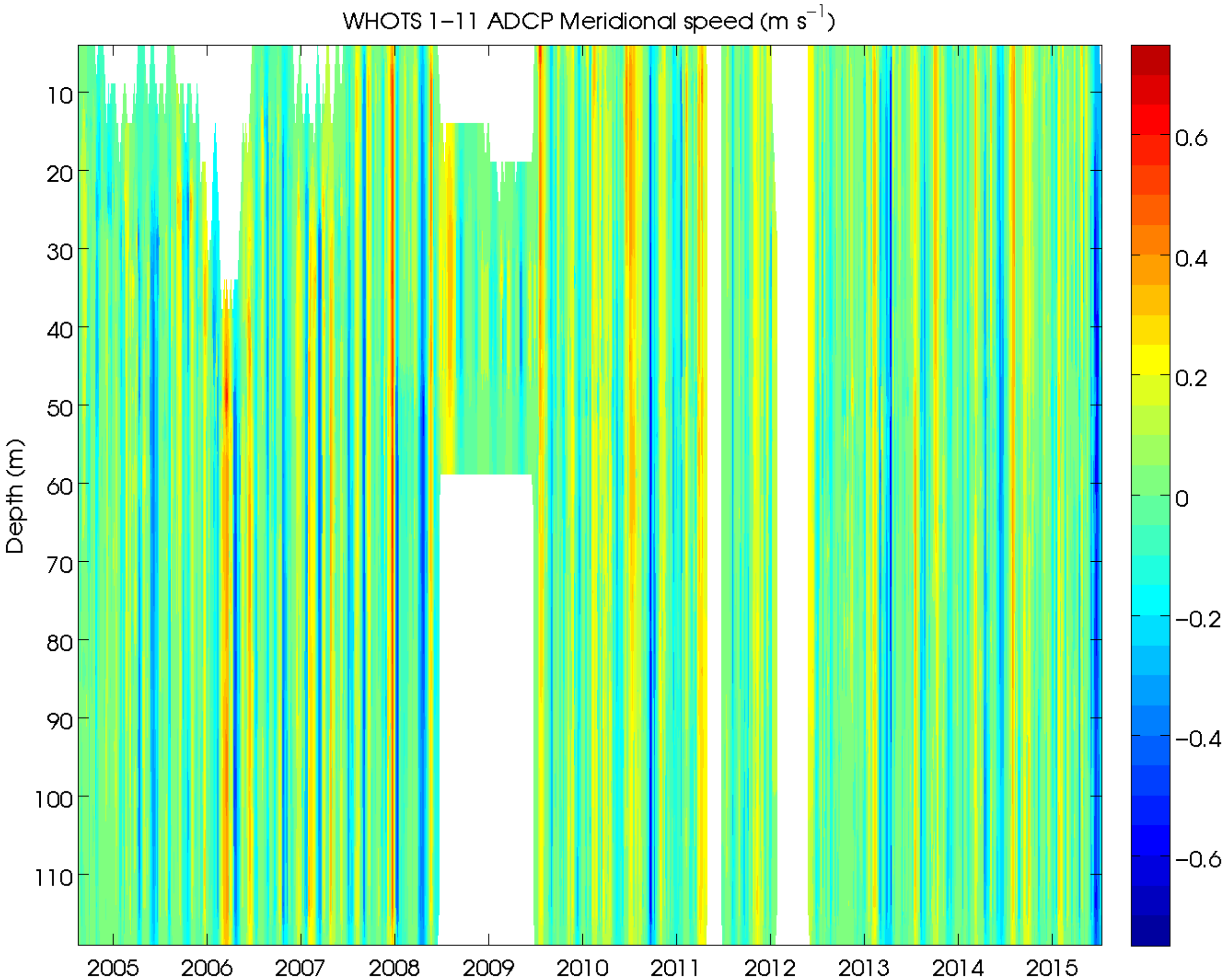

Figure 6-34. Contour plot of north velocity component (m s^{-1}) versus depth and time from the moored ADCPs from the WHOTS-1 through -11 deployments.

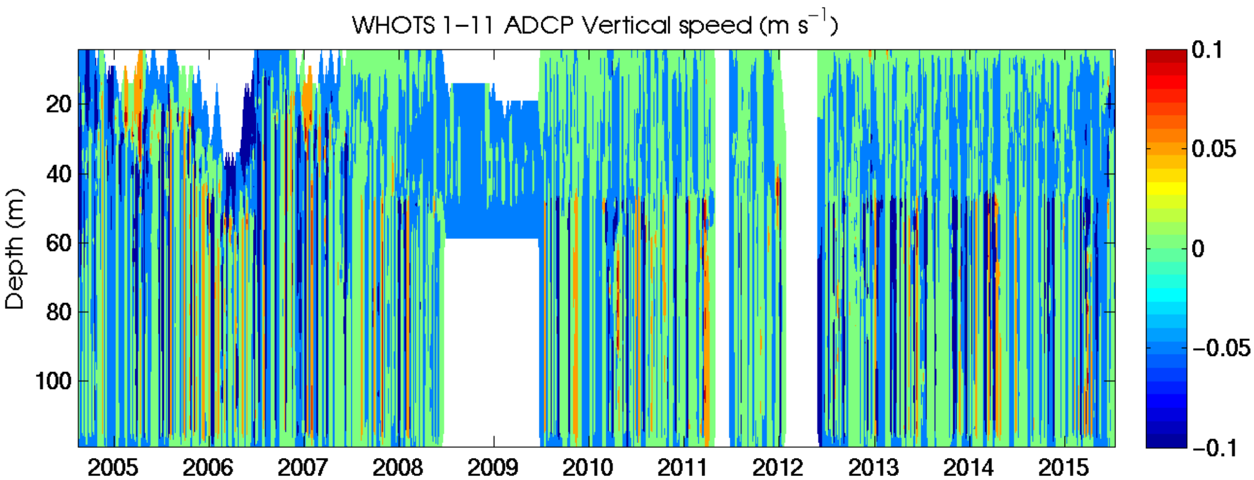

Figure 6-35.Contour plot of vertical velocity component (m s-1) versus depth and time from the moored ADCPs from the WHOTS-1through -11 deployments.

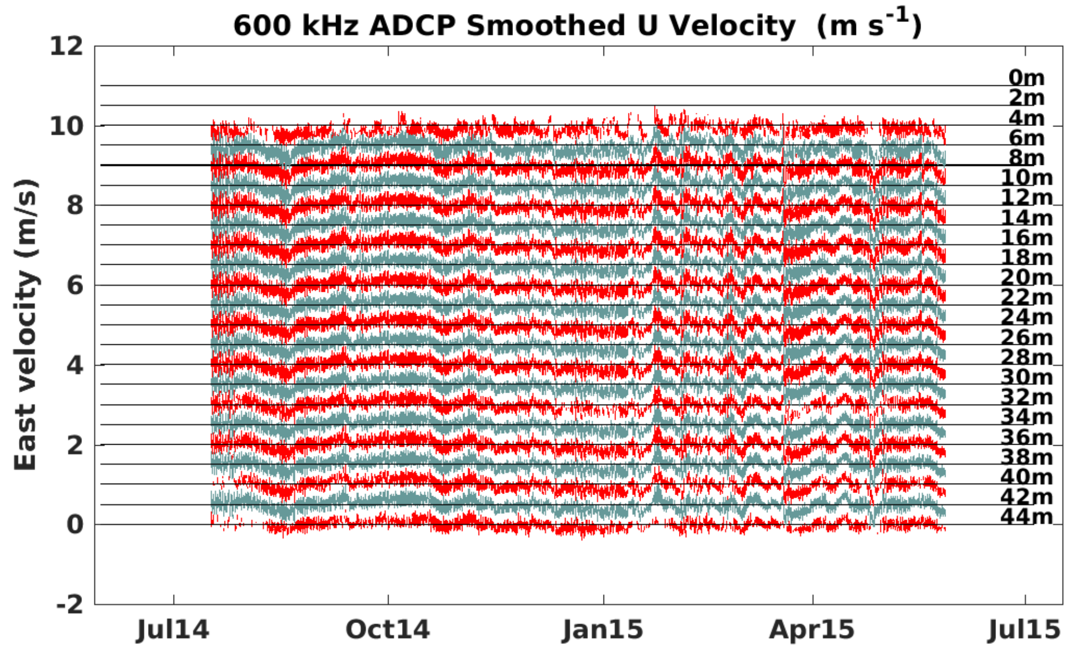

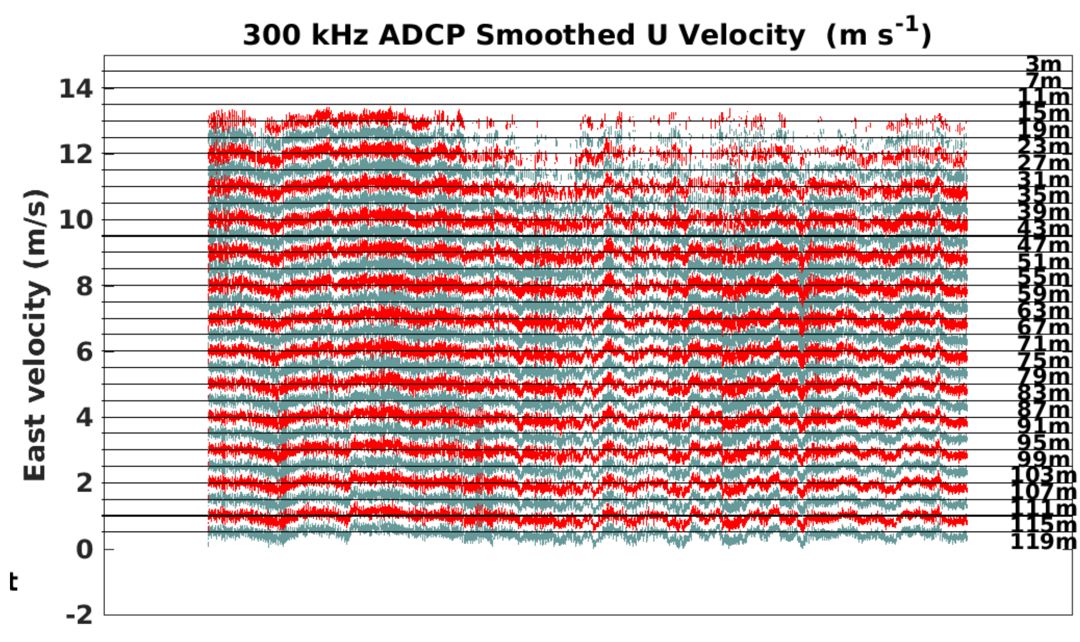

Figure 6-36. Staggered time-series of east velocity component (m s^{-1}) for each bin of the 600 kHz (upper panel), and 300 kHz (lower panel) moored ADCPs during WHOTS-11. The time-series are offset upwards by 0.5 m s^{-1}, the depth of each bin is on the right.

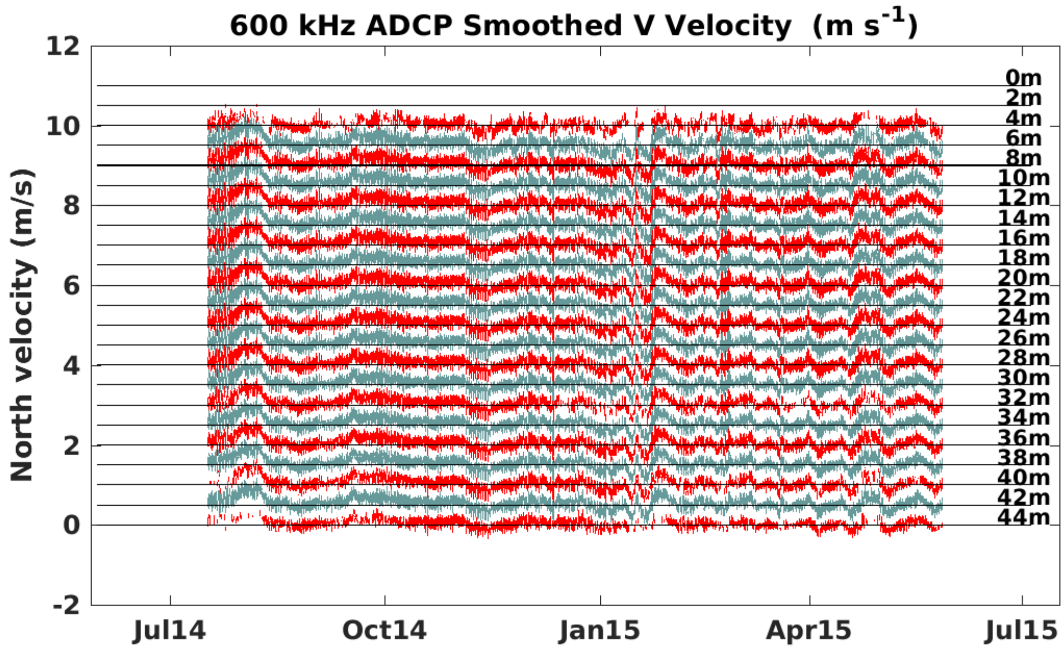

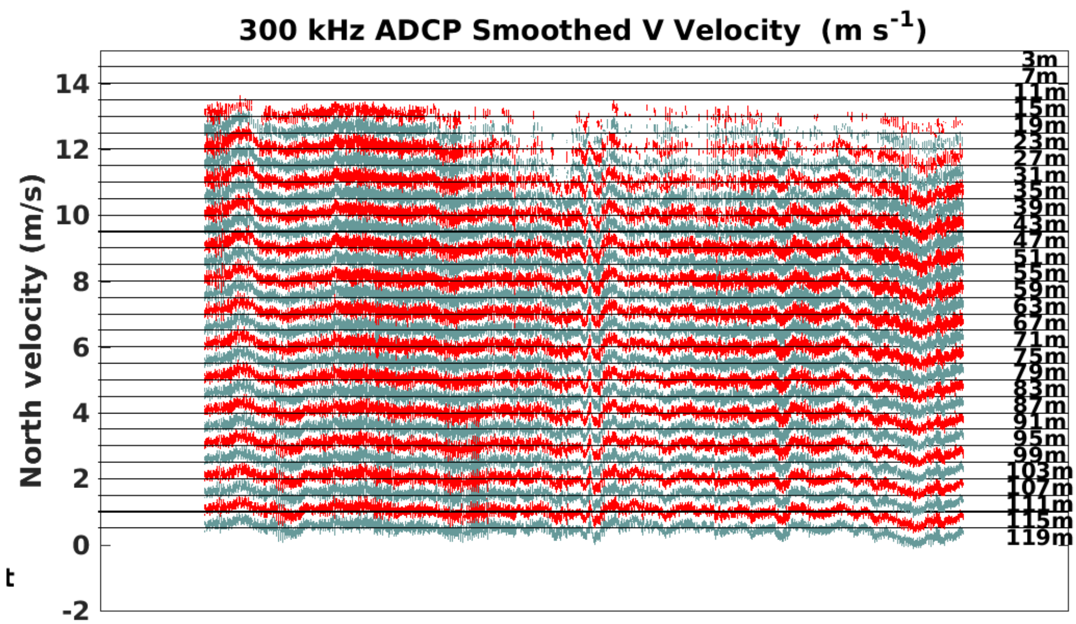

Figure 6-37. Staggered time-series of north velocity component (m s^{-1}) for each bin of the 600 kHz (upper panel), and 300 kHz (lower panel) moored ADCPs during WHOTS-10. The time-series are offset upwards by 0.5 m s^{-1}, the depth of each bin is on the right.

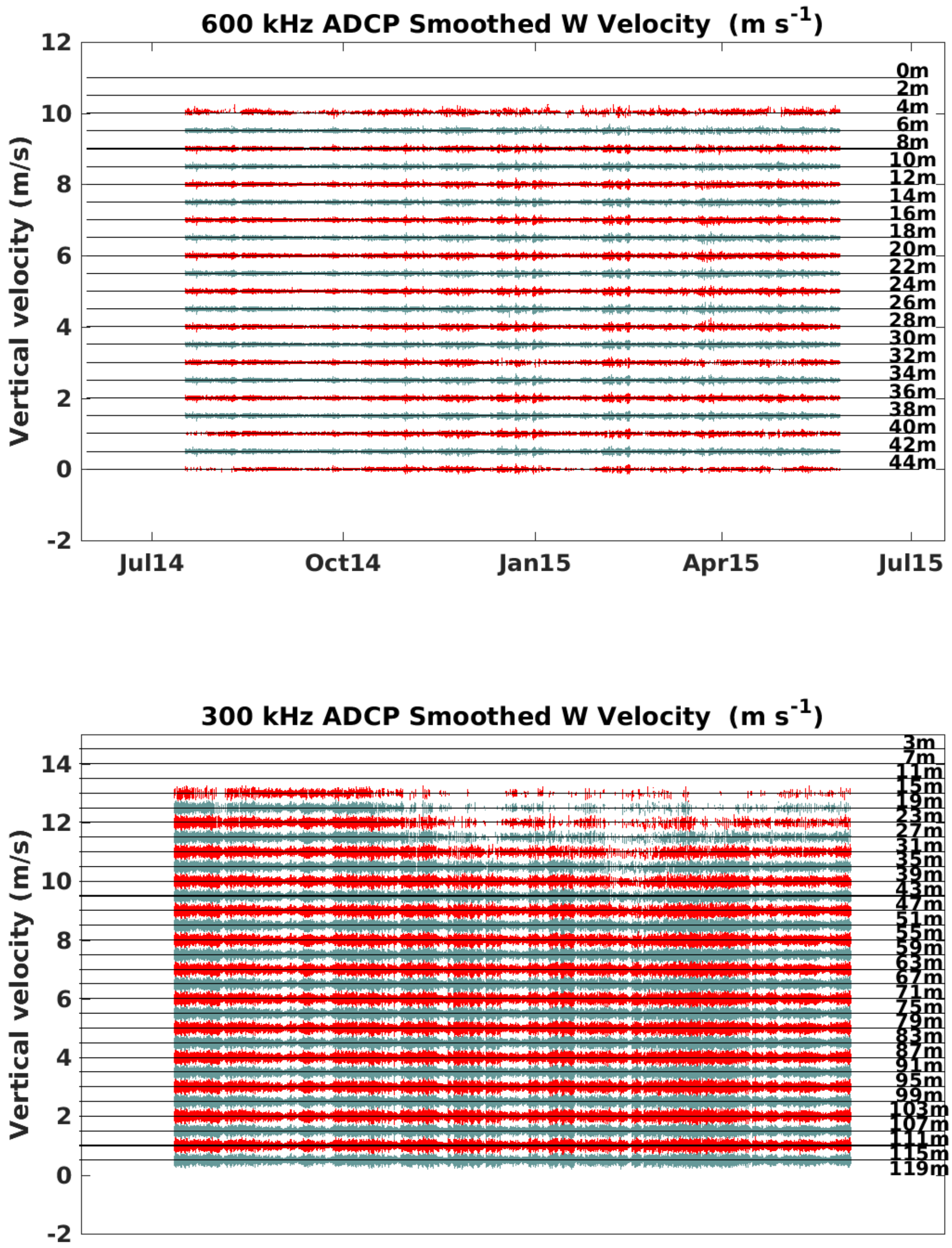

Figure 6-38. Staggered time-series of vertical velocity component (m s^{-1}) for each bin of the 600 kHz (upper panel), and 300 kHz (lower panel) moored ADCPs during WHOTS-11. The time-series are offset upwards by 0.5 m s^{-1}, the depth of each bin is on the right.

E. Moored and Shipboard ADCP Comparisons

Contours of zonal and meridional current components from the Ship *Hi'ialakai's* Ocean Surveyor broadband 75 kHz shipboard ADCP, and the moored 300 kHz ADCP from the WHOTS-11 deployment as a function of time and depth, during the WHOTS-11 cruise are shown in Figure 6-39a and 6-39b. Similar comparisons during the WHOTS-12 cruise are in Figure 6-39a and Figure 6-40b.

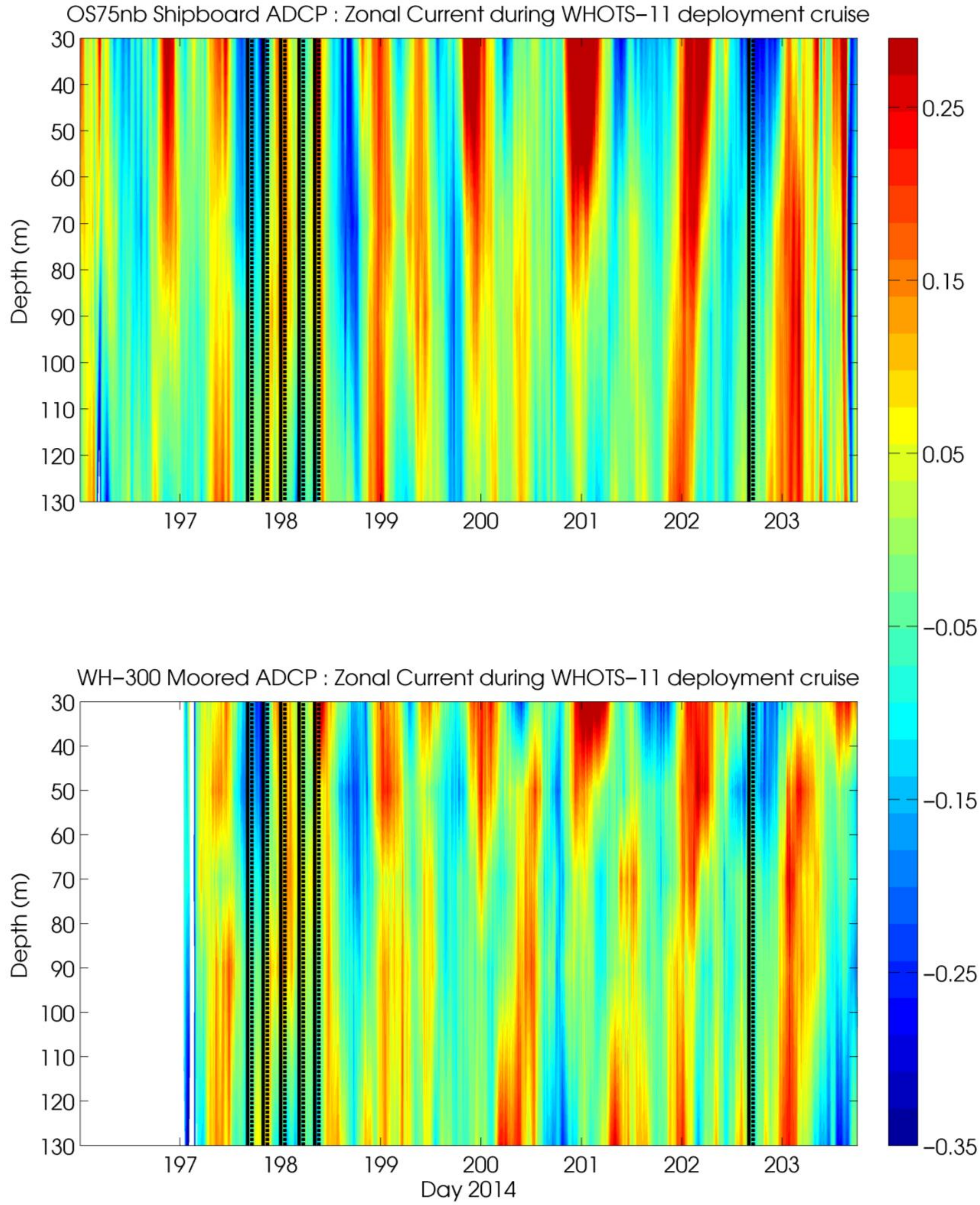

Figure 6-39a. Contour of zonal currents (m s^{-1}) from the Ship Hi'ialakai's Ocean Surveyor narrowband 75 kHz shipboard ADCP (upper panel), and the moored 300 kHz ADCP from the WHOTS-11 deployment (bottom panel) as a function of time and depth, during the WHOTS-11 cruise. Times when the CTD rosette were in the water are identified between solid and dashed black lines.

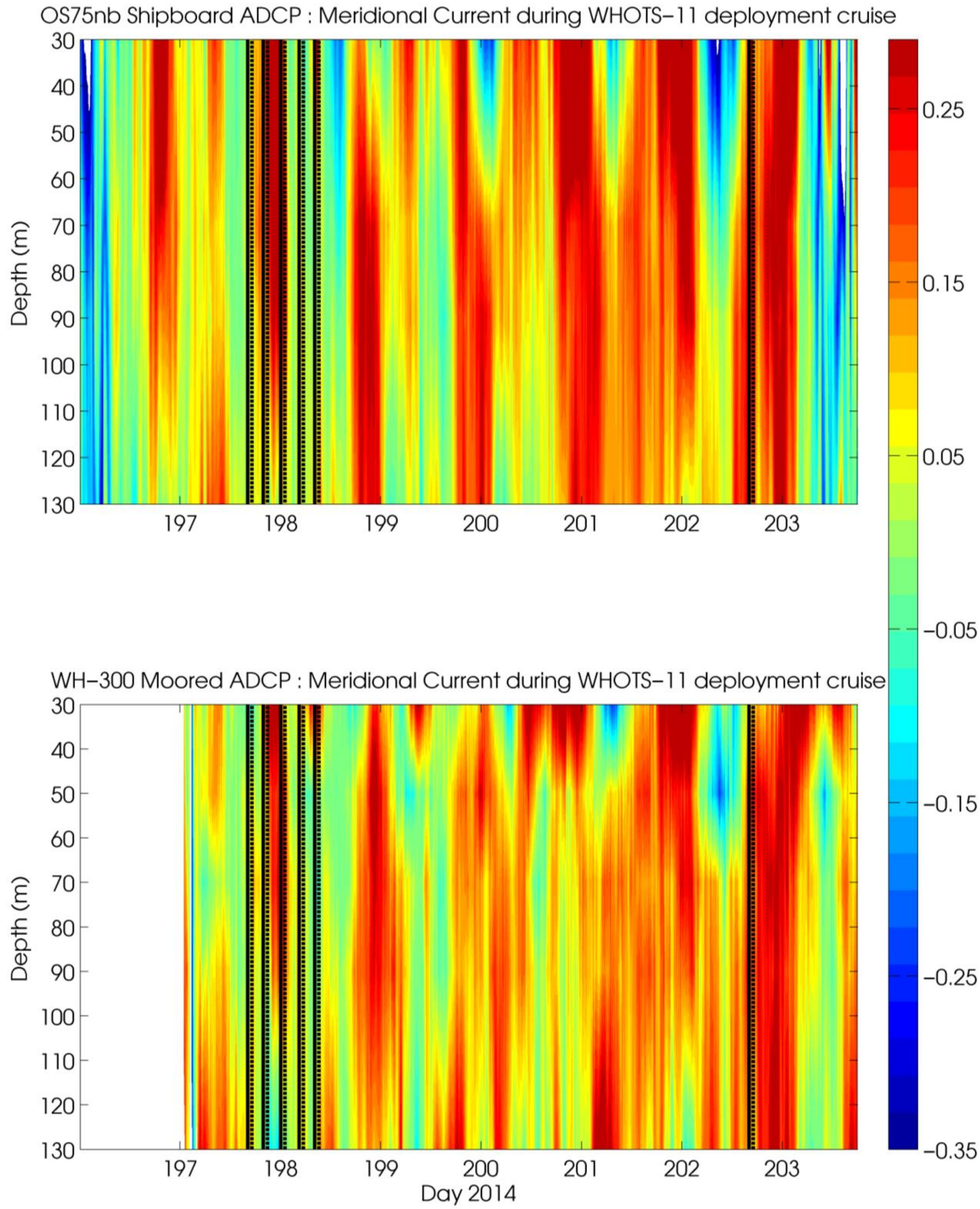

Figure 6-39b. Contours of meridional currents (m s^{-1}) from the Ship Hi'ialakai's Ocean Surveyor narrowband 75 kHz shipboard ADCP (upper panel), and the moored 300 kHz ADCP from the WHOTS-11 deployment (lower panel) as a function of time and depth, during the WHOTS-11 cruise. Times when the CTD/rosette was in the water are identified between the solid and dashed black lines.

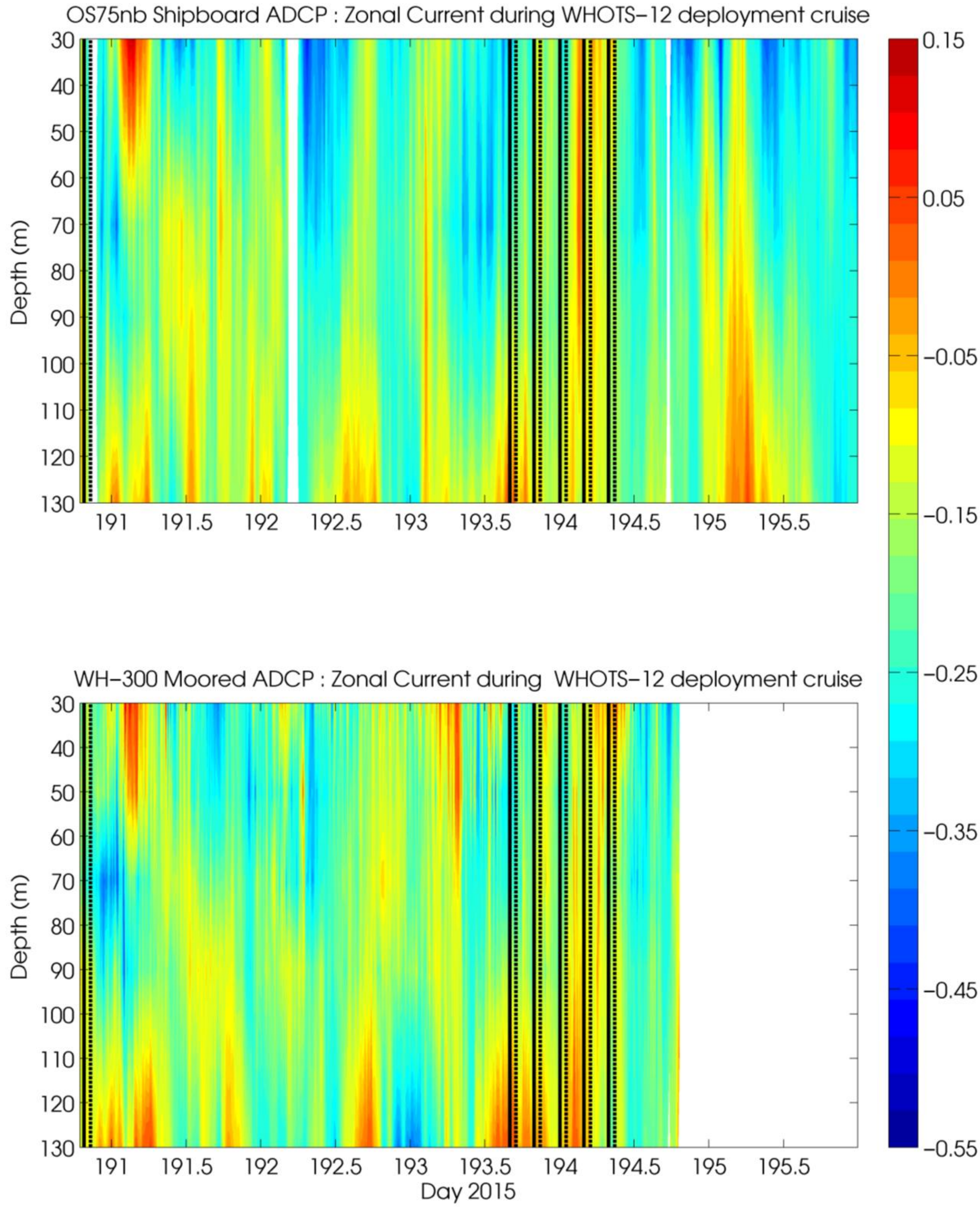

Figure 6-40a. Contour of zonal currents (m s^{-1}) from the Ship Hi'ialakai's Ocean Surveyor narrowband 75 kHz shipboard ADCP (upper panel), and the moored 300 kHz ADCP from the WHOTS-11 recovery (bottom panel) as a function of time and depth, during the WHOTS-12 cruise. Times when the CTD rosette were in the water are identified between solid and dashed black lines.

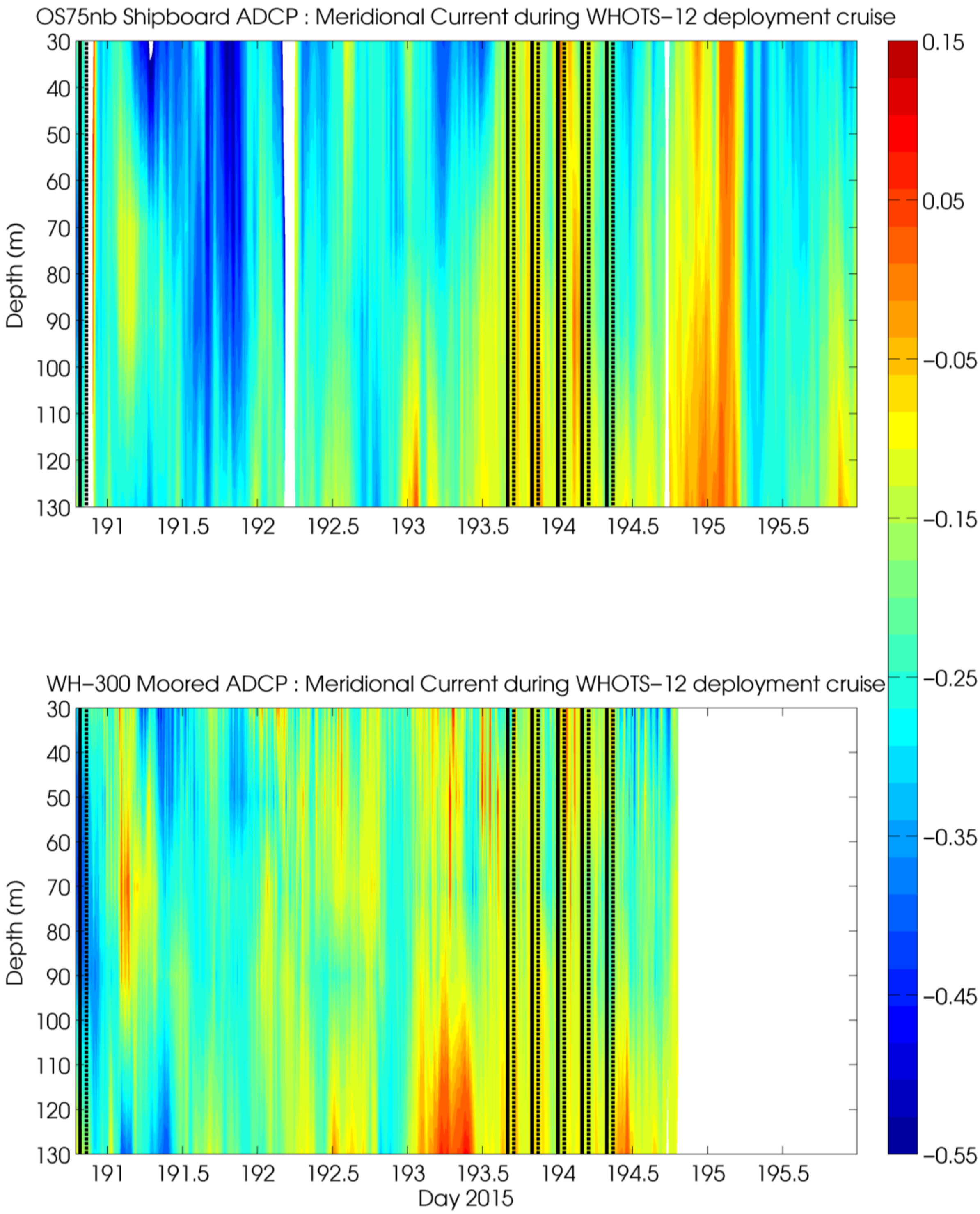

Figure 6-40b. Contours of meridional currents (m s^{-1}) from the Ship Hi'ialakai's Ocean Surveyor narrowband 75 kHz shipboard ADCP (upper panel), and the moored 300 kHz ADCP from the WHOTS-11 recovery (lower panel) as a function of time and depth, during the WHOTS-12 cruise. Times when the CTD/rosette was in the water are identified between the solid and dashed black lines.

Comparisons between quality-controlled moored ADCPs during the WHOTS-11 deployment and available shipboard ADCP obtained during regular HOT cruises 265 to 273 are shown in Figure 6-41 through Figure 6-5045 for the 300 kHz ADCP, and Figure 6-516 through **Error! Reference source not found.** for the 600 kHz ADCP. Median and mean velocity profiles were computed during the time when HOT CTD casts were being conducted near the WHOTS mooring specifically intended to calibrate moored instrumentation (see 5.A.4). The shipboard profiles were taken when the ship was stationary, within 1 km of the mooring, and within 4 hours before the start and 4 hours after the end of the CTD cast conducted near the WHOTS mooring. HOT cruises conducted on the R/V *Kilo Moana* (HOT-265 to 268 and 271 to 273) used data from an RD Instruments Workhorse 300 kHz ADCP (wh300) with 4 m bin size, reaching 100 m, and averaging ensembles every 2 minutes; and from an RD Instruments Ocean Surveyor 38 kHz operating in broad band mode (os38bb) with 12 m bin size, reaching 1200 m, with 5 minute ensemble averages, and in narrow band mode (os38nb) with 24 m bin size, reaching 1500 m and also with 5 minute ensemble averages. Data from the wh300 were used for the comparisons with the moored ADCP data, or from the os75bb if the wh300 data were not available.

The moored ADCP data were collected from the upward facing 300 kHz ADCP located at 125 m and the upward facing 600 kHz ADCP located at 47.5 m over the same time period. Zonal (U), and meridional (V) current components from the shipboard and moored vertical profiles were interpolated to the profile resolution of the shipboard ADCP, and ensemble mean and median profiles were obtained for each data set to compute differences and correlation coefficients between them (Table 6). Bins with less than 50% data were excluded.

Comparisons between the 300 kHz and the shipboard ADCP from HOT-266, 267, 270, and 271 were excluded due to a lack of comparable data. Comparisons between the moored 600 kHz and the shipboard ADCP were only evaluated for cruises featuring the Workhorse 300 kHz ADCP (wh300) due to the larger vertical resolution with the other ADCP models (os38bb, os75bb). The correlations and the vertical mean of the differences between the ensemble median and mean for each of the U and V components are shown in Table 6-1.

Table 6-1. Correlations and differences of zonal (U) and meridional (V) ensemble median and mean currents (10 to 125 m) between WHOTS-11 moored ADCP (300 and 600 kHz) and shipboard ADCP during HOT cruises. Only HOT cruises with a wh300 shipboard ADCP were compared with the 600 kHz ADCP due to lack of shallow current data in the shipboard os38bb and os75bb models (see text).

HOT Shipboard ADCP vs WHOTS Moored 300 kHz ADCP									
Cruise	**Ship ADCP Type**	**Ensemble Median U correlation**	**Vertical Mean of U median differences**	**Ensemble Median V correlation**	**Vertical Mean of V median differences**	**Ensemble Mean U correlation**	**Vertical Mean differences U**	**Ensemble Mean V correlation**	**Vertical Mean differences V**
HOT-265	wh300	0.9906	0.0275	0.9855	0.0014	0.9932	0.0281	0.9848	0.0016
HOT-268	wh300	0.7791	0.0318	0.0253	0.0884	0.5713	0.0321	-0.5829	0.0830
HOT-269	wh300	0.9862	0.0302	0.8823	-0.0361	0.9949	0.0312	0.9100	-0.0366
HOT-272	wh300	0.9679	0.0023	0.7738	0.0193	0.9799	0.0034	0.8674	0.0177
HOT-273	wh300	0.8726	-0.0290	0.8124	-0.0106	0.9538	-0.0161	0.7926	0.0020
HOT Shipboard ADCP vs WHOTS Moored 600 kHz ADCP									
HOT – 265	wh300	0.8184	0.0303	0.5466	-0.0099	0.8671	0.0301	0.4628	-0.0085
HOT – 266	wh300	0.5355	-0.0101	0.5875	-0.0212	0.9482	-0.0128	-0.5180	-0.0296
HOT – 267	wh300	0.8850	0.0054	0.0715	0.0638	0.8776	-0.0004	0.7216	0.0609
HOT – 269	wh300	0.9328	-0.0070	0.9719	-0.0158	0.8774	-0.0073	0.9911	-0.0180
HOT – 270	wh300	0.6018	0.0047	-0.8113	0.0168	0.7760	0.0070	-0.8520	0.0219
HOT - 272	wh300	0.4185	0.0150	0.9924	0.0695	0.6744	0.0194	0.9958	0.0503

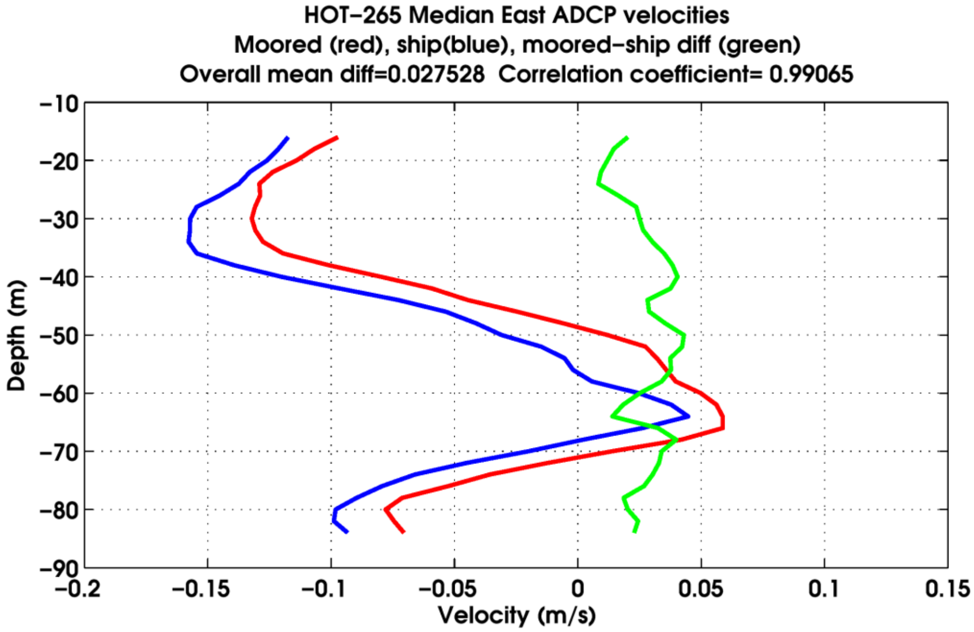

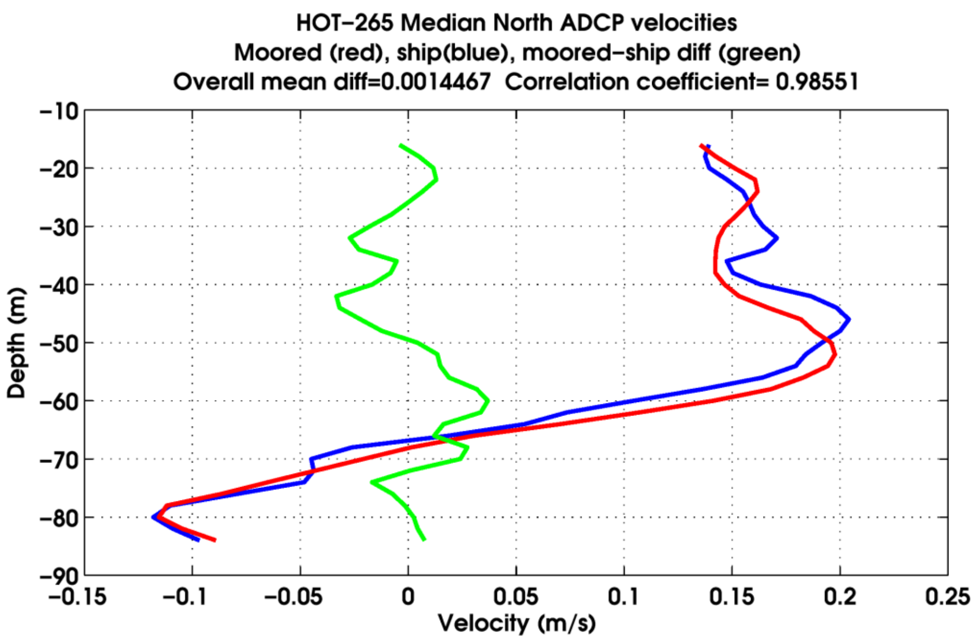

Figure 6-41. Median velocity profiles during shipboard ADCP (blue) versus moored 300 kHz ADCP (red) intercomparisons from HOT-265. Moored minus shipboard ADCP differences shown in green. Top panel shows east velocity components, bottom panel shows north velocity components.

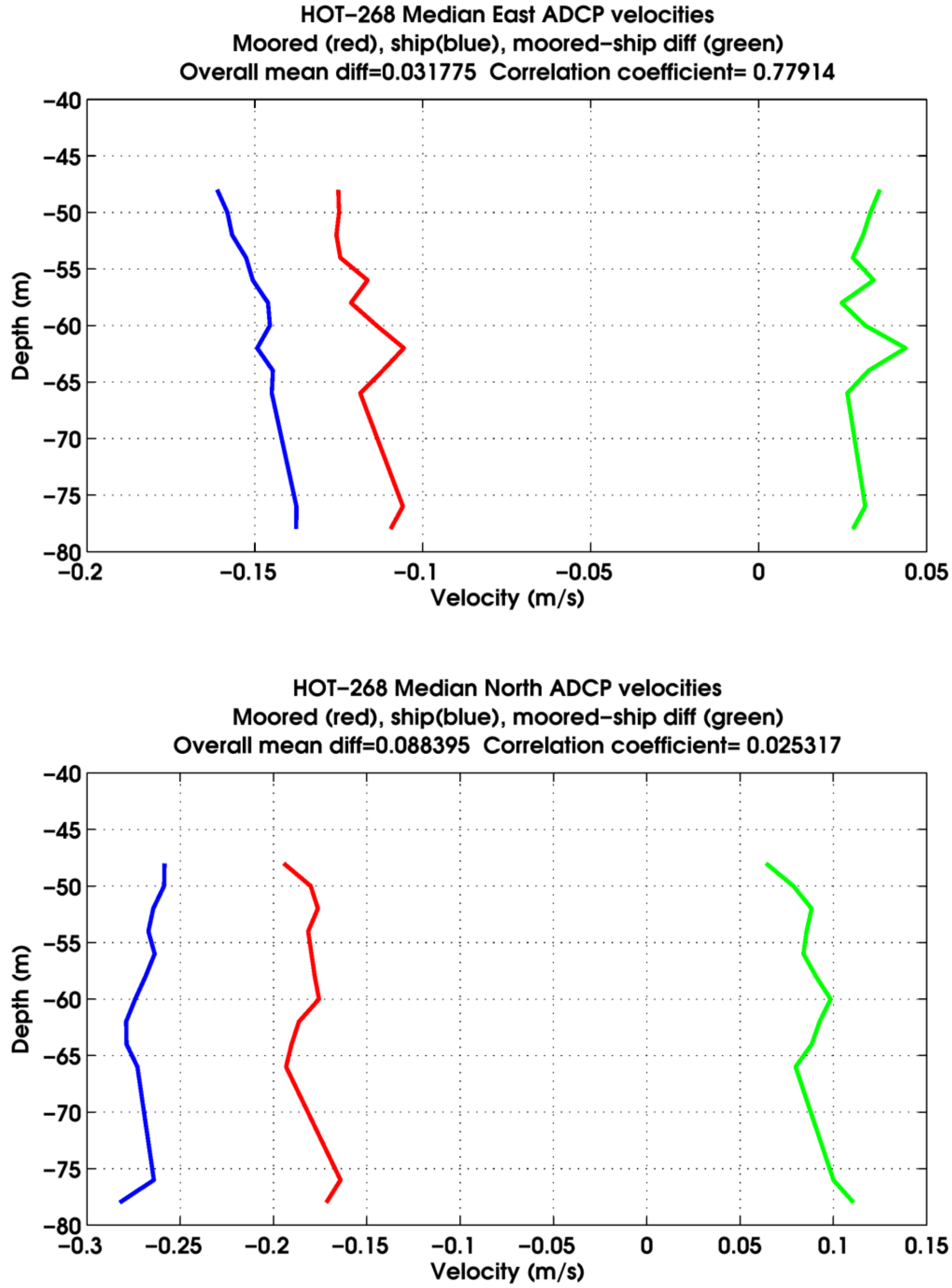

Figure 6-45. Median velocity profiles during shipboard ADCP (blue) versus moored 300 kHz ADCP (red) intercomparisons from HOT-268. Moored minus shipboard ADCP differences shown in green. Top panel shows east velocity components, bottom panel shows north velocity components.

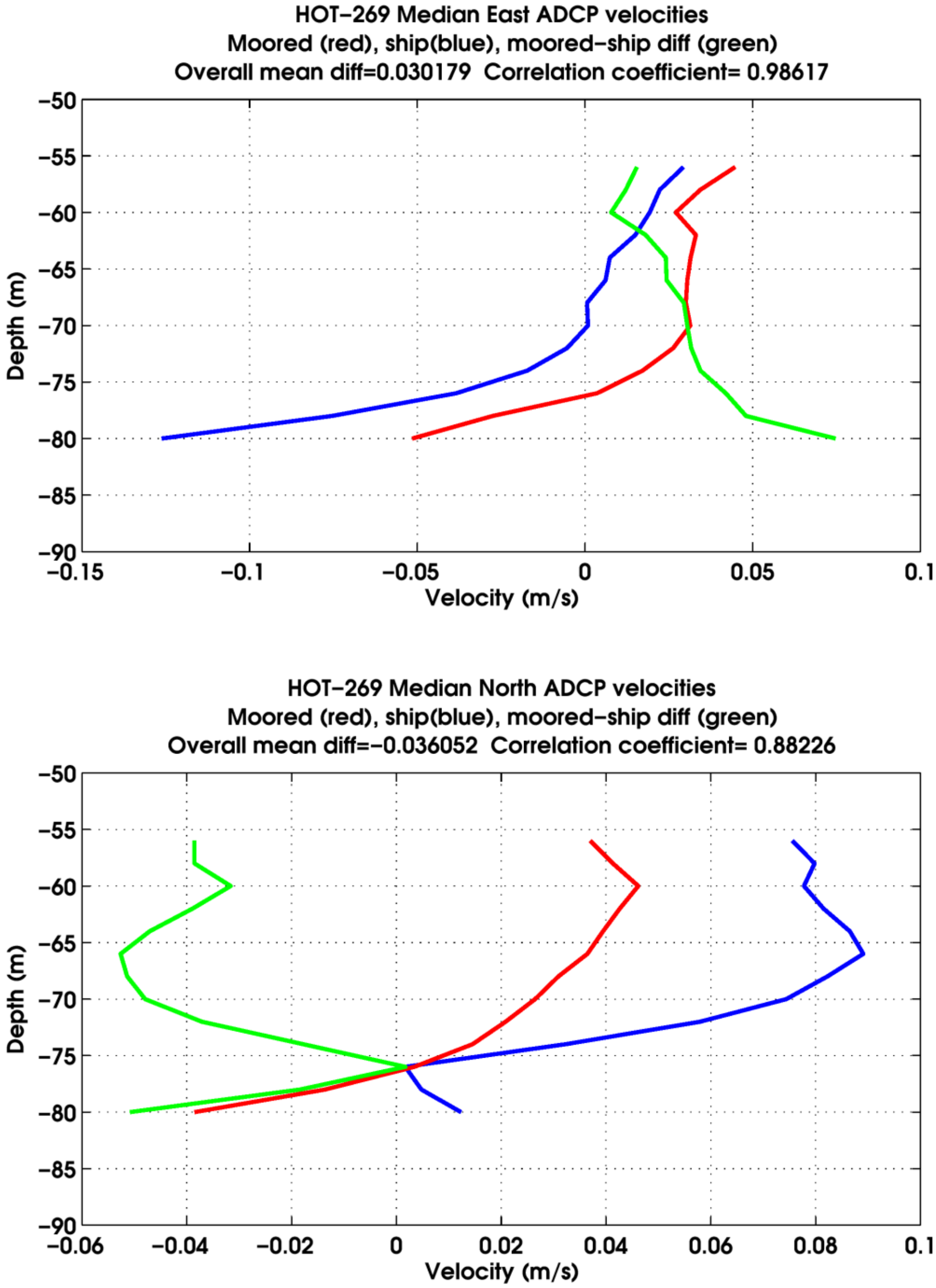

Figure 6-43. Median velocity profiles during shipboard ADCP (blue) versus moored 300 kHz ADCP (red) intercomparisons from HOT-269. Moored minus shipboard ADCP differences shown in green. Top panel shows east velocity components, bottom panel shows north velocity components.

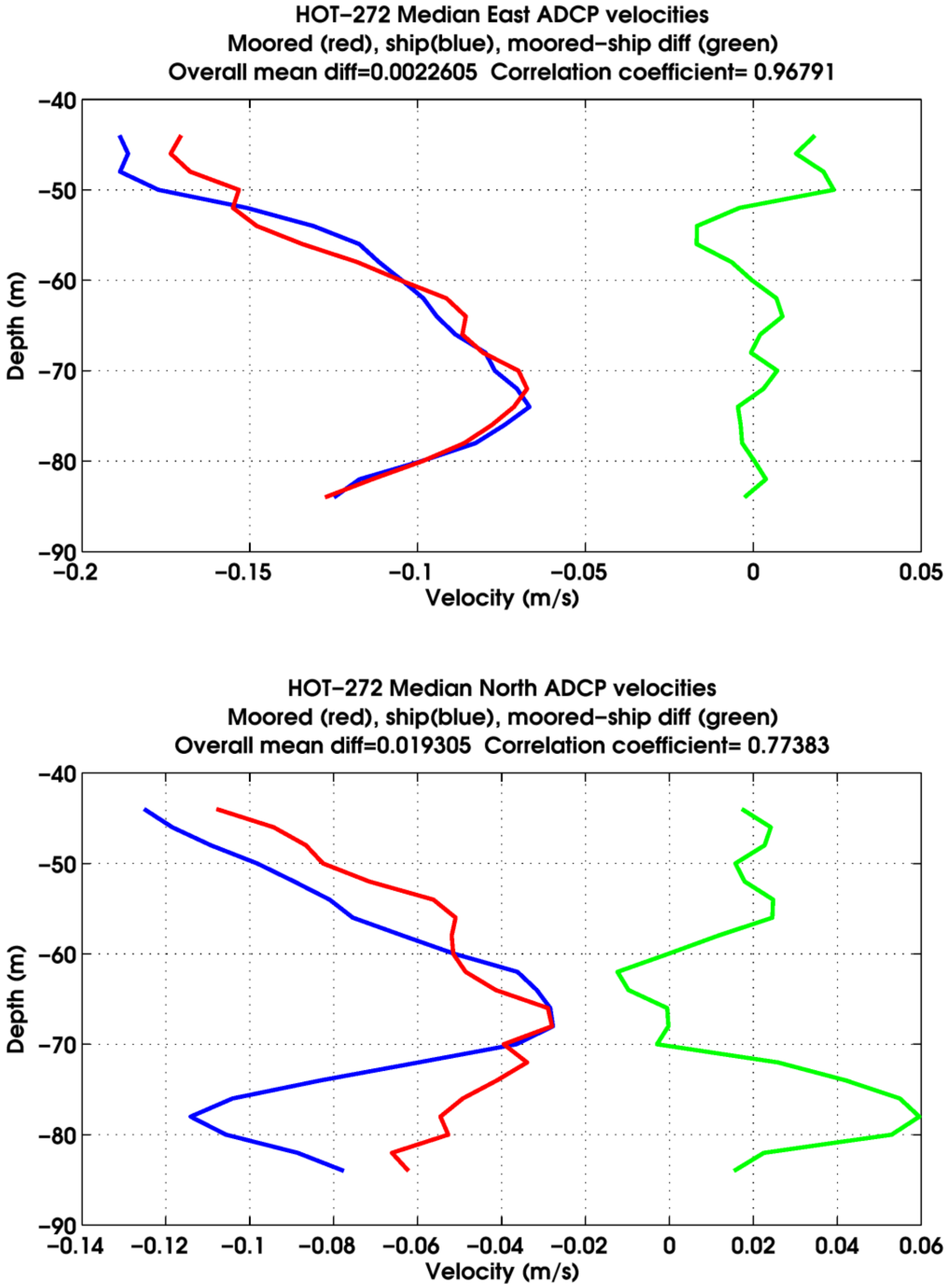

Figure 6-44. Median velocity profiles during shipboard ADCP (blue) versus moored 300 kHz ADCP (red) intercomparisons from HOT-272. Moored minus shipboard ADCP differences shown in green. Top panel shows east velocity components, bottom panel shows north velocity components.

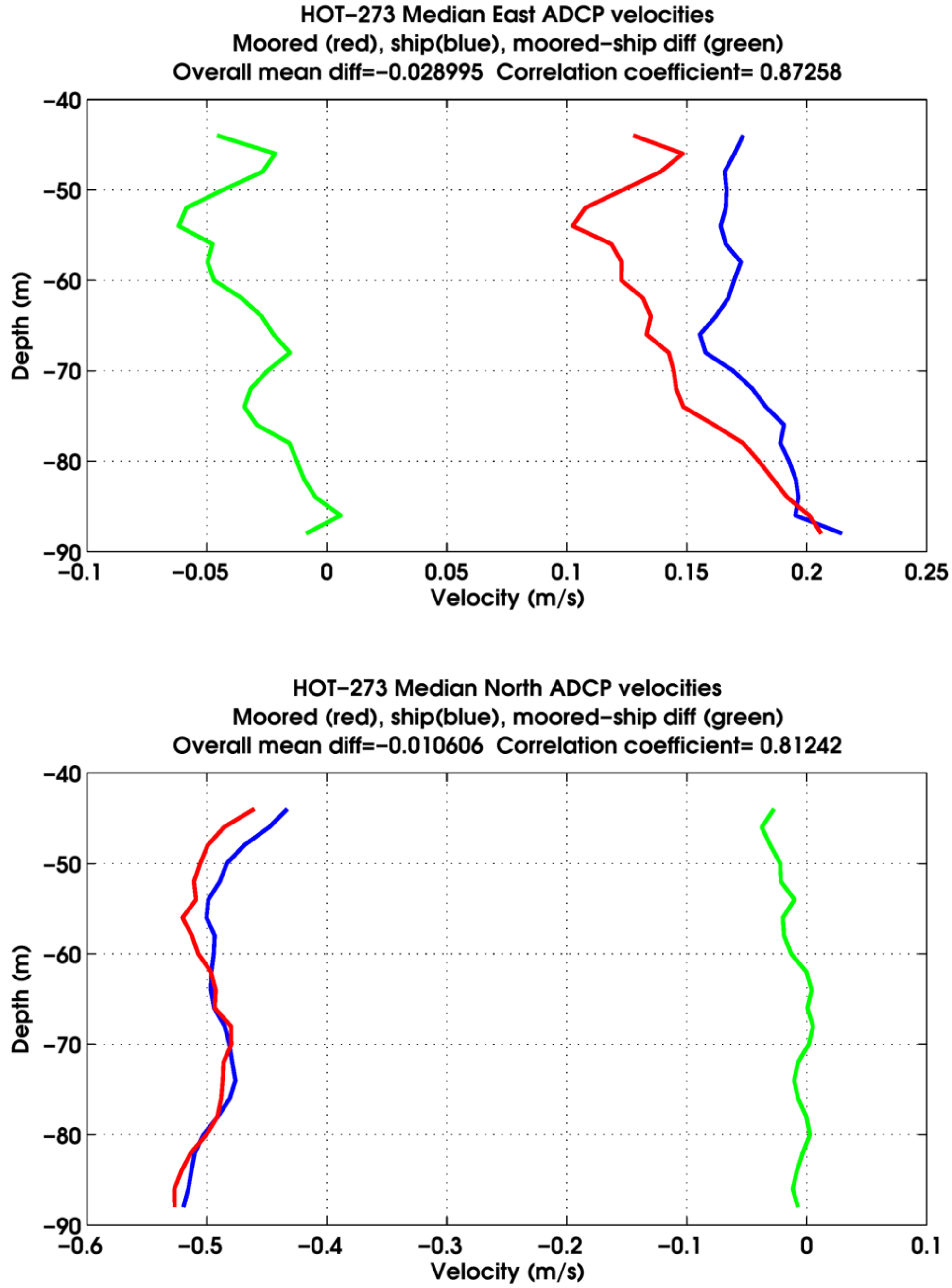

Figure 6-45. Median velocity profiles during shipboard ADCP (blue) versus moored 300 kHz ADCP (red) intercomparisons from HOT-273. Moored minus shipboard ADCP differences shown in green. Top panel shows east velocity components, bottom panel shows north velocity components.

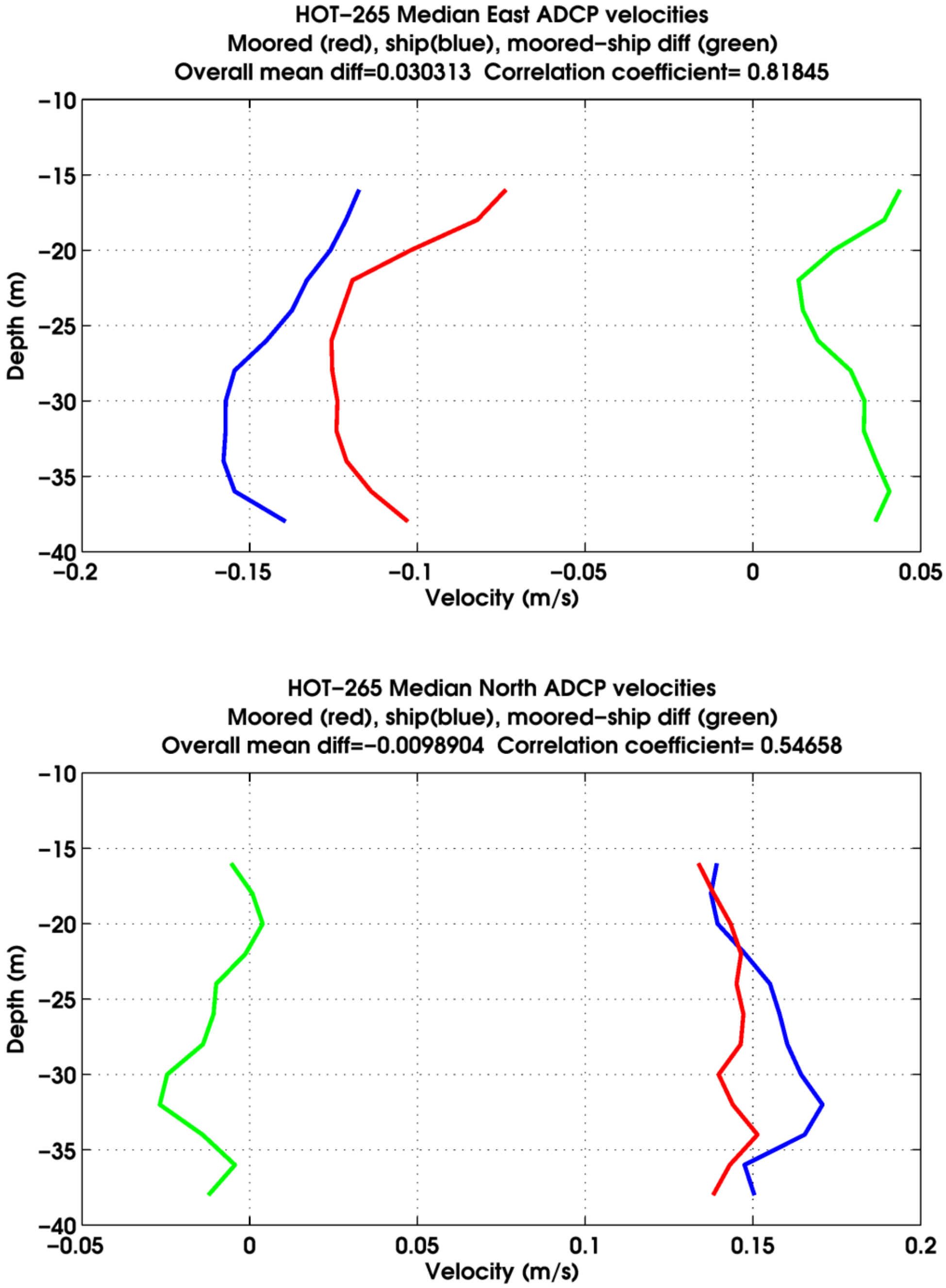

Figure 6-46. Median velocity profiles during shipboard ADCP (blue) versus moored 600 kHz ADCP (red) intercomparisons from HOT-265. Moored minus shipboard ADCP differences shown in green. Top panel shows east velocity components, bottom panel shows north velocity components.

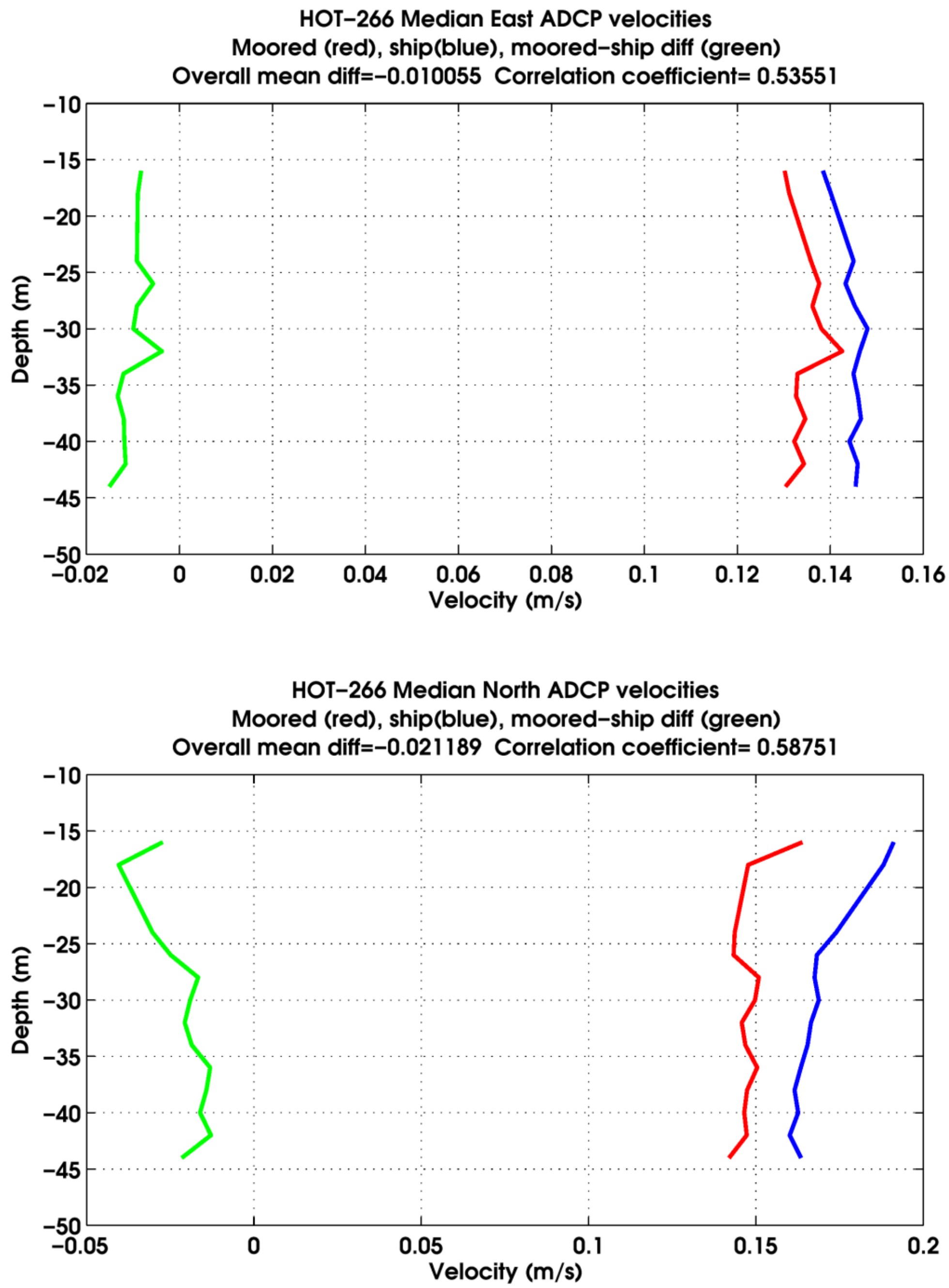

Figure 6-47. Median velocity profiles during shipboard ADCP (blue) versus moored 600 kHz ADCP (red) intercomparisons from HOT-266. Moored minus shipboard ADCP differences shown in green. Top panel shows east velocity components, bottom panel shows north velocity components.

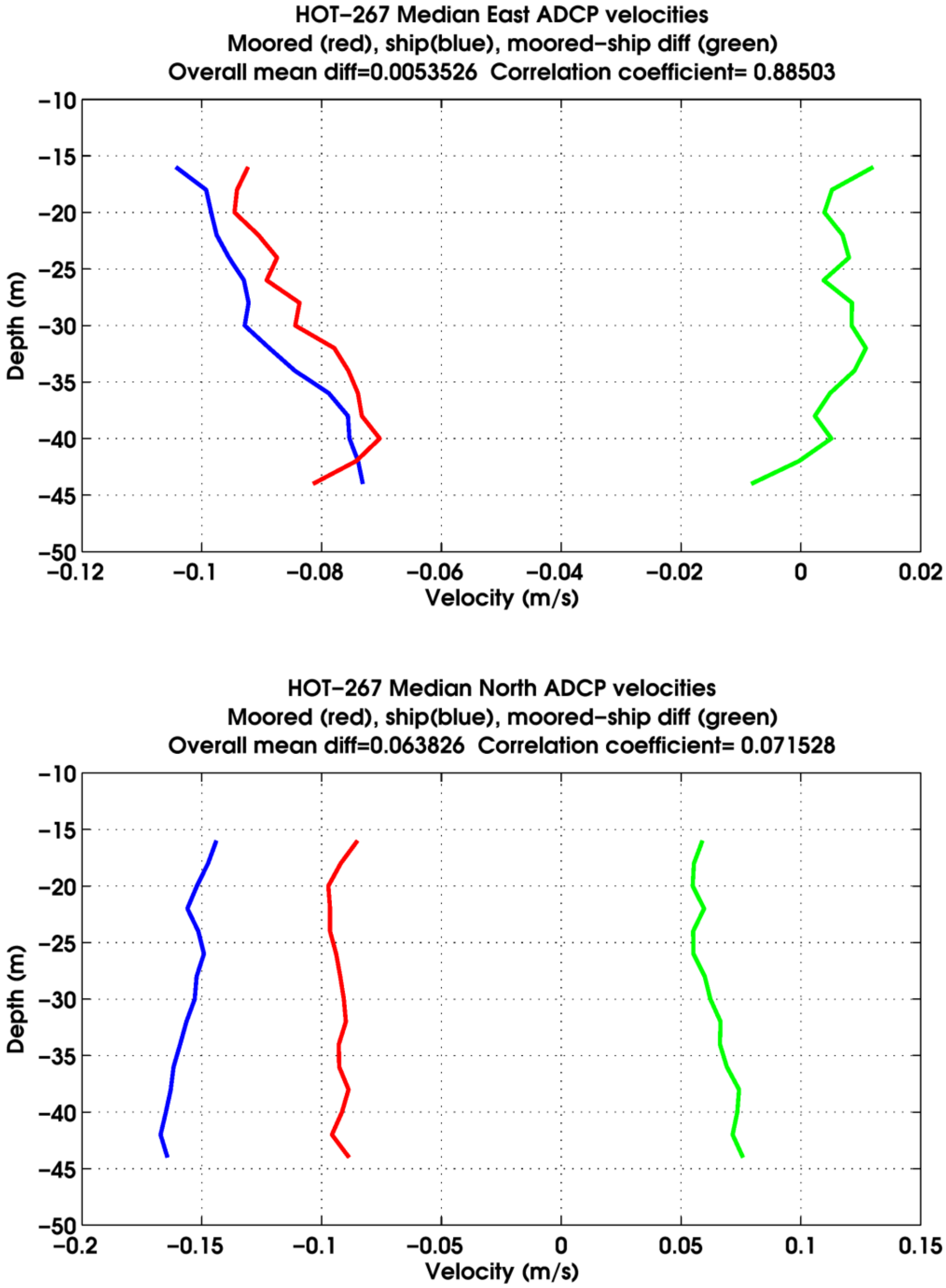

Figure 6-48. Median velocity profiles during shipboard ADCP (blue) versus moored 600 kHz ADCP (red) intercomparisons from HOT-267. Moored minus shipboard ADCP differences shown in green. Top panel shows east velocity components, bottom panel shows north velocity components.

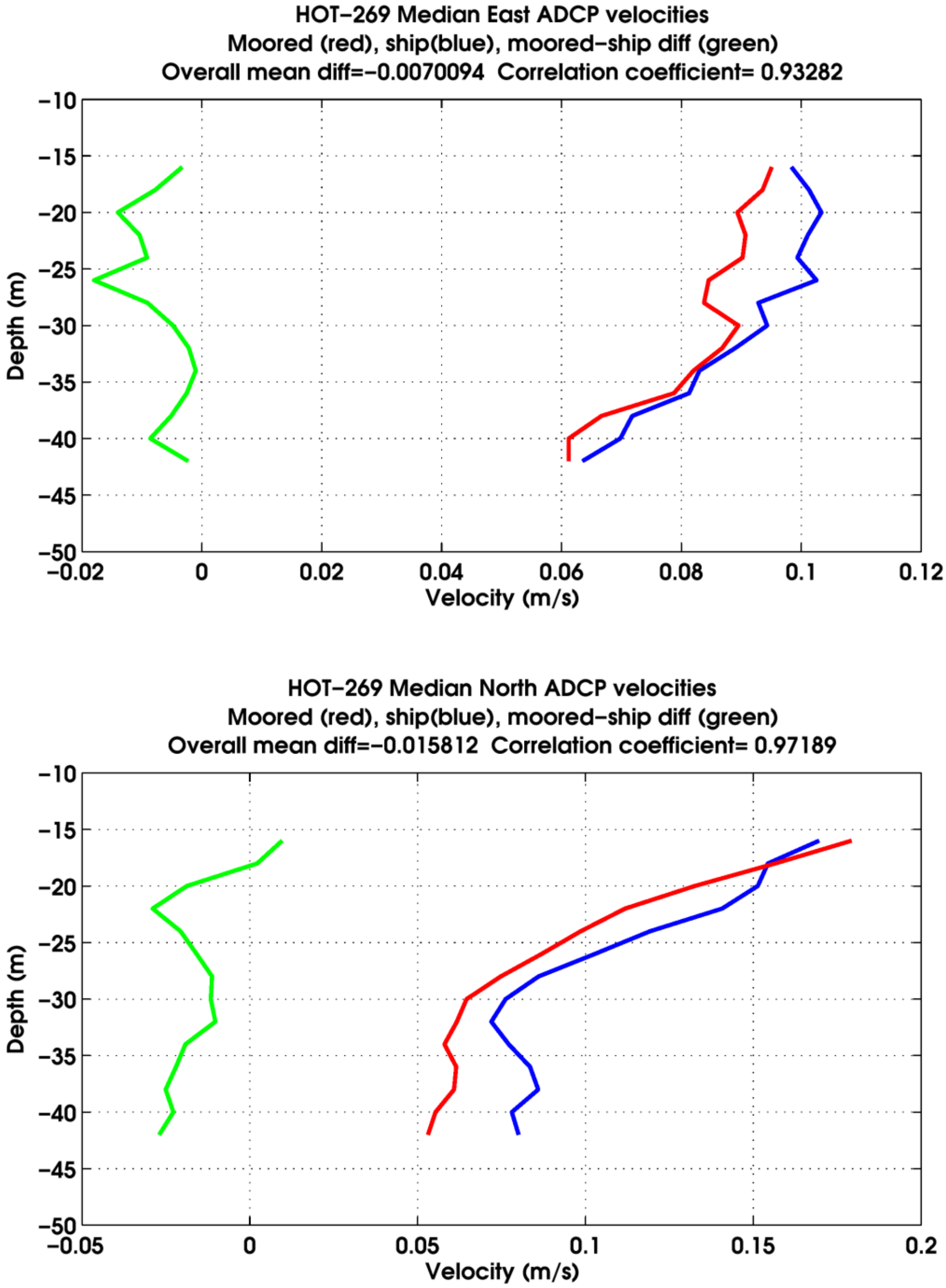

Figure 6-49. Median velocity profiles during shipboard ADCP (blue) versus moored 600 kHz ADCP (red) intercomparisons from HOT-269. Moored minus shipboard ADCP differences shown in green. Top panel shows east velocity components, bottom panel shows north velocity components.

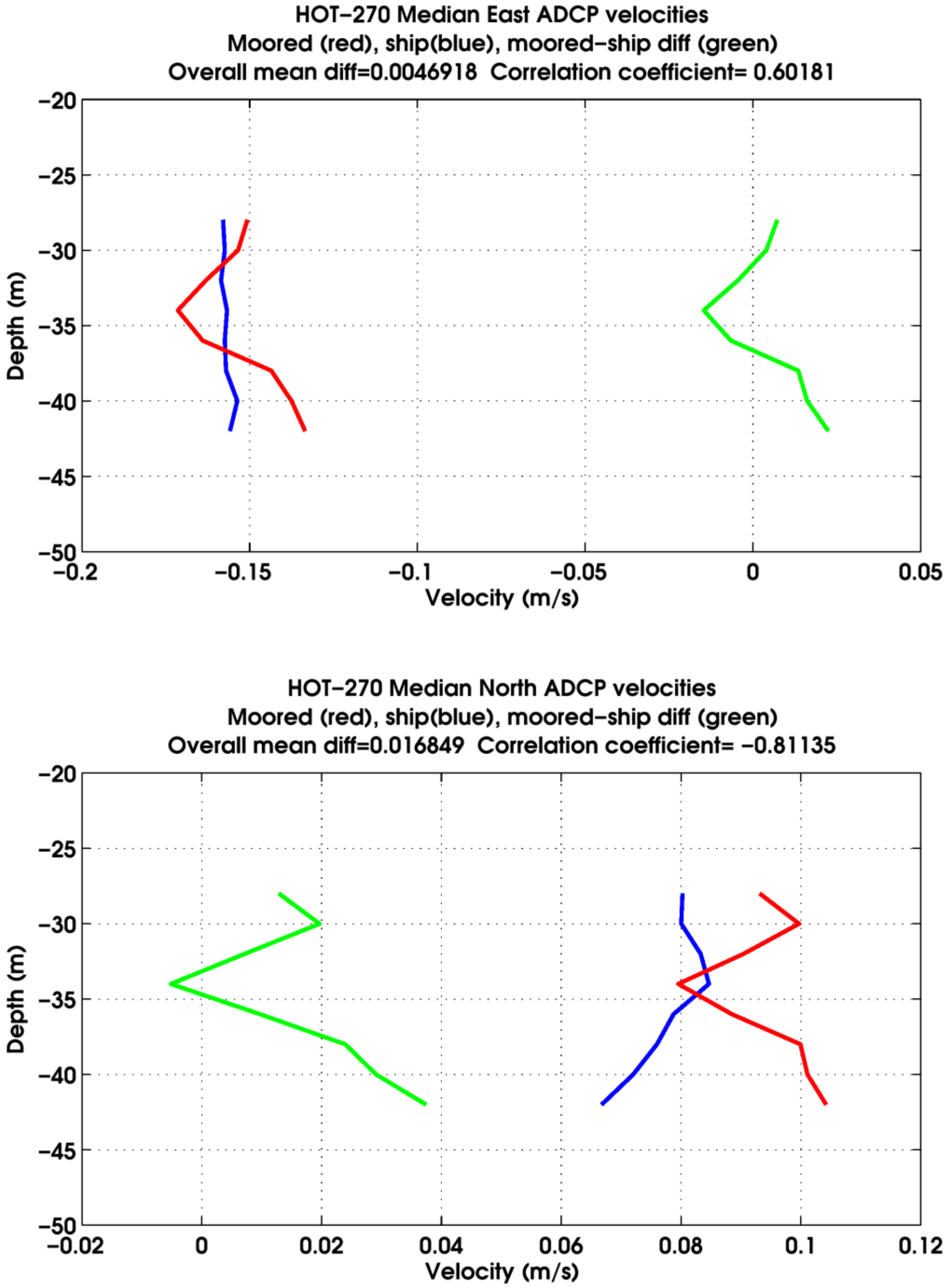

Figure 6-50. Median velocity profiles during shipboard ADCP (blue) versus moored 600 kHz ADCP (red) intercomparisons from HOT-270. Moored minus shipboard ADCP differences shown in green. Top panel shows east velocity components, bottom panel shows north velocity components.

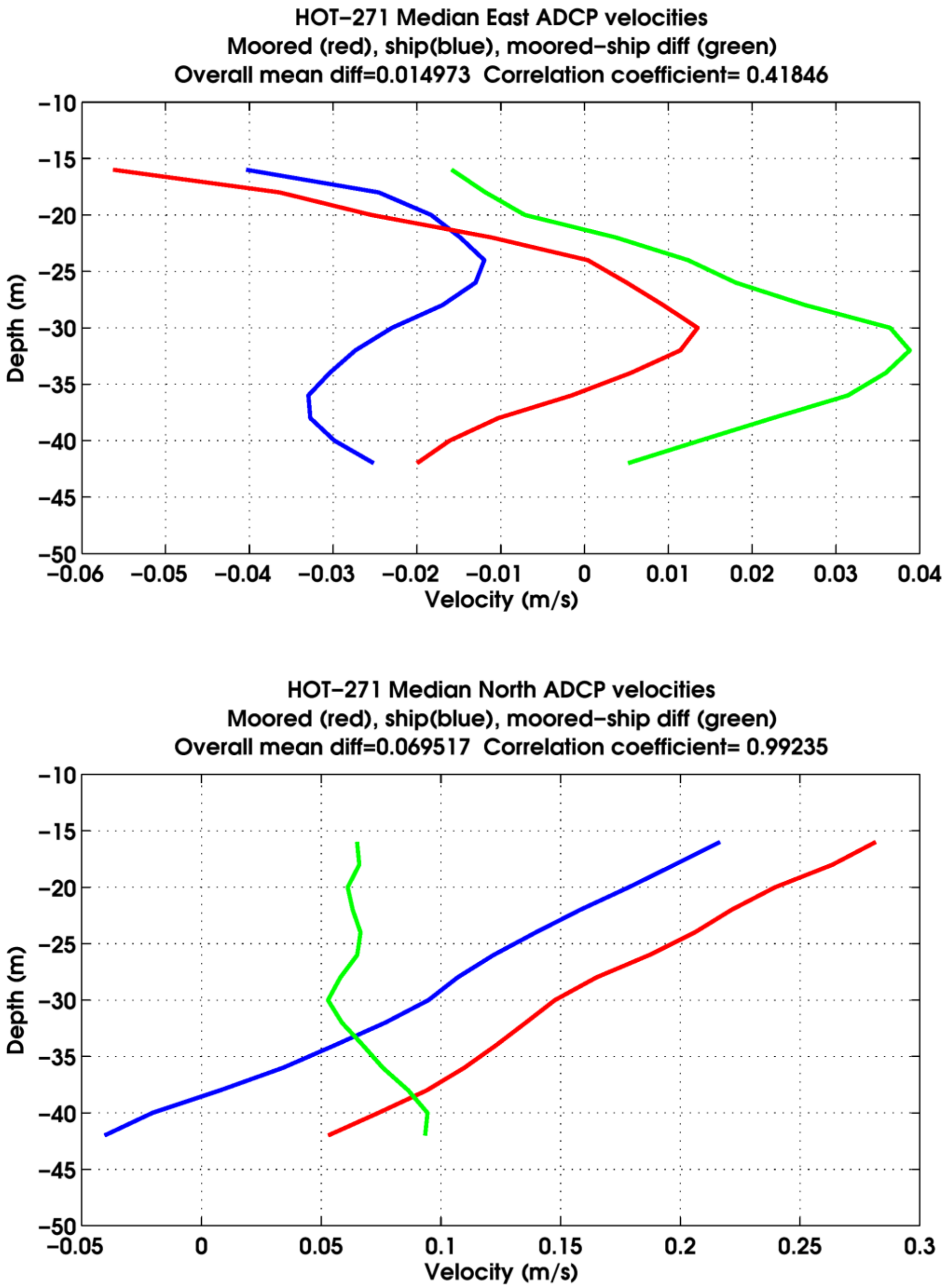

Figure 6-516. Median velocity profiles during shipboard ADCP (blue) versus moored 600 kHz ADCP (red) intercomparisons from HOT-271. Moored minus shipboard ADCP differences shown in green. Top panel shows east velocity components, bottom panel shows north velocity components.

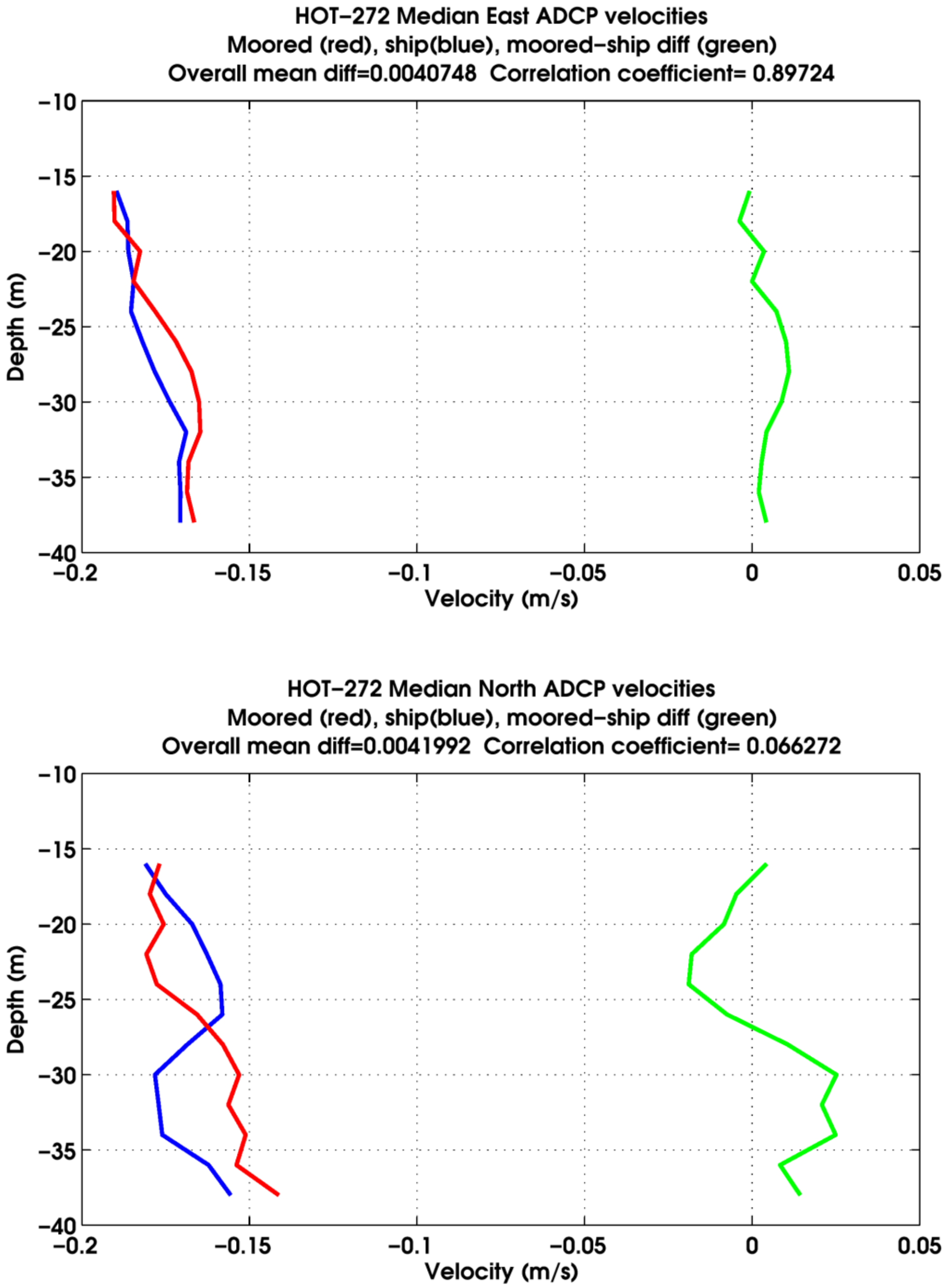

Figure 6-72. Median velocity profiles during shipboard ADCP (blue) versus moored 600 kHz ADCP (red) intercomparisons from HOT-272. Moored minus shipboard ADCP differences shown in green. Top panel shows east velocity components, bottom panel shows north velocity components.

F. Next Generation Vector Measuring Current Meter (VMCM) Data

Time-series of daily mean current speeds for the VMCM current meters deployed during WHOTS-11 at 10 m and 30 m are presented in Figure 6-53.

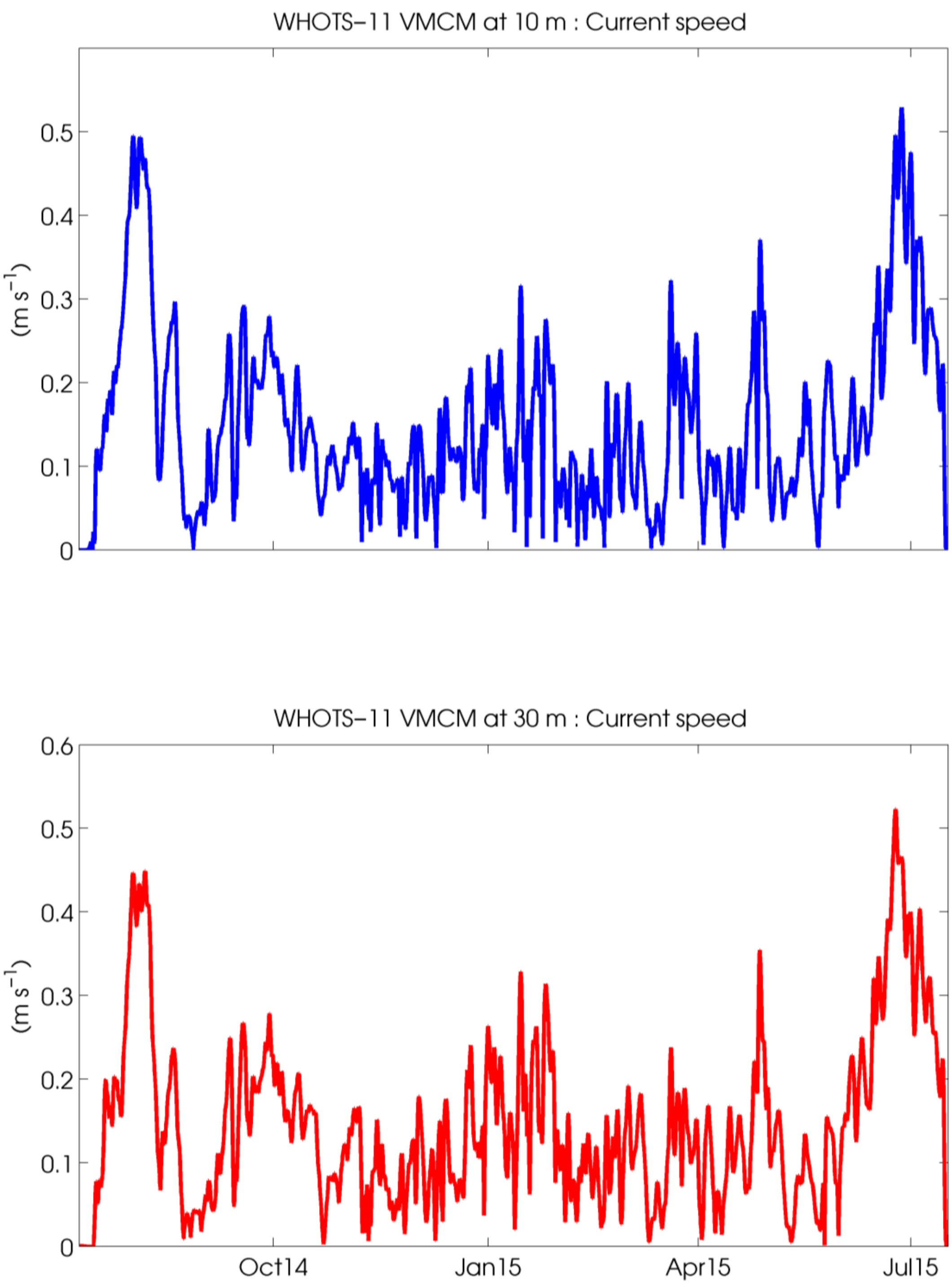

Figure 6-53. Horizontal current speed (m/s) during the WHOTS-11mooring deployment from the VMCMs at 10 m depth (upper panel) and at 30 m depth (lower panel).

G. GPS Data

Time-series of latitude and longitude of the WHOTS-11 buoy from GPS data are presented in Figure 6-54 and spectra of the time-series is shown in Figure 6-5555.

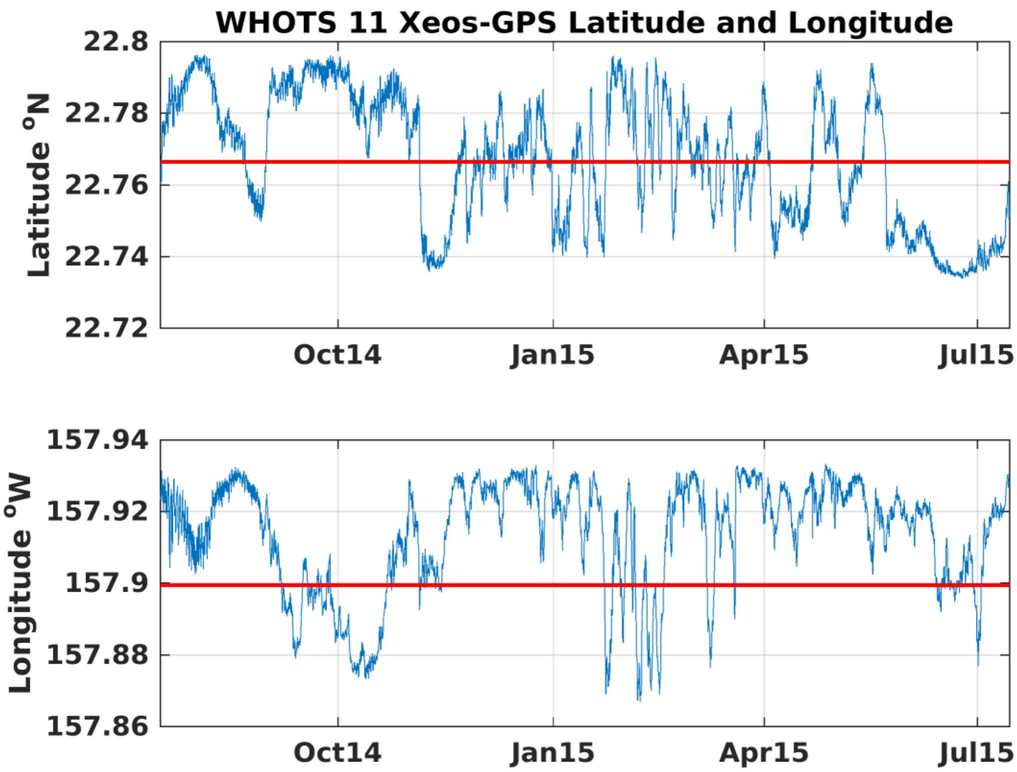

Figure 6-58. GPS Latitude (upper panel) and longitude (lower panel) time series from the WHOTS-11 deployment.

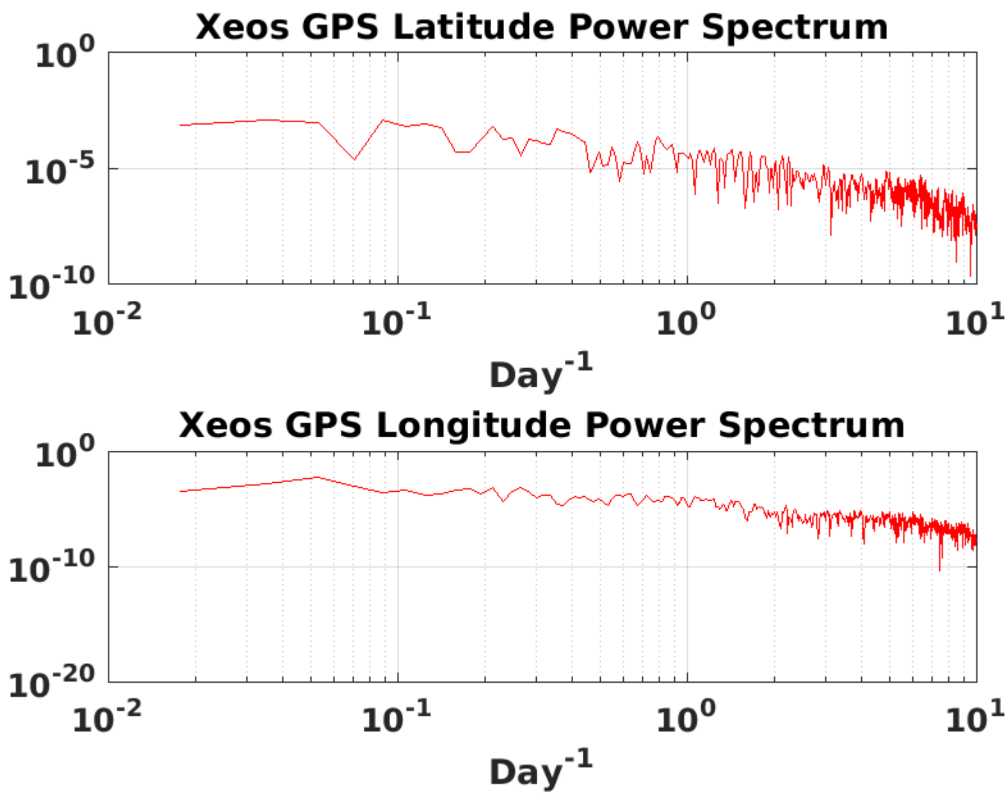

Figure 6-55. Power spectrum of latitude (upper panel) and longitude (lower panel) for the WHOTS-11 deployment.

H. Mooring Motion

The position of the mooring with respect to its anchor was determined from the ARGOS positions as shown in Section 5.D. Additional information of the mooring motion was provided by the ADCP data of pitch, roll and heading, shown in this section.

Figure 6-56 shows the ADCP data of the instrument's tilt (a combination of the pitch and roll), plotted against the buoy's distance from its anchor (derived from ARGOS positions), for both WHOTS ADCP's. The red line in the plot is a quadratic fit to the median tilt calculated every 0.2 km distance bins. The figure shows that during both deployments, the ADCP tilt increased as the distance from the anchor increased. This tilting was caused by the deviation of the mooring line from its vertical position as it was pulled by the anchor. The tilting of the line also caused the rising of the instruments attached to the line.

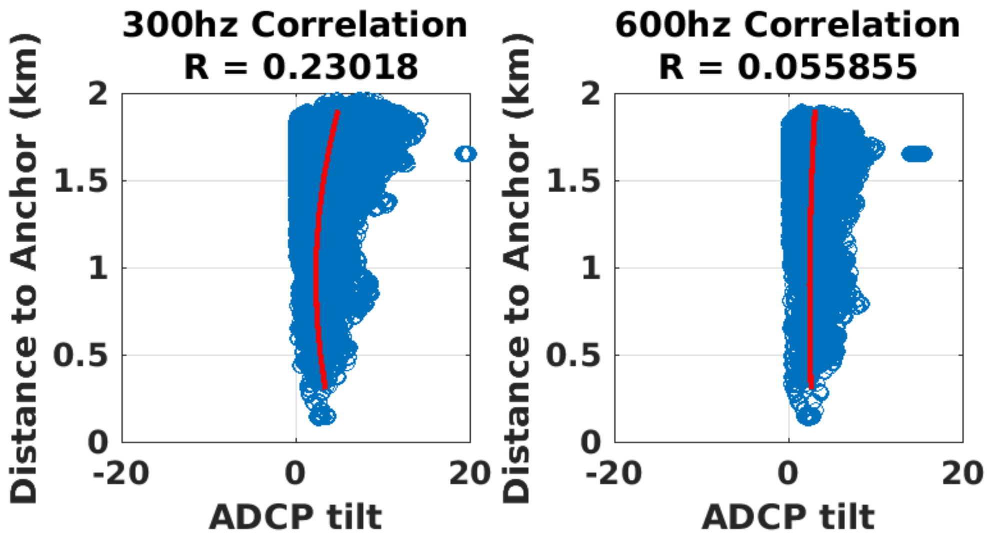

Figure 6-56. Scatter plots (blue circles) of ADCP tilt and distance of the buoy to its anchor for the 300 kHz (left panel), and the 600 kHz (right panel) ADCP deployments. The red line is a quadratic fit to the median tilt calculated every 0.2 km distance bins.

7. References

Colbo, K., R. Weller, 2009. Accuracy of the IMET Sensor Package in the Subtropics. J. Atmos. Oceanic Technol., 26, 1867-1890.

Firing, E., 1991. Acoustic Doppler Current Profiling measurements and navigation. In *WOCE Hydrographic Operations and Methods.* WOCE Operations Manual, WHP Office Report WHPO 91-1,WOCE Report No. 68/91, 144pp.

Freitag, H. P., M. E. McCarty, C. Nosse, R. Lukas, M. J. McPhaden, and M. F. Cronin, 1999. COARE Seacat data: Calibrations and quality control procedures. NOAA Thechnical Memorandum, ERL PMEL-115. 93 pp.

Fujieki, L. A., F. Santiago-Mandujano, W. Deppe, D. McCoy, R. Lukas, and M. Church, 2016. Hawaii Ocean Time-series Data Report 26: 2014. School of Ocean and Earth Sciences and Technology. Publication # 9823.

Fujieki, L. A., F. Santiago-Mandujano, K. Rosburg, A. King, R. Lukas, and D. Karl, 2017. Hawaii Ocean Time-series Data Report 27: 2015. School of Ocean and Earth Sciences and Technology. Publication # 10230.

Hosom, D. R. Weller, R. Payne, and K. Prada, 1995. The IMET (Improved Meteorology) Ship and Buoy Systems. J. Atmos. Oceanic Technol., 12, 527-540.

Howe, B. M., R. Lukas, F. Duennebier, and D. Karl, ALOHA cabled observatory installation, *OCEANS 2011*, 19-22 Sept. 2011.

Kara, A. B., P. A. Rochford, and H. E. Hulburt, 2000. Mixed layer depth variability and barrier layer formation over the North Pacific Ocean, J. Geophys. Res., 105, 16,803–16,821.

Lukas, R., F. Santiago-Mandujano, F. Bingham and A. Mantyla, 2001. Cold bottom water events observed in the Hawaii Ocean time-series: Implications for vertical mixing. *Deep-Sea Res*. I, 48 (4), 995-1021

Owens, W. B. and R. C. Millard, 1985. A new algorithm for CTD oxygen calibration. Journal of Physical Oceanography, 15, 621-631.

Plueddemann, A.J., R.A. Weller, R. Lukas, J. Lord, P.R. Bouchard, and M.A. Walsh, 2006, WHOI Hawaii Ocean Timeseries Station (WHOTS): WHOTS-2 Mooring Turnaround Cruise Repor**t,** Woods Hole Oceanographic Institution, Technical Report WHOI-2006-08, 68 pp.

Plueddemann, A.J., B. Pietro, S. Whelan, R. Lukas, J. Snyder, F. Santiago-Mandujano, B. Nakahara, D. McCoy, R. Tabata, T. Tran, K. Lance, and B. Blomquist, 2015, WHOI Hawaii Ocean Timeseries Station (WHOTS): WHOTS-11 2014 Mooring Turnaround Cruise Repor**t,** Woods Hole Oceanographic Institution, Technical Report WHOI-2015-01, 102 pp.

Santiago-Mandujano, F., P. Lethaby, R. Lukas, J. Snyder, Weller, A. Plueddeman, J. Lord, S. Whelan, P. Bouchard, and N. Galbraith, 2007. Hydrographic Observations at the Woods Hole Oceanographic Institution (WHOI) Hawaii Ocean Timeseries (HOT) Site (WHOTS): 2004-2006. School of Ocean and Earth Science and Technology, University of Hawaii. (http://www.soest.hawaii.edu/whots/data_report1.html)

Santiago-Mandujano, F., D. McCoy, J. Snyder, R. W. Deppe, and R. Lukas, 2015. UH Contributions to the WHOTS-12 Cruise Report. School of Ocean and Earth Science and Technology, University of Hawaii. (http://www.soest.hawaii.edu/whots/proc_reports/WHOTS-12_CruiseRpt.html)

Tupas, L., F. Santiago-Mandujano, D. Hebel, R. Lukas, D. Karl, and E. Firing 1993. Hawaii Ocean Time-series Data Report 4, 1992, School of Ocean and Earth Science and Technology, University of Hawaii, 93-14, 248 pp.

Tupas, L., F. Santiago-Mandujano, D. Hebel, C. Nosse, L. Fujieki, E. Firing, R. Lukas, D. Karl, 1997. Hawaii Ocean Time-series Data Report 8, 1996, School of Ocean and Earth Science and Technology, University of Hawaii, 97-7, 296 pp.

UNESCO. 1981. Tenth Report of the Joint Panel on Oceanographic Tables and Standards. UNESCO Technical Papers in Marine Science, No. 36, UNESCO, Paris.

Whelan S., R. Weller, R. Lukas, F. Bradley, J. Lord, J. Smith, F. Bahr, P. Lethaby, J. Snyder, 2007. WHOI Hawaii Ocean Timeseries Station (WHOTS): WHOTS-3 Mooring Turnaround Cruise Report. Technical Report. Woods Hole Oceanographic Institution, WHOI-2007-03, 103 pp.

8. Appendices

A. Appendix 1: WHOTS-11 300 kHz ADCP Configuration

```
yearbase: 2014
      proc_yearbase: 2014
            nbytes: 752
        nbeams_used: 4
            ncells: 30
          num_pings: 40
              cell: 4
             blank: 1.7600
             pulse: 4.4400
       bin1distance: 6.2300
         head_align: 0
          head_bias: 9.4700
          bt_was_on: 0
        tr_pressure: 125
            convex: 1
        orientation: 'up'
          beamangle: 20
          frequency: 300
        coordsystem: 'earth'
              mode: 1
          code_reps: 9
                EZ: 125
               lag: 0.5000
        sensornames: {'temp'  'cond'  'roll'  'pitch'  'head'  'press'  'sspeed'}
      COR_threshold: 64
       PG_threshold: 0
       EV_threshold: 2
           tpp_secs: 4
       coord_transf: 31
                SA: 29
   cpu_serialnumber: 7.1957e+17
                WB: 0
           pingtype: 'bb'
          sysconfig: [1x1 struct]
                bt: [1x1 struct]
```

Program Version 50.40

Instrument S/N:	7637
System Frequency:	307200 HZ
Configuration:	4 BEAM, JANUS
Match Layer:	10

Beam Angle:	20 DEGREES
Beam Pattern:	CONVEX
Orientation:	UP
Sensor(s):	HEADING TILT 1 TILT 2 TEMPERATURE
Temp Sens Offset:	-0.29 degrees C

False Target	(WA)	70 counts
Band Width	(WB)	0
Blank	(WF)	1.76 m
Bins	(WN)	30
Pings/Ens	(WP)	40
Bin Size	(WS)	4.00 m
Head Align	(EA)	0.00 degrees
Head Bias	(EB)	9.47 degrees
Coord Xform	(EX)	11111 Earth Coordinates Using Tilts, 3 Beam Solutions, and Bin Mapping
Sens Source	(EZ)	1111101 cdhprst
Time/Ping	(TP)	00:04.00 Time per Ping (min:sec.sec/100)

B. Appendix 2: WHOTS-11 600 kHz ADCP Configuration

```
yearbase: 2014
       proc_yearbase: 2014
              nbytes: 652
         nbeams_used: 4
              ncells: 25
           num_pings: 80
                cell: 2
               blank: 0.8800
               pulse: 2.2200
        bin1distance: 3.1100
          head_align: 0
           head_bias: 9.4700
           bt_was_on: 0
         tr_pressure: 4.7000
              convex: 1
         orientation: 'up'
           beamangle: 20
           frequency: 600
         coordsystem: 'earth'
                mode: 1
           code_reps: 9
                  EZ: 125
                 lag: 0.2500
         sensornames: {'temp'  'cond'  'roll'  'pitch'  'head'  'press'  'sspeed'}
       COR_threshold: 64
        PG_threshold: 0
        EV_threshold: 2
            tpp_secs: 2
```

```
      coord_transf: 31
                SA: 29
   cpu_serialnumber: 6.8702e+17
                WB: 0
           pingtype: 'bb'
          sysconfig: [1x1 struct]
                bt: [1x1 struct]
```

```
Program Version 50.4
Instrument S/N:        13917
Frequency:             614400 HZ
Configuration:         4 BEAM, JANUS
Match Layer:           10
Beam Angle:            20 DEGREES
Beam Pattern:          CONVEX
Orientation:           UP
Sensor(s):             HEADING  TILT 1  TILT 2  TEMPERATURE
Temp Sens Offset:       -0.03 degrees C

False Target    (WA)    70 counts
Band Width      (WB)    0
Blank           (WF)    0.88 m
Bins            (WN)    25
Pings/Ens       (WP)    80
Bin Size        (WS)    2.00 m

Head Align      (EA)    0.00 degrees
Head Bias       (EB)    9.47 degrees
Coord Xform     (EX)    11111 Earth Coordinates Using Tilts, 3 Beam Solutions, and Bin Mapping
Sens Source     (EZ)    1111101 cdhprst

Time/Ping       (TP)    00:02.00 Time per Ping (min:sec.sec/100)
```

C. Appendix 3: WHOTS-11 VMCM report

WHOTS 11 Preliminary Processing
and Data Return
2015/12/14 n. galbraith

a. VMCM

read cards and generated matlab files on Oct 29, 2015..
THERE IS NO COMPASS DATA, SO DIRECTIONS WILL BE WRONG.

SN 62 10m
SN 83 30m

S	first	last	#points	#expt	rate	return

N						%
62	17-Jul-2014 04:10:15	14-Jul-2015 16:55:15	522046	522045	1	100
83	17-Jul-2014 04:10:45	14-Jul-2015 16:55:45	522046	522045	1	100